Host-induced gene silencing as resistance strategy against pathogens

Dissertation
zur Erlangung des
Doktorgrades der Naturwissenschaften (Dr. rer. nat.)

der

Naturwissenschaftlichen Fakultät III
Agrar- und Ernährungswissenschaften,
Geowissenschaften und Informatik

der Martin-Luther-Universität Halle-Wittenberg

vorgelegt von
Frau Karolina Maria Słomińska – Durdasiak

Gutachter:
1. Prof. Dr. Jochen Reif
2. Prof. Dr. Holger Deising
3. Prof. Dr. Thomas Miedaner
Verteidigung am: 13.11.2023 in Halle (Saale)

Table of contents

Table of contents I
Abbrevations V
List of figures VIII
List of tables X
1. Introduction 1
1.1 Food security 1
1.2 Plant resistance 2
1.2.1 Mechanism of resistance 2
1.3 Powdery mildew - barley pathosystem 5
1.4 Fusarium head blight (FHB) 6
1.4.1 Current and possible FHB control strategies 8
1.4.1.1 Chemical control 8
1.4.1.2 Genetic control 9
1.4.1.3 Genetically modified plants 9
1.5 Host-induced gene silencing (HIGS) 10
1.6 Natural HIGS phenomenon 11
1.6.1 Spray induced-gene silencing 12
1.6.1.1 HIGS and SIGS to control FHB 12
1.7 Silencing and unconventional protein secretion pathway in plants 13
1.7.1 The RNAi silencing pathway in plants 13
1.7.2 The secretory pathway 15
1.7.3 Plant cytoskeleton 17
1.8 Association mapping 18
1.8.1 Linkage mapping 18
1.8.2 Genome-wide and candidate-gene association mapping 19
1.8.2.1 Control for relatedness within a population 20
1.9 Aims of the thesis 20
2. Materials and methods 21
2.1 Wet lab protocols 21
2.1.1 Plant and fungal material 21
2.1.1.1 Germplasm and FHB disease resistance assessment for the candidate genes approach 22
2.1.2 DNA, RNA isolation, and cDNA synthesis 22
2.1.3 Preparation of TOP10 competent cells 24
2.1.4 Development of vectors for transient-induced gene silencing by particle bombardment 24
2.1.5 Transient-induced gene silencing 25
2.1.6 Inoculation with *Blumeria graminis* f. sp. *hordei* and GUS staining, microscopy, and statistics 26
2.1.7 Amplification of the wheat sequences 27
2.1.8 Virus-induced gene silencing (VIGS) 27
2.1.8.1 VIGS via in vitro transcription 28
2.1.8.2 VIGS via Microprojectile bombardment and mechanical infection of BSMV 28
2.1.8.3 *Fusarium culmorum* inoculation 29
2.1.8.4 Statistical evaluation 29
2.2 Dry lab protocols 30
2.2.1 Selection of HIGS candidate genes 30
2.2.2 HIGS reporter gene for TIGS screening 30
2.2.3 Putative candidate genes involved in HIGS mechanism in wheat 30

2.2.4 Sequences analysis 31
2.2.5 Association studies 31
2.2.5.1 Candidate-gene association mapping 31
2.2.5.2 Phenotype-genotype association in a biparental population 32
2.2.6 Physical and genetic mapping, LD calculation 32
2.2.6.1 Physical mapping 32
2.2.6.2 Linkage disequilibrium (LD) calculation 32
2.2.6.3 Genetic mapping 32
2.2.7 Selection of putative sRNA targets in Fusarium spp. 33
2.2.8 Software and databases 34
3. Results 36
3.1 Mechanism of HIGS 36
3.1.1 Work concept 36
3.1.2 Reporter gene approach 38
3.1.2.1 Selecting HIGS candidate gene orthologues in barley 38
3.1.2.2 Development of a TIGS test system to study the mechanism(s) of HIGS 39
3.1.2.2.1 Selecting a susceptible genotype for the TIGS test system 39
3.1.2.2.2 Failure to find reliable HIGS reporter gene 40
3.1.3 Association approach 44
3.1.3.1 Selection of potential HIGS candidate genes orthologues in wheat 44
3.1.3.2 Three markers associated with *Fusarium* infection in candidate-gene association studies 50
3.1.3.3 Validation of the marker-trait associations in the 'Apache x Biscay' and 'History x Rubens' populations 51
3.1.3.3.1 Confirmation of the marker-FHB infection associations in 'Apache x Biscay' population 51
3.1.3.3.2 Confirmation of marker DCL1(1) - FHB infection association in 'Rubens x History' population 53
3.1.3.4 Analysis of the genes with DCL1(1), DCL1(2) and Ara6 markers 55
3.1.3.5 Physical mapping and analysis of linkage disequilibrium among the significant markers 57
3.1.3.6 Genetic mapping 60
3.2 Naturally occurring HIGS in barley against *Fusarium spp*. 63
3.2.1 Selection of the HIGS candidate genes in *Fusarium* 63
3.2.1.1 Analysis of putative barley sequences creating sRNA tags targeting *Fusarium* genes 64
3.2.2 Stability of the BSMV 67
3.2.2.1 The stability of the virus in 'Black Hulless' is dependent on the length of the insert in the BSMV:γ vector 67
3.2.2.2 The 104 nt and 180 nt Inserts carried in BSMV:γ vectors were mainly stable over the entire VIGS experiment 70
3.2.3 Two of the chosen candidate genes were shown to be essential for FHB development 72
3.2.4 Gene expression analysis vs. stability of the BSMV 77
4. Discussion 81
4.1.1 A critical view on the experimental design for functional validation and study of HIGS candidate genes 81
4.1.2 Selection of genes potentially involved in the HIGS mechanism 85
4.2 Association studies 87
4.2.1 Reasons for choosing candidate-gene association mapping approach 87
4.2.2 Attempts to explore the mechanism of host-induced gene silencing 87

4.2.3 Detected associations verified in RILs populations 90
4.2.4 Ara6 marker associated with plant height 91
4.2.5 The association of candidate genes putatively involved in trans-kingdom RNA trafficking and heading date 92
4.3 Naturally occurring HIGS 93
4.3.1 Selection of the HIGS candidate genes in *Fusarium* 93
4.3.2 VIGS – stability of the insert and validation analysis 94
5. Summary 98
References 99
Appendix: Supplemental tables and figures 113
Supplementary Data M1: Important chemicals used in experiments described in here 113
Supplementary Data M2: The media composition for bacterial and fungal cultures used in the experiments with additional information 115
Supplementary Data M3: The solutions used in the experiments described in Material and Methods. 116
Supplementary Data M4: Specifications of the barley and wheat variaties used in the PhD thesis. 118
Supplementary Data M5: Vectors 119
Supplementary Data M6: cDNA synthesis protocol. 121
Supplementary Data M7: Transformation efficiency equation 121
Supplementary Data R1: Values to Figure R 2. 122
Supplementary Data R2: Values to Figure R 3. 123
Supplementary Data R3: Association of the FHB infection at the different stages of FHB disease development in a biparental population 'Apache x Biscay' and allelic variant of the four markers. 124
Supplementary Data R4: Association of the FHB infection at the different stages of FHB disease development in a biparental population 'History x Rubens' and allelic variant of the four markers. 125
Supplementary Data R5: Association of the FHB infection at the latest stage of FHB disease development in a biparental population 'History x Rubens' and allelic variant of the four markers 126
Supplementary Data R6: sRNA sequences and their targets in *Fusarium graminearum*. 127
Supplementary Data R7: Stability of the long inserts (344, 442 and 495 nt) at the time when 'Apogee' spikelet is inoculated with FHB (~20th day of the experiment). 129
Supplementary Data R8: Relative FHB infection of 'Apogee' wheat plants inoculated with recombinant BSMV, carrying FGSG_06195(164) insert. 130
Supplementary Data R9: Relative FHB infection of 'Apogee' wheat plants inoculated with recombinant BSMV, carrying FGSG_01104(107) insert. 130
Supplementary Data R10: Gene expression analysis and stability of the BSMV 131
Acknowlegment 132
Curriculum vitae 133
List of publications 134
Oral presentations and posters 134
Declaration under oath 135

List of supplemental files provided in the accompanying Compact Disc

Supplementary Data M8: Candidate genes in barley and primers (Data provided as Compact Disc).

Supplementary Data M9: Primers used to amplify sequences of BSMV vectors and Fusarium sequences.
Supplementary Data M10: Barley genes potentially involved in HIGS mechanism divided into gene families (Data provided as Compact Disc).
Supplementary Data M11: Primers used for HIGS reporter gene amplification.
Supplementary Data M12: Primers of potential HIGS orthologs in wheat (Data provided as Compact Disc).
Supplementary Data M13: The primers amplifying KASP markers (Data provided as Compact Disc).
Supplementary Data R11: Identified orthologues in barley.
Supplementary Data R12: Sequence of Ara6 gene in wheat (4D chromosome).
Supplementary Data R13: Sequence of Dicer1 gene in wheat (5A chromosome).
Supplementary Data R14: The barely sequences putatively producing sRNAs targeting *Fusarium* genes.
Supplementary Data R15: Values to Figure R 20-22 and Supplenetary Data 8-9

Abbrevations

Abbreviation	Meaning
AGO	Argonaut
AGT	Appressorial germ tube
BEC	*Blumeria* effector candidates
Bgh	*Blumeria graminis* f. sp. *hordei*
BSMV	Barley stripe mosaic virus
CC	Coiled-coil
CNL	Coiled-coil domains containing NLR
CG	Candidate gene
CPS	Conventional protein secretion
CYP40	Cyclophilin 40
CYP51	Cytochrome P450 lanosterol C-14α-demethylase
DAMP	Damage-associated molecular patterns
DCL	Dicer
DH	Double Haploid
DMI	Demethylation inhibitors
DON	Deoxynivalenol
dsRNA	Long double stranded RNA
ESCRT	Endosomal sorting complex required for transport
EV	Extracellular vesicle
EXPO	Exocyst-positive organelle
FAO	The Food and Agriculture Organization
FHB	Fusarium head blight
FRET	Fluorescence Resonance Energy Transfer
GLS	β-1, 3-glucan synthase
GM	Genetically modified
GPI	Glycosylphosphatidylinositol
GTF	β-glucanosyltransferase
GUS	β-glucuronidase
GWAS	Genome wide association studies
HCG	HIGS candidate gene
HEN1	HUA ENHANCER 1
HIGS	Host-induced gene silencing
HR	Hypersensitive response
HRG	HIGS reporter gene
HSP90	Chaperone heat shock protein 90
IBS	Centered identity by state
ILV	Intraluminal vesicle
IPK	Leibniz Institute of Plant Genetics and Crop Plant Research

KASP	Kompetitive allele specific PCR
LD	Linkage disequilibrium
LDH	Layered double hydroxide
LIP5	LYST-interacting protein 5
LOD	Logarithm of odds
LRR	Leucine rich repeat
MAMP	Microbe-associated molecular patterns
MAPK	Mitogen-activated protein kinases
MAS	Marker assisted selection
miRNA	microRNA
MLO	Mildew resistance locus O
MVB	Multivesicular bodies
MT	Microtubule
NB	Nucleotide binding
NB-ARC	Nucleotide-binding domain shared with APAF1, R gene products, and
NCBI	National center for biotechnology information
NLR	Nucleotide-binding domains and leucine-rich repeats
PAMP	Pathogen-associated molecular patterns
PM	Plasma membrane
Pol II	RNA Polymerase II
PRR	Pattern recognition receptor
PTGS	Posttranscriptional gene silencing
QTL	Quantitative trait loci
R protein	Resistance protein
RdRp/RDR	RNA-DEPENDENT RNA POLYMERASE
Rht-D1	Reduced height-D1
RIL	Recombinant inbred line
RISC	RNA-induced silencing complex
RNAi	RNA interference
RNAse III	Ribonuclease III
ROS	Reactive oxygen
RT	Room temperature
siRNA	Small interfering RNA
SIGS	Sprayed-induced gene silencing
SNARE	Proper soluble N-ethylmaleimide-sensitive factor attachment
SNP	Single Nucleotide Polymorphism
sRNA	Double stranded small RNA
ssRNA	Single-stranded RNA
TGN	Trans-Golgi network
TGS	Transcriptional gene silencing

TIGS	Transient-induced gene silencing
TIR	N-terminal Toll/interleukin-1 receptor-like
TR	Transcription Regulator
UPS	Unconventional protein secretion
URGI	Unité de Recherches en Génomique Info
VIGS	Virus-induced gene silencing
WAK	Wall-Associated Kinase
X-Gluck	5-bromo-4-chloro-3-indolyl-beta-D-glucuronic acid

List of figures

Figure I 1: Simplified model of plant immunity. 3
Figure I 2: Model of the FHB infection in cereal hosts..... 7
Figure I 3: Model of RNA interference in pathogen-infected cells. 15
Figure M 1: Transformed cell with (A) and without (B) *Bgh* haustorium. 26
Figure R 1: Outline of planned experiments leading to understanding HIGS in plants mechanistically.....37
Figure R 2: Susceptibility index (SI) of chosen barley genotypes to *Bgh*. 40
Figure R 3: The search for a reliable HIGS reporter gene among the eight gene candidates. 43
Figure R 4: Alignments of wheat genomic sequences to sequences of HIGS candidates of barley. 46
Figure R 5: Three markers shown to be associated with FHB infection at the latest stage of FHB disease development in 'Apache x Biscay' population. 52
Figure R 6: Marker Ara6 associated with the plant height (PH) in 'Apache x Biscay' population. 52
Figure R 7: No association of the heading date (days) and allelic variant of the markers located in the candidate genes. 53
Figure R 8: Marker DCL1(1), located in *Dicer1* gene, associated with the FHB infection at some stages of FHB development in 'History x Rubens' population. 54
Figure R 9: DCL1(1) and ESCRT-III markers associated with the wheat spike heading date..... 54
Figure R 10: No association of the wheat spike plant height and allelic variants of the four markers in 'History x Rubens' population. 55
Figure R 11: Expression profiles of *Dicer1* and Rab5 GTPase *Ara6* genes. *Dicer1* (TraesCS5A02G516000) and *Ara6* (TraesCS4D02G267900) expression profiles show spikes infected with FHB and leaves, roots of seedlings infected with stripe rust, *Septroria tritici* and powdery mildew. 56
Figure R 12: LD plot of markers DL1(1), DCL1(2) and nearby lying markers on RefSeq v1.0 physical map. 59
Figure R 13: LD plot of Ara6 marker and nearby lying markers on RefSeq v1.0 physical map..... 60
Figure R 14: Genetic map generated using 'Apache x Biscay' population, presenting relative distances of markers in the linkage to the Ara6 marker available for this population. 61
Figure R 15: Genetic map generated using 'Apache x Biscay' population, presenting relative distances of markers being in the linkage to the DCL1(1) and DCL1(2) markers, available for this population. 62
Figure R 16: Amplification of cDNA obtained from the second leaf of 'Black Hulless' barley plants after particle bombardment with BSMV:α, BSMV:β and BSMV:γ / recombinant BSMV:γ showed significant reduction / loss of inserts in BSMV:γ, having a length greated than or equal to 344 nt. 69
Figure R 17: Amplification of cDNA obtained from the second leaf of 'Black Hulless' barley plants after particle bombardment with BSMV:α, BSMV:β and BSMV:γ / recombinant BSMV:γ showed slight reduction/losing of the inserts in BSMV:γ, having a length greated than or equal to 164 nt. 70
Figure R 18: Amplification of cDNA obtained from 'Apogee' wheat plants after the entire VIGS experiment showed that insert carried in BSMVFGSG_06175(104) was intact in most samples, where some deletions/reductions of the insert in BSMVFGSG_06175(180) were observed. 71
Figure R 19: Amplification of cDNA obtained from 'Apogee' wheat plants after the entire VIGS experiment showed some deletions/reductions of the 180 nt insert in $BSMV_{FGSG_06175(180)}$, where insert of 233 nt was deleted in almost all samples in $BSMV_{FGSG_10970(233)}$. 72
Figure R 20: Plants carrying the $BSMV_{FGSG_10970(233)}$ virus showed significantly less FHB disease symptoms than plants carrying BSMV:00 after seven and ten days after the point inoculation.. 74
Figure R 21: Plants carrying the $BSMV_{FGSG_06175}$ virus showed less FHB disease symptoms than plants carrying a non-recombinant vector at some stage of FHB development. 75

Figure R 22: Plants carrying two recombinant viruses ($BSMV_{FGSG_06175(180)}$ and $BSMV_{FGSG_10970}$) showed significantly reduced FHB disease symptoms compared to the control. 76
Figure R 23: Example of the visual assessment of the recombinant BSMV stability of the insert after accomplishing the VIGS experiment. 79
Figure R 24: Graph presenting samples with their gene expression paired with estimated insert stability (0 - insert is lost; 1 - insert is fully intact) and relative gene expression (10 days after *Fusarium* inoculation of the wheat spike). 80
Figure D 1: Candidate genes potentially involved in cross-kingdom RNA silencing were selected in wheat. 90
Figure D 2: Three polymorphic markers (Ara6, DCL1(1), and DCL1(2)) out of twelve detected in the GABI wheat population were found to be associated with the FHB severity. 91

List of tables

Table R 1: HIGS reporter gene candidates tested by particle bombardment. 42
Table R 2: Polymorphisms found in nine genes among eight wheat genotypes 48
Table R 3: Candidate genes potentially involved in HIGS with polymorphisms detected among the selected wheat genotypes. 49
Table R 4: Results of candidate-gene association mapping of polymorphic markers being located in the nine candidate genes. 50
Table R 5: Markers surrounding DCL1(1) and DCL1(2) markers. 57
Table R 6: Markers surrounding Ara6 marker. 58
Table R 7: Sequences in barley genome that may be responsible for sRNA targeting *Fusarium* genes creation. 66
Table R 8: Expected lengths of the PCR product: 68
Table R 9: The number of experiments with the number of BSMV-positive plants performed for each construct. 73
Table R 10: The following relative criteria were used to assess recombinant BSMV stability of the insert after accomplishing the VIGS experiment. 78

1. Introduction

1.1 Food security

Due to novel technologies established in/for Green Revolution and resulting higher efficiencies of land and water usage, agricultural production tripled between 1960 and 2015. Nowadays, however yield increases are slowing (Food and Agriculture Organization of the United Nations, 2017). Since hundreds of millions of people are suffering from hunger (Food and Agriculture Organization of the United Nations, 2019) and the human population is growing, considerable increase in overall food production is required (Food and Agriculture Organization of the United Nations, 2017). There are still some challenges that agriculture and food systems face now and will be facing in the future. One such challenge is the outbreaks of transboundary diseases and pests that threaten food security (Food and Agriculture Organization of the United Nations, 2017). History had already shown that plant diseases like potato late blight in Ireland in the 19th century may be responsible for massive human death and migration. Nowadays, plant diseases are not only persistent, but new ones continue to emerge (Velasquez et al., 2018). Globally, 20 to 40% of the yield is annually reduced by pests. The cost of plant diseases is equivalent to approx. US$220 billion annually (Food and Agriculture Organization of the United Nations, 2017). Moreover, food production is affected by climate changes that have that potential to threaten food security in many ways. Climate change may create weather conditions conducive to the emergence of the new devastating plant diseases in regions critical for food production (Velasquez et al., 2018). It is estimated that in low-latitude countries, crop production will be adversely affected by climate changes. In northern latitudes, the consequences are not certain, as they can be either positive or negative. However, frequent droughts and floods may dramatically reduce overall yield (Food and Agriculture Organization of the United Nations, 2017). Estimates suggest that without significant improvement of the genetic material, global production of wheat, one of the main calories providers for humans, will decrease by approx. 6% for each additional degree centigrade, which is estimated to have increased even by 3,7 degree by the end of the century (Tessmann & Van Sanford, 2018). Besides that, conflicts are often the reason for malnutrition, by reducing food availability as well as access to health care and food (Food and Agriculture Organization of the United Nations, 2017). In addition, around 30% of all food is lost or wasted during harvesting, post-harvesting, processing, packaging, distribution, and consumption. It is estimated that two million people could be saved by reducing food loss and waste by 50% (Food and Agriculture Organization of the United Nations, 2019). Without doubt, improvement and redesign of food supply chains are needed (Food and Agriculture Organization of the United Nations, 2017; Food and Agriculture Organization of the United Nations, 2019).

1.2 Plant resistance

Plants are constantly under biotic and abiotic stresses. Biotic stress may be caused by the action of organisms like bacteria, insects, nematodes, and fungi, which can also lead to plant disease (Gill et al., 2015). The interaction between plants and pathogens is a process in which plants and pathogens exchange molecules, like sugars, proteins, lipopolysaccharides (Boyd et al., 2013), and RNA molecules (Shahid et al., 2018; Wang et al., 2016; Weiberg et al., 2013; Zhang et al., 2016). Pathogens aim to infect a plant, whereas plants try to detect pathogens and induce defense responses (Gupta et al., 2015). Plants developed a wide variety of constitutive and inducible defense responses to protect themselves from the damage. Among constitutive ones are cell walls, waxy epidermal cuticules, or bark, whereas inducible defense responses include the production of low-molecular weight antimicrobial chemicals referred to as phytoalexins, pathogen-degrading enzymes, and hypersensitive response characterized by deliberate plant cell death (Freeman & Beattie, 2008). There are two types of plant resistance, namely race-specific and broad-spectrum resistance. Race-specific resistance relies on single genes (called R genes) that confer a strong effect against single or few pathogen races (Li et al., 2020). The most studied disease resistance (R) proteins are characterized by the nucleotide-binding (NB) and leucine-rich repeat (LRR) domains (Jones & Dangl, 2006; Kanyuka & Rudd, 2019). However, every gene involved in resistance responses may be considered as a resistance gene (Jones & Dangl, 2006). Race-specific resistance is usually easily introduced into a breeding program, but it is easily "broken", and then no longer effective against the disease because of the rapid changing pathogen population (Miedaner & Korzun, 2012). On the other hand, broad-spectrum resistance is controlled by quantitative trait loci (QTL) and is usually race-nonspecific (Periyannan et al., 2017). In general, non-race specific resistance is a quantitative, partial resistance in which pathogen development/growth is slow (Periyannan et al., 2017). Broad-spectrum resistance is difficult to be "broken down", yet it gives only partial protection against infection and is much more difficult to introduce into a breeding program (St Clair, 2010).

1.2.1 Mechanism of resistance

The plant immune system depends on the plant's ability to recognize enemy molecules, pass the signal on and respond defensively via various pathways involving a number of genes and their products (Andersen et al., 2018).

Pattern recognition receptors (PRRs) are able to detect a wide spectrum of microbial components called pathogen-associated molecular patterns (PAMPs), such as fungal chitin, xylanase, bacterial flagellin, or viral nucleic acids. PRRs often have LRRs that bind to an extracellular ligand, a transmembrane domain for their anchoring in the cell membrane and cytoplasmic kinase domains for

signalling through a transfer of a phosphate group onto proteins, in a process called phosphorylation (Andersen et al., 2018). LRRs are highly differentiated, related to their ability to bind different elicitors. On the other hand, wall-associated kinases (WAKs) recognize cellular components that have been disrupted by the action of pathogenic enzymes, called damage-associated molecular patterns (DAMPs). WAKSs possess cytoplasmic kinase domains and an N-terminal, extracellular galacturonan-binding domain interacting with cell wall pectins (Andersen et al., 2018). Pathogens seek to reduce PAMP-triggered immunity efficiency and facilitate their infection of the plant through delivery of effectors (Andersen et al., 2018; Jones & Dangl, 2006). Receptors with nucleotide-binding domains and leucine-rich repeats (NLRs), also known as R genes, are typically located in the cytoplasm and detect pathogen-derived effectors. R genes are activated by direct interaction with the pathogen effector or by detecting modifications to the effector's target or to the NLR itself (Andersen et al., 2018; Dodds et al., 2006; Van der Biezen & Jones, 1998). NLRs consist of an N-terminal domain, a nucleotide-binding domain called NB-ARC (nucleotide-binding domain shared with APAF1, R gene products, and CED4), and a C-terminal LRR. Highly variable LRR domain is involved in recognition of various effector structures when N-terminal Toll/interleukin-1 receptor-like (TIR) or coiled-coil (CC) domains are evolutionarily conserved domains that can cause cell death autonomously and without the presence of the effector (Bentham et al., 2020). The NB-ARC domain acts as a molecular switch, with the detection of pathogenic effectors mediated by this domain through nucleotide exchange (ADP into ATP) (Bentham et al., 2020; van Wersch et al., 2020). Receptors activate various signaling mechanisms, including G-proteins, mitogen-activated protein kinases (MAPKs), ubiquitin and calcium fluctuations (Andersen et al., 2018).

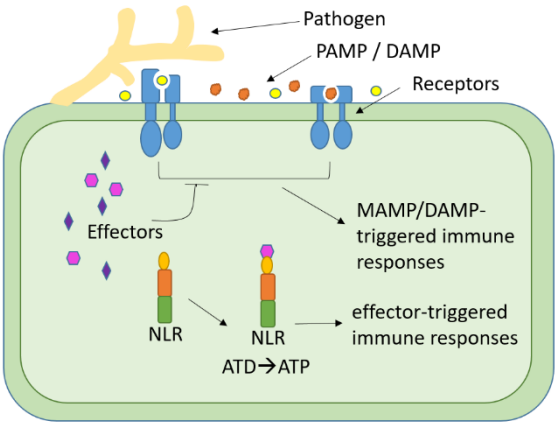

Figure I 1: Simplified model of plant immunity. DAMPs, which are generated by pathogens and PAMPs, can be sensed by receptors and trigger microbe-associated molecular pattern (MAMP)/DAMP immunity responces. Pathogens can release effectors that may interact with host systems to their advantage, for example, by suppressing signalling pathways originating from cell surface receptors. The effectors or their activity can be detected by NLRs to initiate effector-triggered immunity (Bentham et al., 2020). MAMP-recognizing PRRs trigger immune responses resulting in rapid calcium influx, MAPK phosphorylation cascade, defense gene expression, reactive oxygen species (ROS) accumulation, and cell wall changes. Activation of plant NLRs leads to Ca2+ signaling, production of ROS, transcriptional reprogramming of defense genes, programmed cell death, accumulation of salicylic acid and jasmonic acid, and generation of antimicrobial molecules and hydrolytic enzymes (Nishad et al., 2020) (modified Bentham et al. (2020)).

Recently, Bi et al. (2021) have shown that when activated, the *Arabidopsis* NLR protein zygotic arrest 1 (ZAR1) creates a resistosome in the plasma membrane (PM), which is a cation-selective calcium-

permeable channel. The activity of the resistosome triggers immune responses as well as cell death in plants. It is not known whether resistosome and channel activity is conserved among plant coiled-coil domains containing NLR (CNLs), although the results of a study by Forderer et al. (2022) on the wheat resistosome support this thesis. Direct binding of the effector AvrSr356 to the wheat CNL Sr35 was shown to result in the formation of a pentameric Sr35-AvrSr35 complex (Forderer et al., 2022).

Plant Hormones regulate reistance responces depending on pathogen/pest type e.g. jasmonic acid and ethylene are involved in the plant's response to necrotrophic pathogens. Transcription factors (TFs) influence the expression of numerous defense genes. Exposure to the pathogen results in chromatin modification, which affects the expression of various components of the plant defense response. DNA methylation, recombination between homologous chromosomes, RNA interference (RNAi), and histone methylation/acetylation affect plant defense (Andersen et al., 2018).

This leads to a range of defense responses that prevent further infection. Hypersensitive response (HR) induce planned cell death in the region surrounding the infection. This establishes a zone that stops the spread of the pathogen and is an effective technique against pathogens requiring living tissue (biotrophs). The pathogen infection activates the production of peroxidases to generate reactive oxygen species (ROS), and ROS triggers programmed cell death. ROS also creates unsuitable environments for pathogen development and reproduction, referred to as an oxidative burst. In addition, ROS are involved at the level of signal transduction and mediate the crosslinking of glycoproteins, thereby strengthening plant cell walls (Andersen et al., 2018). In response to fungal cellulase enzymes degrading the plant cell wall, plants produce enzyme inhibitors and deposit callose and lignin to strengthen the plant cell wall. In addition, plant enzymes, chitinases, and β-1-3-glucanases are released to degrade the pathogen's carbohydrates. Proteases secreted by plants have evolved to diminish the efficiency of catalytic pathogen proteins. Moreover, plants use protease inhibitors to hinder the activity of fungal proteases. Other plant proteins important in the defense response of plants against pathogen attack are defensins. Plant defensins impair pathogen protein synthesis and enzyme activity. These proteins are involved in the initiation of ROS production, protease inhibition, ion signaling blockade, as well as may cause an increase in pathogen membrane permeability (Andersen et al., 2018). Thaumatin-like proteins are also associated with pathogenesis. Barley thaumatin-like protein were shown to bind to 1,3-β-D-glucans and to be associated with resistance to *Fusarium graminearum* and powdery mildew. Various antifungal thaumatin-like proteins, such as wheat trimatin and barley hordomatin, show fungal membrane-permeabilizing activity. Other compounds that take part in the defense response of plants are phytoalexins. They are produced by plants as a response to an attacking pathogen or to chemical or mechanical injury (Andersen et al., 2018).

1.3 Powdery mildew - barley pathosystem

Blumeria graminis f.sp. *hordei* (*Bgh*), as an obligate biotrophic organism, cannot grow on artificial media (Schweizer, 2014). Spore germination and barley infection happen rapidly (Glawe, 2008). Asexual spores, transported hundreds of kilometers by wind, are responsible for the spread of epidemics (Schweizer, 2014). Upon reaching the surface of the host leaf, the conidium germinates, forming a short primary germ tube after around 1 hour, followed by an appressorial germ tube (AGT). The AGT elongates and swells at its tip, forming a hooked appressorium, out of which emerges a penetration peg (about 12 h) that breaches the cell wall of the host epidermis (Zhang et al., 2005). The tip of the penetration peg then swells into the lumen of the host cell, forming a haustorium. Haustorium is encapsulated in the extrahaustorial membrane formed by the invagination of the host cell's modified plasmalemma (Glawe, 2008; Zhang et al., 2005). After about 24 hours, secondary hyphae begin to grow, and after about 48 hours, hyphal appressoria differentiate from secondary hyphae, and new generations of haustoria are formed. Sexual spores are produced in cleistothecia, which form on aging leaves. Cleistothecia remain dormant under adverse environmental conditions, allowing the fungus to overwinter or survive during periods of high temperature and drought (Zhang et al., 2005).

The interaction between barley and *Bgh* is one of the best-understood plant-pathogen models (Schweizer, 2014). Gene silencing assays, such as transient-induced gene silencing (TIGS) in transformed epidermal cells, have proven to be valuable tools for a better understanding barley - *Bgh* interactions. TIGS, based on biolistic transgene delivery, is a method that enables high throughput silencing of gene expression through RNA interference in barley epidermal cells. In short, detached leaf fragments are bombarded with DNA-coated particles carrying both reporter and test gene constructs. After the powdery mildew challenge, *Bgh* success is assessed on individual epidermal cells, which are distinguished by the expression of marker genes. The effect of the test gene on the outcome of the host-pathogen interaction is indicated by quantifying the success of the pathogen in relation to the transformation of the control gene (Douchkov et al., 2014; Douchkov et al., 2005; Panstruga, 2004). This scientific approach is especially suitable for studying barley-powdery mildew interaction for several reasons. Firstly, the outcome of this interaction seems to be regulated solely in a cell-autonomous manner, which is relevant to the application of single-cell gene expression analysis. Secondly, *Blumeria graminis* attacks only cells of the epidermis, which is also the primary target tissue for particle bombardment, and *Bgh* infection structures (except for haustoria) grow completely epiphytically and develop synchronously. In addition, *Bgh* conidiospores can be generated easily in large quantities, and barley epidermal cells are relatively large. This ensures that, on average, almost every transformed cell will be attacked by the fungus if an appropriate inoculation density is used (Panstruga, 2004).

Numerous dsRNAi constructs can be introduced into single cereal cells simultaneously. Co-silencing of barley genes *HvRar1* and *HvSgt1* of barley in the same epidermal cells reduced race-specific resistance more efficiently than silencing *HvRar1* or *HvSgt1* individually (Azevedo et al., 2002; Panstruga, 2004). However, the effect of co-silencing probably depends on the RNAi target since, in the case of the *Mlo* target gene, the system did not tolerate three more "competing" constructs and showed a minor RNAi effect (Douchkov et al., 2005). Douchkov et al. (2005) calculated that 160 RNAi constructs can be tested in a month in a round of TIGS screening by one person. Using the above-mentioned method, they identified the t-SNARE protein, HvSNAP34, as an essential component of the host basal resistance (Douchkov et al., 2005). Moreover, Douchkov et al. (2014) discovered 90 genes significantly influencing quantitative barley resistance to powdery mildew fungus using TIGS method. This method can also be used to identify *Bgh* genes that are required for development or virulence (Nowara et al., 2010; Pliego et al., 2013). Pliego et al. (2013) identified eight *Blumeria* effector candidates contributing to powdery mildew infection by TIGS methods. The *Bgh* - barley pathosystem seems to be a remarkable system for primary research, which makes it possible to quickly test the function of many genes, not only in the host but also in the pathogen. This allows for narrowing down the list of gene candidates and testing only those selected subsequently with other methods.

1.4 Fusarium head blight (FHB)

Fusarium head blight (FHB) is a disease of different cereals, like wheat, barley, rye, oat, or triticale. Among species causing FHB, predominant are *Fusarium graminearum,* and *Fusarium culmorum*, both belonging to the phylum *Ascomycota*. FHB is responsible for quantitative but also qualitative losses by producing mycotoxins hazardous to humans and animals (Kosova et al., 2009). Both these species can reproduce asexually via macroconidia, while *F. graminearum* also reproduces sexually via ascospores. Sticky ascospore cell walls effectively adhere to the plant surfaces, preventing their displacement (Figure I 2; A). Environmental conditions such as humidity, spore density, or temperature influence the germination of conidia. The infection process of *Fusarium* is shown in Fig. I 2.

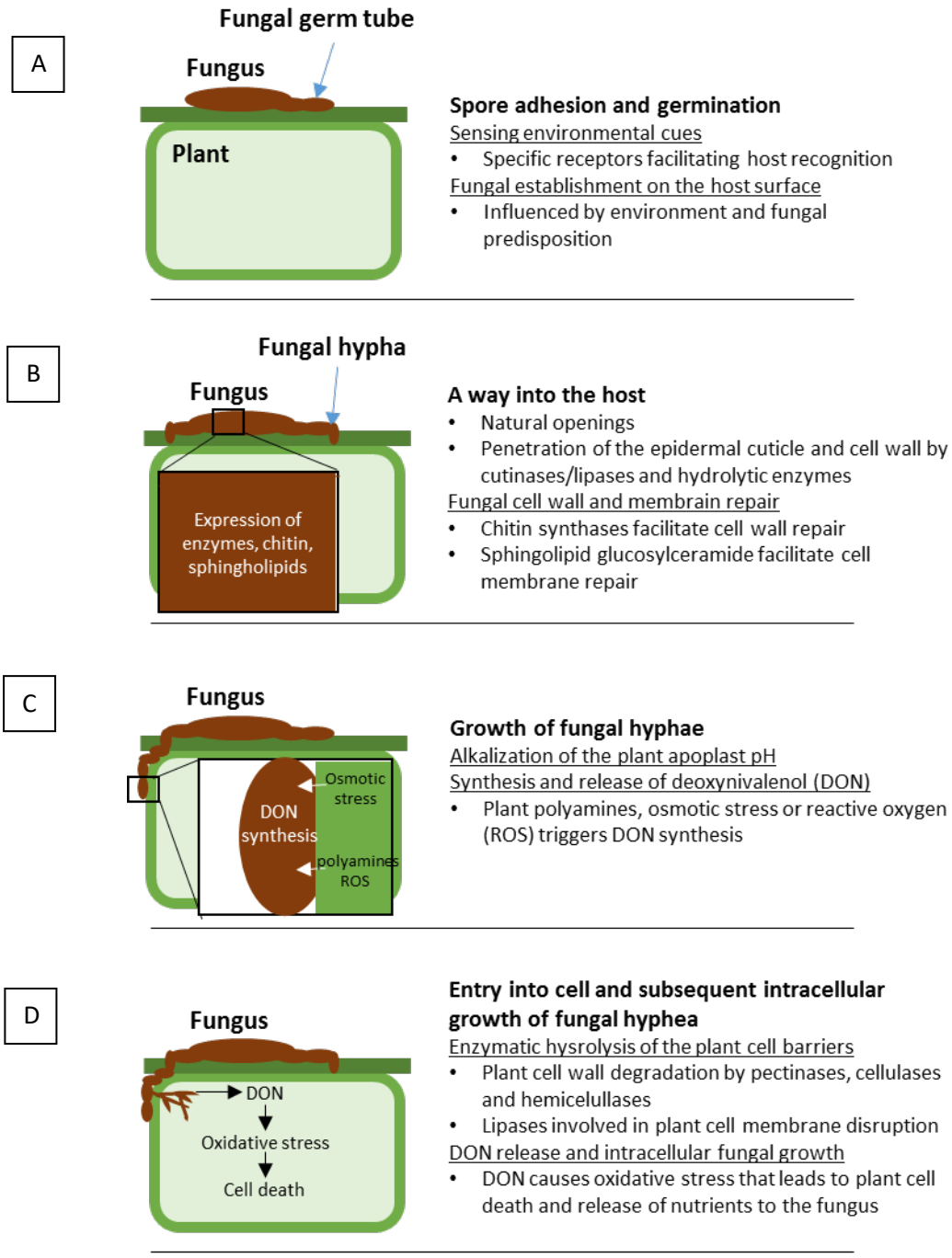

Figure I 1: Model of the FHB infection in cereal hosts.
The model presents *Fusarium* spore adhesion and germination (A), invasion of the host (B), intercellular growth of fungal hyphae (C) and entry and growth of the fungus in the cell (D) (Modified after Walter et al. (2010)).

Subsequently, *Fusarium* fungi are able to invade the floret either through natural openings like stomata or actively by penetration using short infection hyphae. Hydrolyzing enzymes, secreted by *Fusarium*, are most likely involved in penetration. After hydrolysis of the cuticle with cutinases/lipases (Figure I 2; B), *Fusarium* hyphae grow intercellular during the first 2 days after spike infection. Cereal infection

is started with pectin-degrading enzymes released by *Fusarium* that degrade the middle lamella and cell wall. Pectin-degrading enzyme activity enables the degradation of other cell wall polysaccharides by hemicellulases and cellulases. Additionally, *Fusarium* release elicitors that direct repair of the fungal membrane and cell wall-like chitin synthases helping with cell wall repair or sphingolipid glucosylceramide synthase producing sphingolipids for cell membrane repair. Following cell penetration, *Fusarium* may spread in the apoplast, leading to cell death (Walter et al., 2010). One of the mycotoxins produced by both *F. culmorum and F. graminearum* is deoxynivalenol (DON), which belongs to type II trichothecenes. Trichothecenes block protein synthesis in eukaryotes by binding the 60S ribosomal subunit, inhibiting polypeptide chain elongation and preventing chain termination (Mirdita et al., 2015). DON contributes to damage to the ribosomes, chloroplasts, and plasma membranes, triggering hydrogen peroxide production and causing cell death in cereals. *Fusarium* also releases lipases, proteases, and carbohydrate-degrading enzymes to release plant cell compounds, serving as fungal nutrients (Figure I 2; C and D) (Walter et al., 2010).

1.4.1 Current and possible FHB control strategies

1.4.1.1 Chemical control

There are few FHB control strategies like chemical control, irrigation management, or genetic resistance to protect small-grain cereals. Fungicides play an essential role in the FHB disease management strategy. The most common fungicides used against FHB are demethylation inhibitors (DMI). Their mode of action is focused on one specific target, cytochrome P450 lanosterol C-14α-demethylase (CYP51), involved in ergosterol biosynthesis. This sterol is a crucial component of the fungal cell membrane, responsible for PM permeability, fungal growth, and virulence. However, it is impossible to obtain full protection against FHB with DMI treatment, resulting from additional copies of CYP51 gene in *F. greaminarum* genome that provides a higher level of resistance of this pathogen compared with others. *FgCYP51B* encodes the enzyme primarily responsible for sterol 14α-demethylation (Machado et al., 2018). *FgCYP51A* encodes a sterol 14α-demethylase and may compensate for the disruption of *FgCYP51B* function, moreover is also responsible for variation in sensitivity to different azoles. *FgCYP51C*, is a *Fusarium*-specific *CYP51* gene and is required for full virulence on host wheat spikes (Fan et al., 2013). Under field conditions, the efficiency of fungicides may be highly variable and often insufficient (Shah et al., 2018). Their application to control FHB is also not trivial since the plants' chemical treatment must be applied during its highest sensitivity to FHB (before flowering). However, cereal spikes do not always flower synchronously. That is why multiple treatments are required, which raises the cost and makes chemical treatment more laborious (Machado et al., 2018).

1.4.1.2 Genetic control

The most cost-effective way to control FHB is by breeding for resistance, even though it is a slow and complex process, as the inheritance of the trait is controlled by multiple quantitative loci and depends on environmental factors like temperature or humidity (Machado et al., 2018). Many studies were conducted to reveal QTL responsible for this trait, using different molecular markers (Arruda et al., 2016; Kollers et al., 2013). The finding of such QTL allows breeders to combine QTL against pathogens like *Fusarium* in one cultivar (Kosova et al., 2009). However, it can be difficult because additional genes carried by QTL negatively impact the other features. An example is a negative association between some dwarfing alleles like Reduced height-D1 (Rht-D1), giving plants higher resistance to lodging but the same decreasing FHB resistance (Buerstmayr & Buerstmayr, 2016; Herter et al., 2018). An explanation of such association would be the indirect resistance mechanisms of tall plants, which have a different microclimate in the ear and a bigger distance between spikelets (Buerstmayr et al., 2000). Nevertheless, the second dwarfing allele, Rht-B1b, has similar effects on plant height, is less affecting FHB severity (Buerstmayr & Buerstmayr, 2016). That would indicate a different mechanism than the passive resistance of this phenomenon.

So far, only moderate wheat FHB resistance has been achieved, although more than 50 QTL were discovered until 2017 (Machado et al., 2018). The most prominent source of FHB resistance is taken from the Chinese cultivar Sumai-3. The major QTL from this cultivar, *Fhb1,* restrains the spread of infection in the wheat spike and provides resistance to deoxynivalenol by mycotoxin detoxification (Lemmens et al., 2005; Machado et al., 2018). *Fhb1* was confirmed in various genetic wheat backgrounds, and the QTL explains 20-40% of phenotypic variation. Another identified QTL is *Qfhs.ifa-5A*. This QTL accounts for 23% of phenotypic variation in the mapping population. However, the introgression of both QTL into spring wheat lines gave only a 10% reduction of the FHB disease for each QTL (Miedaner & Korzun, 2012). These QTL are rarely used in Europe because of their linkage with increased lodging and smaller yield (Steiner et al., 2017). The situation in barley looks even worse as only a few QTL with small effects have been identified (Machado et al., 2018; Massman et al., 2011). To overcome the negative drag effects of the genes carried in the QTL intervals, a candidate-gene association mapping may also be performed, taking into consideration markers in genes involved in wheat resistance against FHB (Slominska-Durdasiak et al., 2020).

1.4.1.3 Genetically modified plants

Another important strategy can be using genetically modified (GM) plants with a more efficient response to the FHB (Yu et al., 2017). One of the possibilities for obtaining plants with higher resistance is the overexpression of defense response genes. For example, the transgenic wheat overexpressing the defense response genes α-1-purothionin, thaumatin-like protein 1, and β-1,3-glucanase provide a resistance level above the one present in controls (Mackintosh et al., 2007). Another example of such

a strategy is the overexpression of a gene called WFhb1-1. Although still in dispute, this candidate gene may be responsible for FHB resistance provided by the QTL Qfhb1. Overexpression of this gene in wheat lacking Qfhb1 resulted in a significant decrease in *Fusarium*-diseased kernel rate and DON content in harvested kernels (Paudel et al., 2020). An alternative GMO strategy would be to silence susceptibility genes. For example, disruption of the potential susceptibility gene to FHB, *TaHRC*, encoding a putative histidine-rich calcium-binding protein suspected of being responsible for QFhb1-mediated resistance to FHB, resulted in increased wheat FHB resistance (Su et al., 2019). Another possible strategy is to modify the systemic resistance. For example, wheat expressing *Arabidopsis thaliana* gene *NPR1* (*AtNPR1*), which regulates systemic acquired resistance activation, showed higher resistance to FHB, likely due to faster activation of defense response in FHB-challenged wheat (Makandar et al., 2006). Moreover, GM plants that would inhibit the expression of crucial fungal genes by transfer of RNA molecules from plants to the pathogen in the phenomenon called host-induced gene silencing (HIGS) is also a promising strategy (see next chapter) (Jiao & Peng, 2018; Nowara et al., 2010; Shahid et al., 2018; Wang et al., 2016; Zhang et al., 2016).

1.5 Host-induced gene silencing (HIGS)

Host-induced gene silencing (HIGS) allows the development of plants that can silence essential fungal genes, thereby increasing plant resistance. HIGS is a mechanism based on RNA interference (RNAi) and occurs between two organisms. One organism produces RNA molecules that can be transported subsequently to the other organism to reduce transcript abundance of the target gene(s). This phenomenon was reported to work against various pathogens like nematodes (Huang et al., 2006), fungi (Nowara et al., 2010), and insects (Han et al., 2017). Transgenic *Arabidopsis thaliana* plants expressing dsRNA, targeting gene 16D10 of *Meloidogyne incognita*, showed a 90% reduction in the number of feeding structures of nematodes compared to the vector-transformed lines (Huang et al., 2006). HIGS was shown to be also effective against insects. Transgenic cotton plants, silencing a molt-regulating transcription factor gene of the lepidopteran pest *Helicoverpa armigera*, were shown to cause high larval mortality. The newly hatched larvae, third or fifth instar larvae of *H. armigera* eating the transgenic plant, had deformations in pupae and at the adult stage (Han et al., 2017). The phenomenon of HIGS can also be used against fungi. In 2010, HIGS of the two *Blumeria graminis* 1,3-β-glucanosyltransferases, *GTF*1 and *GTF*2, upregulated during early stages of infection, inhibit fungal development (Nowara et al., 2010; Pliego et al., 2013). Experiments using virus-induced gene silencing showed that silencing of *GTF*1 strongly reduced initial haustorium formation, whereas silencing of *GTF*2 reduced the elongation of secondary hyphae of *Blumeria graminis* f. sp. *tritici* on wheat (Nowara et al., 2010). Similarly, transgenic barley plants, silencing *Blumeria graminis* f. sp. *hordei GTF*1 gene, were more resistant to the pathogen (Nowara et al., 2010). The other example of HIGS against fungi

was provided by stable transformed *Arabidopsis thaliana*, silencing the three *CYP51* genes of *Fusarium graminearum*, taking part in fungal ergosterol biosynthesis (see above). Fungal growth in transgenic *Arabidopsis plants* was restricted almost entirely (Koch et al., 2013). Again this phenomenon was shown to work against fungi by using transient-induced gene silencing (TIGS) single-cell assay in the barley – *Blumeria graminis* f. sp. *hordei* interaction. Fifty *Blumeria* effector candidates (BEC) were screened, and eight contributed to infection with the highest value for BEC1011, reducing infection by almost 70%, compared to the control. BEC1011 intervenes in pathogen-induced cell death (Pliego et al., 2013). It was also shown that stable transgenic wheat plants carrying a construct silencing the β-1, 3-glucan synthase gene *FcGls1* of *F. culmorum* exhibit enhanced resistance to the fungus (Chen et al., 2016). On the other hand, there are systems in which cross-kingdom RNAi could not be confirmed (Kettles et al., 2019). dsRNA applied in-vitro, or RNA molecules produced by VIGS wheat plants targeting crucial *Zymoseptoria tritici* genes did not result in reduced disease levels. That may be explained by incapability or inefficiency in taking up exogenous RNA molecules (Kettles et al., 2019). Even though the HIGS phenomenon seems to be promising in pathogen control, it may not work in each pathosystem, possible due to the lack of canonical RNA-silencing machinery in some fungal pathogens (Hudzik et al., 2020).

1.6 Natural HIGS phenomenon

With the discovery of the HIGS phenomenon caused by a transgene, a question appeared if a naturally occurring HIGS exists. Indeed, HIGS has been shown to operate in various interactions between organisms, including plants and fungi (Zhang et al., 2016). For example, *Botrytis cinerea*, causing the gray mold disease, delivers small RNAs (sRNAs) into *Arabidopsis* and tomato to silence genes involved in their defense. However, these plants can also produce sRNAs targeting the *Botrytis* genes *Bc-DCL1* and *Bc-DCL2*, impeding fungal development and virulence (Wang et al., 2016; Weiberg et al., 2013). Several other cases of cross-kingdom RNAi between plant and fungi were reported. Cotton (*Gossypium sp*.) plants transfer microRNAs to *Verticillium dahlia* to reduce transcript abundance of genes contributing to fungal virulence (Zhang et al., 2016). There is also an example of the transport of the sRNAs from the parasitic plant *Cuscuta campestris* to hosts such as *Arabidopsis thaliana* or *Nicotiana benthamiana* (Shahid et al., 2018). Other examples are the defense response of the *Arabidopsis thaliana* to the infection of *Phytophthora capsici* by siRNAs generation from pentatricopeptide repeat (PPR) encoding genes (Hou et al., 2019), and suppression of host immunity of mammalian cells by miRNAs produced by *Heligmosomoides polygyrus* (Buck et al., 2014). It seems that the exchange of small RNAs between organisms may be a common way to manipulate defense response (Wang et al., 2017).

1.6.1 **Spray induced-gene silencing**

Introducing long double-stranded RNA (dsRNA) and sRNA that target essential pathogen genes by spraying on the plant surface is known as Spray-Induced-Gene Silencing (SIGS). The mechanism that underlies this phenomenon is still not well understood. It was demonstrated that both dsRNA and sRNA could effectively silence the fungal genes' expression when sprayed on the barley leaves, subsequently infected with *Fusarium graminearum* (Koch et al., 2016). It was also shown that long dsRNA, just as well as pre-digested with RNase III, could reduce the target gene expression and inhibit *Botrytis cinerea* virulence on fruits, vegetables, and flower petals (Wang et al., 2016). Thus, it is still unknown in which form RNA molecules are transported from the plant to the pathogen. Fungi can likely process long dsRNA using their own silencing machinery; therefore, both long dsRNA and sRNA may be efficient in silencing the targeted mRNA (Koch et al., 2016; Wang et al., 2016). The interaction between *Arabidopsis thaliana* and *Botritis cinerea* demonstrated that the majority of sRNA produced in a plant is transported through exosome-like extracellular vesicles. However, the process seems selective, as some of the most abundant sRNA produced by the plant are not present in the fungal protoplast, while some lowly abundant ones can be detected in the pathogen's cells. Approximately 75% of the *Arabidopsis* sRNAs transported to *B. cinerea* could be detected in vesicles, where they are thought to be protected from nuclease activity (Cai et al., 2018). The remaining sRNA, not detected in vesicles, may be transported to the fungus in a different way.

As already mentioned, the process of HIGS is not entirely understood. A closer look into the silencing and secretory pathways of plants may reveal which plant genes are involved in the HIGS mechanism and, eventually, to use some of these genes to increase HIGS efficiency and FHB resistance.

1.6.1.1 HIGS and SIGS to control FHB

SIGS application would be an option to control FHB and other diseases caused by different pathogens. The benefit of such an approach would be avoiding the problems associated with public acceptance of the GMO approach and applying synthetic chemistries. Still, many technical issues have to be first overcome, like longevity of dsRNAs, production costs, and application method (Machado et al., 2018). The instability of naked dsRNA is one of the most significant drawbacks of SIGS. However, loading dsRNA on degradable, non-toxic, layered double hydroxide (LDH) nanosheets protects it from washing away by increasing the adhesion to the leaf surface. The negatively charged dsRNA binds to the positively charged nanosheet. Carbon dioxide and moisture are slowly reacting with LDH leading to the release of dsRNA. Such dsRNA loaded on LDH nanosheet can be detected 30 days after application (Machado et al., 2018; Mitter et al., 2017). RNA production cost is still an obstacle. A few years ago, the production of a gram of RNA, sufficient for treating a small field, cost more than $100 000. Nevertheless, new technologies are addressing the decrease in this price. Some companies aim to produce RNA for less than $2 per gram (Machado et al., 2018; Page, 2017).

Using HIGS or SIGS for pest control in the field may bring several advantages. Using this kind of control may reduce or completely replace the application of multiple fungicides. As based on nucleic sequence-similarity, the target specificity of the RNAi pesticides is much higher than those of the chemical agents, nevertheless able to target multiple pathogens by using a common target sequence. At the same time, designing an RNAi protection strategy is still a highly empirical process due to significant variations of efficiency that depend on the target sequence and construct design, amenability of the different pathogen species and population to RNAi, and environmental factors (Hudzik et al., 2020; Machado et al., 2018). Some important questions concerning the application of RNAi pesticides are still open. The persistence and movement of the dsRNA and sRNA in the environment are not well studied, and the potential consumption related toxicity and side effects are still unknown.

1.7 Silencing and unconventional protein secretion pathway in plants

Recent reviews summarize the current knowledge about different components of the HIGS machinery (Hudzik et al., 2020; Wang & Dean, 2020), but a precise understanding of which elements of plant silencing and secretory pathway are involved in sRNA trafficking is still missing. Both pathways are complex and involve many genes. Systematic RNAi-based functional studies may help clarify these mechanisms and answer the question of how the RNA molecules are transferred across the kingdoms.

1.7.1 The RNAi silencing pathway in plants

RNAi typically begins with the introduction of double-stranded RNA (dsRNA) into the cell. dsRNA or RNA hairpins are recognized and cleaved by ribonuclease III (RNAse III) into small double-stranded RNAs (sRNAs): siRNAs or miRNAs, which are usually 20-25 nucleotides long (Bologna & Voinnet, 2014; Borges & Martienssen, 2015; Iki et al., 2012; Majumdar et al., 2017; Sinha, 2010). miRNA and siRNA are processed from a single-stranded hairpin RNA precursor or dsRNA, respectively (Zhu et al., 2019). miRNA precursors usually give rise to a single duplex, whereas siRNA precursors are a source for multiple duplexes (Moran et al., 2017). Genes encoding miRNAs are transcribed by RNA Polymerase II (Pol II) that are processed into a stem-loop structure. Longer Pol II-derived hairpins, termed hairpin-derived siRNAs, might originate from inverted repeats. These hairpins might evolve into miRNAs. Natural-antisense siRNAs are produced from dsRNAs originating from overlapping transcription or highly complementary transcripts originating from different loci. The precursors of secondary siRNAs are transcribed by Pol II and may originate from non-coding loci, protein-coding genes, and transposable elements. They are divided into trans-acting siRNAs, phased siRNA, or epigenetically-activated siRNA. Heterochromatic siRNAs may be derived from transposable elements and repeats located at pericentromeric chromatin (Borges & Martienssen, 2015).

Arabidopsis Dicer-like 1 (DCL1) is involved in miRNA generation in two cycles: pri-to-pre-miRNA and pre-to-mature-miRNA processing when Dicer-like 2 (DCL2), Dicer-like 3 (DCL3) and Dicer-like 4 (DCL4) are generating siRNAs. DCL3 is involved in transcriptional gene silencing (TGS), mediated by 24-nt siRNAs. DCL4 mediates posttranscriptional gene silencing (PTGS) by 21-nt siRNAs and DCL2 acts in TGS, and PTGS mediates by 22-nt siRNA (Bologna & Voinnet, 2014). All siRNAs from plants have to be modified at the 3'-end to confer stability and protection against uridylation, being a signal for degradation. This process is called 2'-O-methylation and is done by HUA ENHANCER 1 (HEN1) (Bologna & Voinnet, 2014; Borges & Martienssen, 2015). sRNA is always composed of two strands, a passenger and a guide. The guide strand of double sRNA is loaded into an RNA-induced silencing complex (RISC), which makes it recognize complementary mRNA and cleave it through the action of Argonaute protein (Ago), a component of the RISC complex. *Arabidopsis* genome has ten *AGO* genes, which usually contain four major domains: variable N-terminal domain and highly conserved PAZ, MID, and PIWI that are responsible for the correct positioning of single-stranded RNA (ssRNA) to its target. The assembly of plant AGO1-containing RISC is dependent on chaperone heat shock protein 90 (HSP90) and cyclophilin 40 (CYP40). These two proteins and F-box protein (FBW2) regulate AGO1 loading/chaperoning and are part of the control mechanism enabling AGO1 to have stable levels under stress conditions. Transcripts targeted independently by two 21-nucleotide miRNAs or by a single 22-nucleotide miRNA can initiate secondary RNA production from the mRNA. Such a cleaved transcript may be a template for dsRNA synthesis by RNA-DEPENDENT RNA POLYMERASE 6 (RDR6) aided by SUPPRESSOR OF GENE SILENCING 3 (SGS3) (Bologna & Voinnet, 2014; Borges & Martienssen, 2015; Iki et al., 2012; Majumdar et al., 2017; Sinha, 2010). A model of RNA interference in pathogen-infected plant cells is presented in Figure I 3.

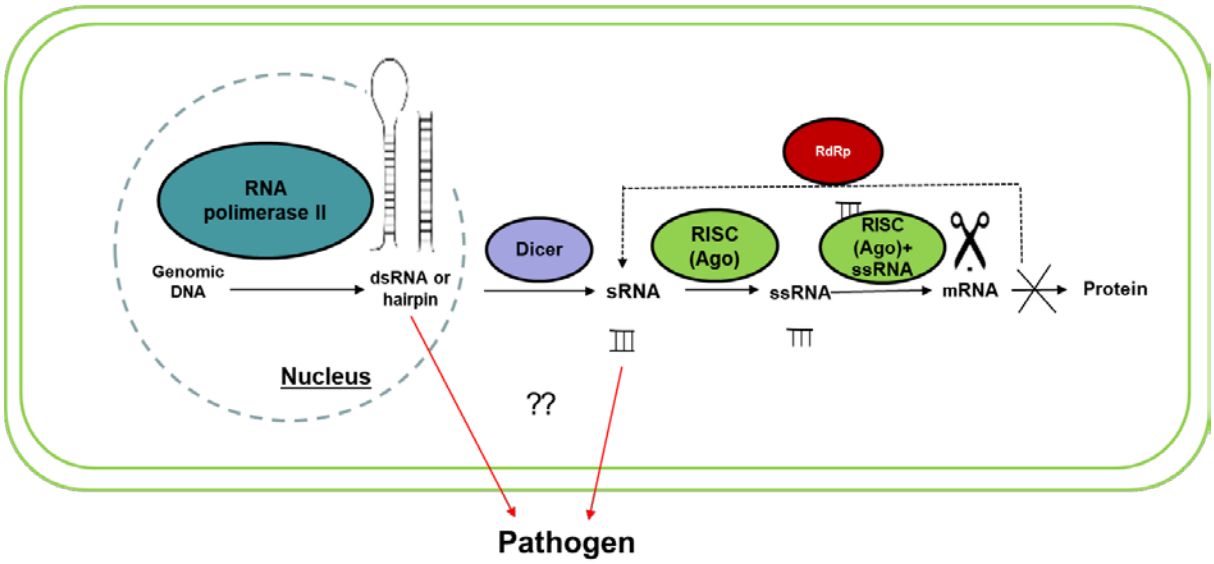

Figure I 2: Model of RNA interference in pathogen-infected cells.
Genomic DNA is transcribed by RNA polymerase II (Guilfoyle & Dietrich, 1987), and dsRNA or hairpin is created. RNase III, such as Dicer, processes these precursors into small double-stranded RNA. The passenger strand of sRNA is eliminated, and the guide single-stranded RNA associates with Ago, directing the RISC complex to bind the target mRNA, resulting in transcript degradation. Unbound siRNA may bind to complementary mRNA and promote the synthesis of new dsRNA through the action of RNA-dependent RNA polymerase (RdRp). The new dsRNA is cut again into sRNA by RNase III (sRNA amplification). RNA molecules are exported from plant cell to the pathogen, where they can silence the expression of its genes (From: Nunes and Dean (2012), modified).

1.7.2 The secretory pathway

The secretory pathway is crucial during cellular growth and development and response to biotic and abiotic stresses (van de Meene et al., 2017). Recent research suggested a role of extracellular vesicles in the sRNA transport from *Arabidopsis thaliana* to *Botrytis cinerea* (Cai et al., 2018; Hudzik et al., 2020) and *Phytophthora capsici* (Hou et al., 2019; Hudzik et al., 2020). In conventional protein secretion (CPS), cargo proteins possess an N-terminal leader sequence; they are post-transcriptionally modified and directed at the *Trans*-Golgi network (TGN) to the PM in secretory vesicles (van de Meene et al., 2017). The unconventional protein secretion (UPS) pathway differs from the CPS pathway enabling proteins lacking a signal peptide to reach the cell exterior (Robinson et al., 2016; van de Meene et al., 2017).

Especially interesting concerning this work is the unconventional protein secretory pathway, as it is supposed to be the pathway responsible for RNA transfer. It was shown that in humans, exosomes selectively load mRNA and miRNA from the cytosol into the lumen of the intraluminal vesicle (ILV) of the multivesicular bodies (MVB) (Robinson et al., 2016; Valadi et al., 2007). In plants, during oomycete infection, MVBs accumulate near the structure penetrating the cuticle and epidermal cells, called penetration peg, and MVBs then can fuse with haustoria (Bozkurt et al., 2014; Robinson et al., 2016). Two siRNAs, silencing target genes in *P. capsici*, were cargos of extracellular vesicles (EVs) in *A. thaliana*

(Hou et al., 2019; Hudzik et al., 2020). Finally, the release of the EVs at the infection sites of *B.cinerea* by fusion of MVBs with PM was shown using electron microscopy (Cai et al., 2018).

UPS in plants can be mediated by MVB or exocyst-positive organelles (EXPO). In UPS mediated by MVB, it seems that MVBs develop out of TGN in the process of maturation in which endosomal sorting complexes required for transport (ESCRT) proteins are involved (Robinson et al., 2016; Scheuring et al., 2011). The possible mechanism behind forming ILVs in MVB is invagination through (ESCRT)III. The action of AAA-type ATPase Vps4 enables the release of ESCRTs from the MVB membrane. LYST-interacting protein 5 (LIP5) is a positive regulator of MVB biogenesis. The alternative proposed ILV formation mechanism would be ceramide-induced MVB invagination (Robinson et al., 2016). Transport vesicles can only fuse with the target membrane if both membranes, vesicles and targeted ones, have the proper soluble N-ethylmaleimide-sensitive factor attachment protein receptors (SNAREs). SNAREs, called tethering factors, help the vesicle to find its targets by exposing tSNAREs. They also regulate the SNARE complexes assembly together with SM (Sec1/Munc18) proteins. In response to *Blumeria graminis f. sp. hordei*, PM-located SNAREs: PENETRATION1 (PEN1, also known as AtSYP121), ROR2 (required for mlo-specified resistance 2) and AtSNAP33 (barley orthologue HvSNAP34) were accumulated in the papillae of barley and *Arabidopsis*. It was observed that only Rab GTPase, ARA6 labeled MVBs are accumulating at the attack site, but not the one labeled with other Rab GTPases like Ara7 or Rha1 (Ding et al., 2014a). GTPase RABG3c after oomycete infection is found not as usual in late endosomes and tonoplast, but at the extrahaustorial membrane, resulting from the fusion of MVBs with the PM (Bozkurt et al., 2014; Robinson et al., 2016). It was presented that TETRASPANIN8 (TET8)-associated vesicles are secreted to the infection sites of *Botrytis cinerea* (Cai et al., 2018). It seems that ARA6 is associated with the outer membranes of MVB that fuse with PM and remain there (Cai et al., 2018).

The other UPS pathway involves exocyst-positive organelles (EXPOs) that can also take part in the sRNA transport. The fusion of EXPO with PM was shown by using electron microscopy (Ding et al., 2014b). EXPO is a double-membrane-bound organelle that consists of eight proteins: Exo70, Exo84, Sec3, Sec5, Sec6, Sec8, Sec10, and Sec15. In *Arabidopsis*, only Sec6 and Sec8 are single-copy genes. For example, Exo70 exists in 23 paralogs in *Arabidopsis* genome (Robinson et al., 2016). AtExo70E2 was shown to be a key player in exocyst complex formation (Ding et al., 2014b). The role of EXPOs in the plant can be more diversified than the known ones in yeast and mammals. EXPOs may play roles in plant defense and cell wall biosynthesis. *Arabidopsis* EXO70 isoforms take part in biotic interactions. *Arabidopsis* knock-out mutant studies show that *Exo70B2* gene takes part in the host and non-host defense response of the plant to the pathogens (Pecenkova et al., 2011). The potential model demonstrating putative RNA molecules secretion is presented in Figure I 4.

1.7.3 **Plant cytoskeleton**

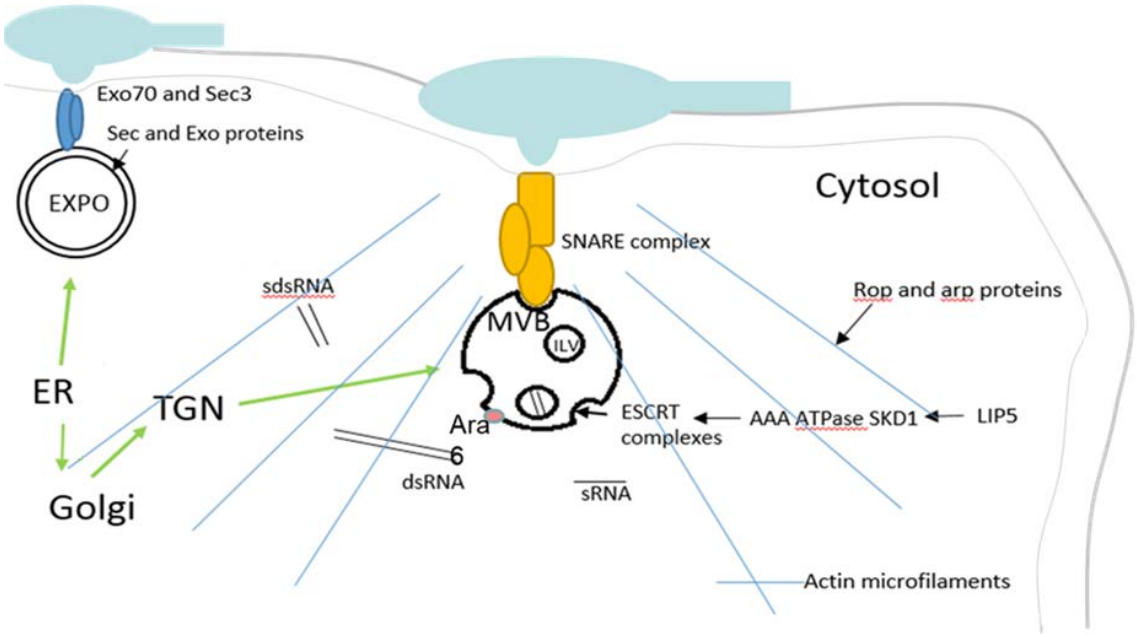

Figure I 3: Potential pathways involved in RNA molecules transport from plant cell via UPS. Putative proteins that may be important in RNA molecules transport from plant cell are highlighted (modified after Ding et al. (2014a)).

Plant cytoskeleton, which consists of microtubules (MTs) and actin microfilaments, plays a key role in penetration resistance, often based on their role in forming the cell wall appositions or papilla representing a chemical and physical barrier against the pathogen. It was shown for a wide range of plant-fungal interactions that the localized reinforcement of the plant cell wall depends on the plant cytoskeleton, and it is characterized by the secretion of antimicrobial compounds and site-directed deposition of callose at the infection site. Alteration of MTs organization leads to the increased transport of cellular components to the site of the attack (Park et al., 2018; Schmidt & Panstruga,

2011). MICROTUBULE-ASSOCIATED PROTEIN 65-3 (MAP65-3) affects MT depolymerization and defense against powdery mildew (Park et al., 2018). The network of MTs delivers cell wall components and likely other defense agents. It is also possible that MTs are involved in the release of exosomes.
Other groups of proteins impacting plant defense responses are ACTIN DEPOLYMERIZING FACTORS, which control the actin microfilaments network (Park et al., 2018) and Arp2/3 complex regulating actin dynamics depending on the presence of complex activators (Frank et al., 2004). It was shown that actin arrays are involved in forming cell wall appositions at the fungal penetration site (Hardham et al., 2007; Opalski et al., 2005; Park et al., 2018).The MLO (Mildew resistance locus O) protein and potential susceptibility factor RACB modulate actin polarization during barley-powdery mildew interaction. RACB proteins belong to the barley RAC/ROP protein family, playing a role in MLO-mediated susceptibility to *Blumeria graminis sp. hodrei*. The knockdown of this protein caused actin focusing, whereas the active form of RACB antagonized this process (Opalski et al., 2005). Barley plants bearing *mlo* null-alleles exhibited the same action pattern as *racb* plants. Such plants showed polarized actin filaments towards the attempted penetration site of *Bgh* and increased defense against *Bgh* (Park et al., 2018).

1.8 Association mapping

Identifying the link between natural or induced genetic polymorphism and phenotypic differences between individuals is of fundamental interest. One way to accomplish this is to perform linkage mapping based on biparental populations (Korte & Farlow, 2013). Another possibility is genome-wide association studies (GWAS), which use historical recombination in genetically diverse populations (Korte & Farlow, 2013). If relevant genes are known, allele mining can identify advantageous gene variants (Buschges et al., 1997; Herter et al., 2018; Slominska-Durdasiak et al., 2020) and use this information to develop molecular markers for marker-assisted selection (MAS). MAS offers the possibility of reducing selection costs in breeding by providing the ability to select with high precision at a very early stage of development. MAS has been successfully used in practical breeding, e.g., for *mlo* against barley powdery mildew or for the wheat rust resistance genes *Lr34* and *Yr36* (Miedaner and Korzun 2012). MAS is particularly attractive when trait detection is time-consuming or expensive (e.g., DON content), the trait is dependent on a particular environment or plant stage, or the goal is to pyramid a few traits together or multiple QTL for a single trait (Miedaner and Korzun 2012).

1.8.1 Linkage mapping

Linkage mapping allowed identifying many broad-spectrum resistant loci and QTL for FHB resistance (Buerstmayr et al., 2009; Miedaner et al., 2012; Waldron et al., 1999). However, limited genetic variation and the considerable amount of time and money needed to develop the experimental populations are evident drawbacks of such a strategy (Korte & Farlow, 2013).

The majority of studies aiming to reveal the QTL for FHB resistance in wheat are based on visual FHB symptoms (Buerstmayr et al., 2009). Sometimes they were performed with a limited population size of the biparental population (Arruda et al., 2016). In a few mapping experiments, mycotoxin contamination was measured. Nevertheless, such analyses are performed relatively rarely due to the associated high costs (Buerstmayr et al., 2009). A QTL with a strong effect, called *Fhb1*, appears in many studies. It is derived from spring wheat from Asia, Sumai3 (Hao et al., 2012). However, the use of this QTL brings difficulties in getting rid of adverse pleiotropic effects or linkage drag (Mirdita et al., 2015). Nowadays, biparental populations are also used to validate the results obtained, e.g., in association mapping, which often gives false-positive results. It was shown that only 33% of the marker-trait associations detected in GWAS approaches could be confirmed in validation studies (Luders et al., 2016; Navara & Smith, 2014).

1.8.2 Genome-wide and candidate-gene association mapping

There are two broad categories of association mapping, depending on the scale and the focus of the study. The first one is candidate-gene association mapping (CG), in which the polymorphisms in the gene of interest, supposed to have a role in phenotypic variation, relate to a specific trait. The second one is genome-wide association mapping (GWAS), in which the genetic variations in the whole genome are used to find associations with a trait (Zhu et al., 2008). In the CG approach, the selection of relevant candidates may be based on the information from genetic or biological studies and literature (Zhu et al., 2008). So far, this approach was rarely used in wheat for finding correlations to the FHB severity (Slominska-Durdasiak et al., 2020), even though it was shown to have mostly high statistical power in other systems (Amos et al., 2011). It was shown, particularly for infectious diseases like tuberculosis, that the CG approach tends to have greater statistical power than GWAS, nearly independent of the markers number used in the study (Amos et al., 2011).

GWAS was used to identify markers associated with FHB resistance. In 2011, Miedaner et al. found chromosomal regions impacting FHB resistance among 455 European breeding lines. In 2013, Kollers et al. identified almost eight hundred significant associations between SSR-loci and FHB severity. In 2015, Jiang et al., using 782 SSR, 9k SNP, and 90K markers, genotyped European wheat varieties, and detected several significant marker-FHB severity associations. In 2016, Arruda et al. performed GWAS on 273 wheat breeding lines from the United States, identifying 19992 SNPs significantly associated with FHB resistance. In 2019, Tessmann et al. evaluated plant height, heading date, FHB rating, incidence, severity, index, DON levels, and *Fusarium*-damaged kernels. The group used GWAS approach to find 16 SNPs associated with disease traits in a large, diverse soft red winter wheat mapping panel (Tessmann et al., 2019). In 2020, another group testing 240 leading Chinese wheat cultivars and elite lines identified five QTL, in which three were probably novel (Zhu et al., 2020). Identified markers can significantly accelerate and reduce the cost of breeding programs. However, so

far, MAS for FHB resistance in Europe was not very successful because of the absence of the major effect loci in elite germplasm (Mirdita et al., 2015).

1.8.2.1 Control for relatedness within a population

Thoughtful population selection is a crucial element to consider in association mapping studies. The resolution power of the study will be improved if more recombinations are observed. Generally, a diverse population should be considered rather than a structured one (Ibrahim et al., 2020). Variations in allele frequencies occur due to non-random mating within a species in a population structure. This is considered a limiting factor in association mapping, being the origin of false positives (Ibrahim et al., 2020). The false positive associations detected in association mapping can be limited by using several statistical methods like structured association or genomic control, where the information from random molecular markers from the genome is used to control for genetic relatedness (Zhu et al., 2008). An important step in improving statistical methodology for association mapping has been obtained by using the mixed linear model methods (Korte & Farlow, 2013; Zhang et al., 2010). Such a model can provide control for population structure and relatedness within the population and reduces the number of false-positive associations (Korte & Farlow, 2013).

1.9 Aims of the thesis

The goal of this work is to understand the mechanism of HIGS better. Candidate genes of the silencing and secretory pathways are to be tested in a transient assay to see which genes affect the production and transport of RNA molecules in barley. Additionally, candidate-gene association mapping performed in wheat may allow to find new QTL and potentially genes responsible for an FHB resistance QTL, as well as to breed for FHB resistance and potentially for HIGS in wheat.

The other aspect of this work was to explore HIGS as a naturally occurring phenomenon in barley-*Fusarium* interaction. That would further confirm the occurrence of bidirectional cross-kingdom dsRNA trafficking between fungi and plants and can lead to new, essential natural gene targets in *Fusarium.*

2. Materials and methods

2.1 Wet lab protocols

Detailed information on the chemicals, the composition of the media for the bacterial and fungal cultures, and solutions used in this work are available in Supplementary Data M1-M3. More information on the plant material employed here is provided in Supplementary Data M4. Maps/descriptions of previously made vectors used in this work can be found in Supplementary Data M5.

2.1.1 Plant and fungal material

For transient-induced gene silencing assays, the barley (*Hordeum vulgare* L.) cultivars 'Golden Promise'; 'Manchuria'; 'Ingrid'; 'Pallas'; 'Maythorpe'; 'Hanna' and the landrace 'HOR728' were used. They were grown in pots (12 cm diameter) filled with soil (from the IPK nursery) without fertilizer in a plant growth cabinet (Sanyo/Panasonic MLR-352H-PE Versatile Environmental Test Chamber, white LED upgrade; Panasonic Healthcare Co., Ltd. ,Tokyo, Japan) at 20°C, 60% relative humidity and a photoperiod of 16 h light with white light LED. The pathogen isolate *Blumeria graminis* f. sp. *hordei* (*Bgh*) CH4.8 was maintained on barley seedlings in a plant growth cabinet (Sanyo/Panasonic MLR-352H-PE; Panasonic Healthcare Co., Ltd. ,Tokyo, Japan) at 20°C and a photoperiod of 16 h. 7-9 days after seedling inoculation with *Bgh* conidia were used for detached leaves inoculation by conidia blowing inside an inoculation tower.

For virus-induced gene silencing (VIGS) assay, the spring wheat 'Apogee' was grown in pots containing soil with one dose of pellet fertilizer in a climatized greenhouse at 18°C and 16 h light. Fungicide (Capitan, Spiess-Urania Chemicals, Hamburg, Germany) and insecticide (Confidor, WG 70, Bayer CropScience, Langenfeld, Germany) treatment was given to the three weeks old plants. For plant inoculation, glycerol stock of the Dutch isolate FC46 (IPO 39-01) of *Fusarium culmorum* was spread onto PDA and kept at 20°C in a plant growth chamber (Sanyo/Panasonic MLR-352H-PE; Panasonic Healthcare Co., Ltd. ,Tokyo, Japan) 16 h with white LED lights. After 7 days of inoculation, a piece of fresh mycelium was transferred onto SNA medium, which was kept overnight in dark at room temperature (RT) and incubated under black light for 2-4 weeks. Alternatively, large-scale *Fusarium culmorum* (*Fc*) propagation of conidia was performed. Mixed seeds of wheat 'Apogee' (75 g) and barley 'Flavour', 'Hanna', 'Golden Promise', 'Morex' (75 g) were crushed and transferred to a foil bag where 60 ml of 2% malt extract solution was added. The bag was closed with a cotton plug and rubber bands, then sealed with aluminium foil. The grain – malt extract mix was then autoclaved twice at 121°C for 20 minutes. The next day, half of the week-old PDA plate colonized by *Fc* was transferred to the bag and mixed. It was stored at RT for at least 20 days till grains were colonized. The bag was then drying at 4°C in an aluminum foil on silica gel beads and was stored for half a year.

For Single Nucleotide Polymorphism (SNP) detection in candidate genes potentially taking part in HIGS mechanism and/or plant defense response, two references ('Chinese Spring' and 'Julius'), three susceptible ('Biscay', 'Florett' and 'Rubens') and three moderately resistant ('History', 'Apache' and 'Arina') wheat varieties were used. These genotypes were selected from a broad set of wheat genotypes previously evaluated for FHB resistance (Kollers et al. 2013, seeds provided by KWS LOCHOW GmbH, Bergen Germany). They were grown in pots with soil (from the IPK nursery) without fertilizer in a plant growth cabinet (Sanyo/Panasonic MLR-352H-PE; Panasonic Healthcare Co., Ltd. ,Tokyo, Japan) at 20°C, 60% relative humidity, and a photoperiod of 16 h light.

2.1.1.1 Germplasm and FHB disease resistance assessment for the candidate genes approach

The germplasm and disease assessment used in candidate-gene (CG) association mapping are described in Kollers et al. (2013). In short, the phenotypic data of 345 winter and 11 spring wheat lines from GABI wheat population, with three replicates per location, were obtained from two locations in Germany in season 2008/2009 (2009.AHL (Ahlum), 2009.CEC (Cecilienkoog)) and in the season 2009/2010 (2010.BOD (Halle-Bodenwerder) and 2010.AHL). All wheat varieties were sprayed with a mixture of *Fusarium graminearum* and *Fusarium culmorum* spores (1/3 F.g.:2/3 F.c.) in an amount of 50,000 spores per ml using 600L/ha of water volume. Inoculations with spore suspension were performed thrice with 3 days intervals, starting from a wheat stage BBCH 61 (beginning of flowering) till stage BBCH65/69 (the end of the flowering). Such an approach aimed to get at least one inoculation of wheat during its flowering time, even though it can lead to some experimental variation between early and late flowering varieties. The FHB incidence (Type I resistance) and severity (Type II resistance) were assessed as in Kollers et al. (2013).

The mapping populations of recombinant inbred lines (RILs) were used for the validation study of the results obtained in the CG approach. The populations of 100 and 48 RILs were developed from a cross between 'Apache' and 'Biscay'; and 'History' and 'Rubens', respectively. The phenotypic data of the population with two replicates were obtained from four locations based in Germany - Hohenheim, Oberer Lindenhof, Wetze, and Wohlde. The populations were evaluated by KWS LOCHOW GmbH (Bergen, Germany) for plant height, heading date, and FHB as outlined in detail in Herter et al. (2018). The populations 'Apache x Biscay' and 'History x Rubens' were genotyped in KWS LOCHOW GmbH (Bergen, Germany), and the biparental population 'Apache x Biscay' was additionally used for the genetic mapping of markers Ara6, DCL1(1), and DCL1(2).

2.1.2 DNA, RNA isolation, and cDNA synthesis

For DNA isolation, wheat tissue from eight genotypes was collected and frozen eight days after sowing and disrupted using Tissue Lyser (Qiagen, Hilden, Germany). The DNA was isolated using DNeasy Plant Mini Kit (Qiagen, Hilden, Germany) according to the manufacturer's protocol. The DNA concentration was measured with the Colibri Microvolume Spectrometer (Titertek Berthold, Bad Wildbad, Germany).

Isolation of DNA from *Bgh* was based on a modified protocol described in Zierold et al. (2005). The conidia from *Bgh* were used as a material for genomic DNA isolation. Heavily infected plants with sporulating fungal colonies were shaken over Petri dishes (Greiner Bio-One, Kremsmünster, Austria), and the collected spores transferred into Eppendorf (Hamburg, Germany) reaction vessels (~50 mg). Then, 1 ml of QBT buffer, 1 µl of Proteinase K (10 mg/ml), and 1 µl of RNAse A (10 mg/ml) were added to the harvested spores. The Eppendorf reaction vessels were inverted a few times, frozen in liquid nitrogen, and thawed in hot water twice. Subsequently, they were centrifuged for 5 minutes in Mikrocentrifuge 5417R (Eppendorf, Hamburg, Germany) (14,000 rpm, 4° C). The Qiagen-tip 20 (Qiagen, Hilden, Germany) was equilibrated with 2 ml of QBT wash buffer, and the supernatant obtained by centrifugation was loaded on the Qiagen-tip 20. The column was washed with 4 ml of QC buffer to separate the DNA bound to the anion-exchange column from the remaining constituents. Next, the DNA was removed from the Qiagen-tip 20 with 2 ml QF elution buffer into 15 ml tube (Greiner Bio-One, Kremsmünster, Austria). The DNA was precipitated with 1.6 ml of isopropanol, then centrifuged (4,600 rpm, 40 minutes) (Eppendorf Centrifuge 5810 R, Hamburg, Germany). The pellet was washed with 1 ml of 70% EtOH, and all was transferred into an Eppendorf reaction vessel and centrifuged (10 min, 14,000 rmp). The pellet was dried for 10 minutes at RT and dissolved in 10 µl of H_2O.

For total RNA isolation, plant tissue was frozen in liquid nitrogen and disrupted using Tissue Lyser (Qiagen, Hilden, Germany). The total RNA was isolated using GenUP™ Plant RNA Kit (biotechrabbit GmbH, Berlin, Germany) or using QIAzol Lysis Reagent (Qiagen, Hilden, Germany) according to the manufacturer's protocols. The RNA concertation was measured with the Colibri Microvolume Spectrometer. The trace genomic DNA in the samples was removed by DNase I (Thermo Scientific, Waltham, USA) treatment (Supplementary Data M6). The first-strand cDNA was synthesized by using the Oligo(dT)18 primer and RevertAid Reverse Transcriptase (Thermo Scientific, Waltham, USA) in 20 µl volume according to the manufacturer's protocol (detailed protocol in Supplementary Data M6) or using iScript™ cDNA Synthesis Kit (Bio-Rad, Hercules, USA) according to the manufacturer's protocol in a Biometra TAdvanced thermal cycler (Analytic Jena AG, Jena, Germany). The 7900HT fast real-time PCR system (Applied Biosystems/Life technologies, Waltham, USA) was used for the amplification and detection of fluorescent signal. A 10 µl final volume of GoTaq® Probe qPCR Master Mix (Promega, Madison, USA) in triplicates in a 384-well PCR plate (Applied Biosystems, Waltham, USA) was used for quantitative PCR (qPCR). The qPCR reaction proceeded as follows: activation of GoTaq® DNA Polymerase for 2 minutes at 95°C, followed by 40 cycles (95°C for 15 seconds; 55°C for 30 seconds; 72°C for 30 seconds). The relative quantity of the target candidate transcripts was normalized to the gene encoding translation elongation factor 1 of *Fusarium culmorum* (*Fc*EF1, accession no. JF740860.1) (Chen et al., 2016). A standard curve, based on the cDNA from FHB infected plants, was made for each

tested gene with five-fold standard dilutions. SDS2.4 software (Applied Biosystems, Waltham, USA) was used to determine transcript quantity.

2.1.3 Preparation of TOP10 competent cells

The modified method described by Hanahan (1983) was used to prepare TOP10 chemically competent cells. The glycerol stock of the One Shot™ TOP10 Chemically Competent *Escherichia coli* (Thermo Fisher, Waltham, USA) was spread on an LB plate to obtain single colonies, used to inoculate a pre-culture in 3 ml LB, incubated overnight at 37°C and 220 rpm shaking. Next, 0.6 ml of the pre-culture was used to inoculate 100 ml LB supplemented with 2.5 M $MgSO_4$ and 2.5 M $MgCl_2$ and incubated at 37°C and 220 rpm. After reaching an optical density of 0.3-0.4, the bacterial culture was transferred on ice in 50 ml tubes (Greiner Bio-One, Kremsmünster, Austria) and centrifuged in 3,000 rpm for 15 minutes at 4°C. The bacterial pellet was resuspended in buffer 1 (Supplementary Data M3), incubated for 2 hours on the ice, and centrifuged (3,000 rpm,15 min, 4°C). Pellet was again resuspended in 4 ml of buffer 2 (Supplementary Data M3). The ready competent cells were distributed to the tubes (50 µl) or micro-titer plates (20 µl) (Thermo Scientific, Waltham, USA), immediately frozen in liquid nitrogen, and transferred to -80°C, till their usage. Their competence was checked with a pUC19 vector (Invitrogen, Carlsbad, USA) by heat-shock transformation and overnight incubation at 37°C. Then the number of colonies was counted, and the efficiency was calculated (Supplementary Data M7).

2.1.4 Development of vectors for transient-induced gene silencing by particle bombardment

The sequences of the barley HIGS-candidate genes were used to design RNAi constructs using the Gateway cloning system. The RNAi-trigger sequences were amplified from cDNA obtained from three barley genotypes combined together ('Maythorpe'; 'Golden Promise' and 'Ingrid') with *Taq* PCR Master Mix Kit (Qiagen, Hilden, Germany) in 10 µl reaction using specific primer pairs (Supplementary Data M8). The touch-down PCR reaction was done in a PCR machine (Biometra TAdvanced Thermal Cycler, Analytic Jena AG, Jena, Germany) as follows: Initial denaturation for 3 min at 94°C, then 9 cycles (94°C for 30 sec, 65°C→55°C for 30 sec, 72°C for 1 minute), followed by 30 cycles (94°C for 30 sec, 55°C for 30 sec, 72°C for 1 minute) and then final extension for 10 minutes at 72°C. Subsequently, 1 µl of PCR reactions were checked on 1% TAE-Agarose gel. The rest of the PCR product was purified using MinElute 96 UF PCR Purification Kit (Qiagen, Hilden, Germany), according to the manufacturer's protocol, and dissolved in 30 µl of deionized water. Subsequently, for 6 µl reaction, 0.2 µl pCR™8/GW/TOPO vector (1-2 ng, Thermo Fisher, Waltham, USA, Supplementary Data M5) was mixed with 1 µl of salt solution (1.2 M NaCl, 0.06 M MgCl), 0.8 µl water and 4 µl purified PCR product. The TOPO cloning reaction was mixed gently and incubated at 25°C for 30 minutes, then in-house prepared chemically competent *E. coli* TOP10 cells were transformed by the heat-shock method with the

recombinant plasmid. Positive colonies were selected on 100 µg/ml spectinomycin LB agar plates. Then plasmids were confirmed by restriction analysis using FastDigest *Eco*RI (Thermo Fisher, Waltham, USA). Afterward, a Gateway LR recombination reaction between the entry clone and a destination vector pIPKTA30N (Douchkov et al., 2005) (Supplementary Data M5) was performed, combining 1 µl (150 ng) of pIPKTA30N, 2 µl of water, 1 µl of LR ClonaseR Mix II and 1 µl (150 ng) of recombinant pCRTM8/GW/TOPO vector. The reaction was incubated at RT overnight and transformed into chemically competent cells from *E. coli* strain TOP10 by the heat-shock method. The positive colonies were selected on LB agar plates with ampicillin (100 µg/ml). The presence of the sequences in the destination vector was confirmed by restriction analysis using FastDigest *Eco*RV (Thermo Fisher, Waltham, USA) and sequencing of the random samples from the plate. To avoid potential sequencing problems due to the presence of the inverted repeats, the recombinant destination plasmids were digested with FastDigest *Eco*RV (Thermo Fisher, Waltham, USA), which separates the repeats into different fragments. After confirmation, plasmid DNA was isolated using PureLink™ HiPure Plasmid Midiprep Kit (Invitrogen, Carlsbad, USA) according to the manufacturer's protocol.

2.1.5 Transient-induced gene silencing

Microprojectile bombardment was performed according to Douchkov et al. (2005) with minor changes. 27,5 mg of the gold particles (1 µm Gold Microcarriers, Bio-Rad, Hercules, USA) were washed twice in 1 ml of sterile H_20 and once in ethanol (>96%). After each washing step, the gold suspension was mixed, ultrasonicated with 35 kHz (Sonorex RK 31, Bandelin, Berlin, Germany) for 30 seconds, and centrifuged (14,000 rpm, 30 seconds), then the supernatant was removed. Subsequently, the gold pellet was dried at 50°C for 5-10 minutes in thermomixer (Eppendorf, Hamburg, Germany) and suspended in 1 ml of 50% Glycerol stock. The gold suspension was kept at -20°C until use.

The coating of the DNA was done as follows: 7 µg of pUbiGUS reporter gene (Schweizer et al., 1999) (Supplementary Data M5) was mixed with 7 µg of each construct of interest or negative/positive control, then 2.4 mg (87.5 µl) of gold suspension was added. Subsequently, calcium nitrate ($Ca(NO_3)_2$), pH 10 was slowly added to the mix to a final concentration of 0.5 M. After 25-30 minutes of incubation at RT, with inversion every 5 minutes, the suspension was centrifuged (14,000 rpm, 30 seconds, RT), and washed with 70% ethanol, and then with 96% ethanol. The gold pellet was resuspended in 32 µl of ethanol (>96%).

For biolistic transformation, leaf segments from the first leaf of seven-day-old barley plants were transferred to Petri dishes (9 cm diameter) filled with 0.5% phyto agar and 0.002% of benzimidazole and seven leaf segments were fixed with the adaxial surface up with stirrer bars on the media surface. Ethanol pre-washed macrocarriers (Bio-Rad, Hercules, USA) were fixed in a hepta-adaptor (Bio-Rad, Hercules, USA); subsequently, the resuspended gold particles were spread uniformly onto macrocarriers and allowed to dry. The PDS-1000/He model (Bio-Rad, Hercules, USA) with a vacuum of

27 mm of mercury (Hg) and a helium pressure of 900 psi was used as a biolistic particle delivery system. The distance between the targeted leaves and microcarriers was 6 cm. After particle bombardment, the leaves on Petri dishes were incubated in a plant growth cabinet (Panasonic, Tokyo, Japan) at 20°C and a photoperiod of 16 h illuminated by LEDs for three days before inoculation with *Bgh* conidia.

2.1.6 Inoculation with *Blumeria graminis* f. sp. *hordei* and GUS staining, microscopy, and statistics

The bombarded leaves were incubated for three days to deplete the products of the targeted by the RNAi construct gene. Afterward, the transformed leaves were inoculated with 150-250 conidia/mm^2 of *Bgh*. Inoculation was performed in an inoculation tower by blowing spores from heavily infected plants with pressurized air (ca. 6 bar). The number of spores per mm^2 and uniformity of spore distribution was controlled by placing microscopic slides in four different locations on the inoculation table. The infected leaves were incubated in a plant growth cabinet (Sanyo/Panasonic MLR-352H-PE, Tokyo, Japan) at 20°C and a photoperiod of 16 h illuminated by LEDs. Detection of transiently transformed epidermal cells was done by co-transformation of vector (pUbiGUS) overexpressing β-glucuronidase (GUS) reporter gene controlled by maize ubiquitin promoter. The GUS enzyme cleaves X-Gluck (5-bromo-4-chloro-3-indolyl-beta-D-glucuronic acid; Biosynth AG, Staad, Switzerland), producing colorless glucuronic acid and an intense blue precipitate of chloro-bromoindigo, easily detectable under a light microscope (Figure M 1).

The GUS staining was performed by vacuum infiltration of the leaves with X-Gluc solution, as in Douchkov et al. (2005). The reaction was made in 15 ml falcon tube and incubated for 24 hours at 37°C. Afterward, X-Gluc solution was removed, and the leaves were destained in TCA solution until complete decoloration of the chlorophyll. Then, leaves were washed thrice with water and stored not longer than a month in water at 4°C.

Microscopy was performed under Axio Scope.A1 microscope (Carl Zeiss AG, Jena, Germany) at 100X magnification. GUS-transformed cells with and without haustoria (Figure M 1) were counted in all seven leaves and subsequently used to calculate the susceptibility index (SI, number of transformed cells with haustoria / total number of transformed cells).

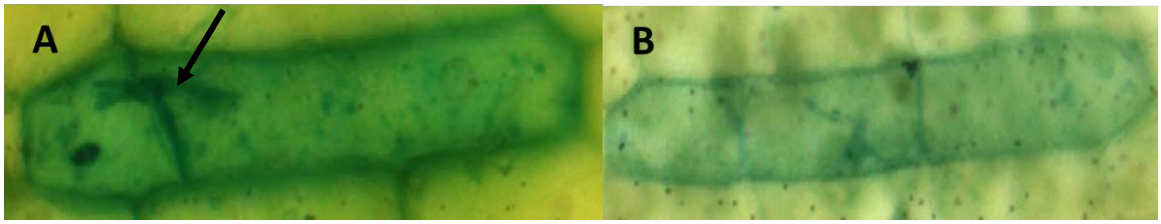

Figure M 1: Transformed cell with (A) and without (B) *Bgh* haustorium.
Haustorium marked with an arrow.

A positive (pIPKTA36, Supplementary Data M5) and three negative (pIPKTA30N) controls were also included in each experiment. The pIPKTA36 is an RNAi vector, silencing the expression of the barley *Mlo* gene and causing mlo-mediated resistance to powdery mildew. The pIPKTA30N is an empty RNAi vector. Both vectors were generated and described in detail by Douchkov et al. (2005). An experiment was considered technically successful if the number of transformed cells was above 90. A mean SI of all three negative control transformations was used for the calculation of relative SI and comparison of the experiments. The six standard barley genotypes ('Manchuria', 'Hanna', Golden Promise', 'Pallas', 'Ingrid' and 'HOR728') were tested for their susceptibility to powdery mildew. At least five independent experiments were performed for each genotype, except for 'Pallas', because of the technical issues. Moreover, the genes that potentially could serve as HIGS reporter genes (HRG) from *Bgh* were tested in 'Manchuria', later also in 'Hanna', and standard barley genotype 'Golden Promise'. At least 2 independent repetitions were performed, testing each HRG candidate.

2.1.7 Amplification of the wheat sequences

The PCR amplification of the fragments of the wheat candidate genes putatively taking part in the HIGS mechanism were done with *Taq* PCR Master Mix Kit (Qiagen, Hilden, Germany) in 35 µl reaction for eight wheat genotypes: three susceptible ones (Rubens, Florett and Biscay), three moderately resistant (History, Arina, Apache) and two references (Chinese Spring and Julius). The touch-down PCR reaction was done in PCR machine (Analytic Jena AG, Jena, Germany) as follows: Initial denaturation for 3 min at 94°C, then 9 cycles (94°C for 30 sec, 65°C→55°C for 30 sec, 72°C for 1 minute), followed by 32 cycles (94°C for 30 sec, 55°C for 30 sec, 72°C for 1 minute) and then a final extension for 10 minutes at 72°C. Subsequently, 2 µl of PCR reaction were checked on 1% TAE-Agarose gel, and the rest was purified using MinElute 96 UF PCR Purification Kit or NucleoFast® 96 PCR (Macherey-Nagel, Düren, Germany) according to manufacturer's protocols. The sequencing of the PCR products was done at the IPK Sequencing core facility using the Sanger sequencing method in 3730xl DNA Analyzer (Applied Biosystems, Waltham, USA) starting from both T3 and T7 promoter sequencing primers.

2.1.8 Virus-induced gene silencing (VIGS)

The VIGS method was used to validate the function of the sRNA target genes in *Fusarium* attacking wheat spike. Chen et al. (2016) showed that barley stripe mosaic virus-mediated transient gene silencing (BSMV-VIGS) in wheat spikes is a convenient and reliable technique to assess HIGS targets in *Fusarium culmorum*. The BSMV vectors were kindly provided by Dr. Chen (IPK). The description of BSMV-VIGS vectors introduces into the plant via *in vitro* transcription or via biolistic bombardment is described in details in Bruun-Rasmussen et al. (2007) and Meng et al. (2009), respectively (Supplementary Data M5). Shortly, for BSMV-VIGS, the heterologous sequences of interest were inserted directly downstream of the stop codon of the γb ORF, which encodes a protein involved in

viral pathogenicity (Lee et al., 2012). The candidate gene sequences were checked for off-targets in wheat and *Fusarium* species using si-Fi21 tool (Luck et al., 2019). Gene-specific primers derived from the *F. graminearum* cDNA sequences were used to amplify the target sequences from *F. culmorum* cDNA (Supplementary Data M9), which was possible because of the highly similar sequences between two *Fusarium* species. Amplified *F. culmorum* cDNA sequences were bluntly inserted into the *Sma*-I digested recombinant RNAγ of BSMV, and then the constructs with antisense-oriented insertions were selected.

2.1.8.1 VIGS via in vitro transcription

The BSMV-VIGS via *in vitro* transcription was performed as in Bruun-Rasmussen et al. (2007) with some modifications. The viral genomic cDNAs were cloned into a vector under the control of the T7 promoter and linearized by enzyme digestion. *Spe*I enzyme was used to digest plasmid containing BSMV:β, and *Mlu*I for plasmids having BSMV:α or BSMV:γ / recombinant BSMV:γ. The linearized DNA fragments were *in vitro* transcribed using AmpliCap-Max™T7 High Yield Message Maker Kit (CELLSCRIPT, Madison, USA) accordingly to the manufacturer's protocol. Then capped viral RNAs were mixed (~6 ug each construct per plant) and were rubbed into 'Apogee' wheat flag leaf with ~40 µl of FES buffer.

2.1.8.2 VIGS via Microprojectile bombardment and mechanical infection of BSMV

Biolistic bombardment of 'Black Hulless' barley plants was performed using PDS-1000/He system (Bio-Rad, Hercules, USA), according to Meng et al. (2009) with minor changes. Gold particles (Bio-Rad, Hercules, USA) were coated with all three plasmids together: BSMV:α, BSMV:β and BSMV:γ / recombinant BSMV:γ mixed in a ratio 1:1:1 (7 µg of each plasmid) and precipitated on the particle surface by dropwise adding calcium nitrate ($Ca(NO_3)_2$) under continuous vortexing. Six days old seedlings were bombarded with the DNA-coated particles using helium pressure of 900 psi, 27 mm of mercury (Hg) vacuum in the chamber, and 6 cm distance between targeted seedlings and microcarriers. Afterward, seedlings were kept for one hour in water and then transferred to pots (8 cm diameter) with soil (from the IPK nursery) without fertilizer for eight days in the growth chamber (Panasonic, Tokyo, Japan) at 22°C, 60% humidity, 16 hours of light illuminated with LEDs and at 20°C for 8 hours darkness. Eight days after bombardment, some of the barley plants developed BSMV infection symptoms (brown stripes on the first leave and chlorotic symptoms on the second one). Symptomatic second leaves were collected, weighed, and kept at -80°C until the wheat infection. cDNA obtained from the collected 'Black Hulles' leaves were used to check stability of the insert of different length in recombinant BSMV:γ that supposed to be used for VIGS experiments. cDNA was amplified using DreamTaq PCR Master Mix (2X) (Thermo Scientific, Waltham, USA) in 10 µl reaction. cDNA of all examined samples were amplified with primer pairs BSMV:gamma (Supplementary Data M9) amplifying part of BSMV:γ, which is carrying insert. cDNA from barley leaves carrying BSMV:FGSG_10970 (442), BSMV:FGSG_01104 (334) and BSMV:FGSG_06175 (495) were additionally

amplified with inserts' specific primers (Supplementary Data M9) and with the primers from inserts and BSMV γ sequence. The PCR reaction was done in a PCR machine (Biometra TAdvanced Thermal Cycler, Analytic Jena AG, Jena, Germany) as follows: initial denaturation for 2 min at 95°C, followed by 30 cycles (95°C for 30 sec, 54°C for 30 sec, 72°C for 1 minute) and then final extension for 10 minutes at 72°C. 10 µl PCR reaction was checked on 1% TAE-Agarose gel. To inoculate wheat plants with BSMV, prepared earlier leaves of 'Black Hulless' were grounded with Celite® 545 and three volumes of 0.05M phosphate buffer (pH 7.2) in a cold mortar. Four weeks old 'Apogee' plants were infected with mixed appropriate three viral parts by rubbing flag leaf with 60 µl of the extract.

2.1.8.3 *Fusarium culmorum* inoculation

Fusarium culmorum spores were diluted with 0.05% Tween-20 to 50 spores/µl and used for point inoculation of one middle 'Apogee' spikelets at the stage of early anthesis. The inoculated spikelets were labeled with a black dot and covered with a moistened, transparent plastic bag for 24 hours. FHB infection was calculated as the ratio of the blighted spikelets to the total number of spikelets per spike, five, seven, and ten days after inoculation. Spikes with no FHB symptoms were removed from the analysis. Plants were assessed as BSMV-positive phenotypically and partially confirmed using molecular biology techniques. cDNA obtained from RNA isolated from wheat spikes was amplified with primer pairs BSMV:gamma (Supplementary Data M9) in the PCR reaction, as described in the previous chapter. The insert stability throughout the entire experiment was also examined with this method, as there are reports that the virus tends to lose its insert during replication (Bruun-Rasmussen et al., 2007; Yin et al., 2011). Plants showing symptoms of BSMV were used for statistical evaluation of FHB severity.

2.1.8.4 Statistical evaluation

Relative FHB infection of each plant was normalized to corresponding mean values of control plants infected by virus strain BSMV:γ that carries the empty multiple-cloning site (BSMV:00). Then results of all experiments of each HIGS construct were combined; outliers were removed by applying the ROUT method (Motulsky & Brown, 2006) and analyzed using Wilcoxon Signed Rank Test (Wilcoxon, 1946) for not normally distributed data.

2.2 Dry lab protocols

2.2.1 Selection of HIGS candidate genes

The choice of the candidate genes for transient-induced gene silencing studies was based on the broad literature studies (Bohlenius et al., 2010; Bologna & Voinnet, 2014; Borges & Martienssen, 2015; Bozkurt et al., 2014; Cai et al., 2018; Ding et al., 2014a; Ding et al., 2014b; Du et al., 2018; Frank et al., 2004; Hardham et al., 2007; Huckelhoven, 2007; Li et al., 2004; Majumdar et al., 2017; Nagawa et al., 2010; Naramoto et al., 2014; Opalski et al., 2005; Park et al., 2018; Pecenkova et al., 2011; Robinson et al., 2016; Robinson et al., 1998; Scheuring et al., 2011; Sinha, 2010; Valadi et al., 2007; van de Meene et al., 2017; F. Wang et al., 2014; Weiberg et al., 2013; Yang & Huang, 2014; Yang et al., 2014; Zarsky et al., 2013). The genes from the plant silencing and secretory pathway, putatively involved in HIGS mechanism, were described for *Arabidopsis thaliana* or *Zea mays*. Subsequently, their orthologues in barley were selected using nucleotide and protein sequence homology search with blastx or blastp (National Center for Biotechnology Information) and ViroBLAST (Deng et al., 2007). The candidate genes from barley were divided into 28 gene families (Supplementary Data M10). Multiple sequence alignment for each gene family and selection of conservative regions was done by S. Lück (IPK). By using si-Fi21 tool (Luck et al., 2019), RNAi targets were selected in the conservative regions of each gene family by simultaneously avoiding regions that may generate putative off-targeting siRNA outside the gene families. Primers for amplifying the target regions were designed using PrimerFactoryQt v.1.0.3 program (http://www.snowformatics.com/primer-factory.html).

2.2.2 HIGS reporter gene for TIGS screening

The choice of a silencing reporter gene targeting *Bgh* transcript was based on literature data (Chen et al., 2016; Koch et al., 2013; Nowara et al., 2010; Oliveira-Garcia & Deising, 2013; Oliveira-Garcia & Deising, 2016; Pliego et al., 2013). Selected were targets previously reported to reduce *Bgh* virulence. The GTF1, GTF2, BEC1011, HO06F11 RNAi constructs were kindly provided by Dr. D. Nowara and S. Lueck (IPK). For the rest of the genes, specific primers for approx. 500 bp long amplicons were designed using the Primer3 software (Koressaar & Remm, 2007; Untergasser et al., 2012) (Supplementary Data M11). The specificity of the selected targets in the genomes of barley and *Bgh* was checked with the help of the si-Fi21 tool (Luck et al., 2019). The silencing vectors were made by using Gateway Recombination Cloning Technology, as described in Chapter 2.1.4.

2.2.3 Putative candidate genes involved in HIGS mechanism in wheat

Wheat orthologues of the barley HIGS-candidates genes were found by sequence similarity search in URGI Blatst server (https://urgi.versailles.inrae.fr/blast/) against wheat TGACv1 whole-genome shotgun assembly database of International Wheat Genome Sequencing Consortium. The specific primers (Supplementary Data M12) were designed with Primer3 software (Koressaar & Remm, 2007; Untergasser et al., 2012) to amplify 400 to 500 bp long specifics genomic regions. Primers were usually

targeted to the intron region of the gene, where the highest polymorphism between homologs was observed. The intron-exon structure of the gene was checked using Splign program comparing barley mRNA to wheat gDNA using discontiguous megablast used for cross-species (Kapustin et al., 2004; Kapustin et al., 2008). T3 and T7 sequencing tags were added to each forward, respectively, reverse primer (tag sequences are marked in red in Supplementary Data M12) to facilitate and uniform the sequencing.

2.2.4 Sequences analysis

The sequence analysis and SNPs detection in the wheat sequences were performed in SeqMan Pro (DNASTAR Lasergene7 (DNASTAR, Inc., Madison, USA)). The fragments of the candidate genes in the eight mentioned earlier genotypes were compared to each other, and polymorphisms between sequences were analyzed manually due to poor sequencing quality. Subsequently, real SNPs occurring between the genotypes were selected for further steps. DNA extraction from GABI-wheat population and biparental populations was performed in KWS LOCHOW GmbH (Bergen Germany), as described in Tinker et al. (1993). Kompetitive Allele Specific PCR (KASP) markers were developed in KWS LOCHOW GmbH (Bergen, Germany) (Supplementary Data M13) based on selected SNPs. KASP genotyping is based on competitive allele-specific PCR that enables distinguishing SNPs, and insertions/deletions (Indels) at specific loci using fluorescence resonance energy transfer (FRET) to generate a signal (Zhao et al., 2017). The target DNA region is amplified using an allele-specific forward primer (matching the target SNP) with a unique tail sequence. Then, the allele-specific tail sequence is integrated into the PCR product using a common reverse primer. The fluorometric dye-labeled oligo of the FRET cassette is complementary to the tail sequence and binds, generating a fluorescent signal by releasing fluorometric dye from the quencher (https://www.biosearchtech.com/how-does-kasp-work). The GABI-wheat population was genotyped by Illumina Technology (Illumina, San Diego, USA) with newly developed markers and a 90k iSelect chip (S. C. Wang et al., 2014). Biparental populations were also genotyped with newly developed markers by KWS LOCHOW GMBH, Bergen, Germany.

2.2.5 Association studies

2.2.5.1 Candidate-gene association mapping

TASSEL 5 program (Bradbury et al., 2007) was used to generate a centered IBS kinship matrix to minimize the genetic relatedness effects between tested genotypes. The calculation was based on a set of 79,962 markers provided by KWS LOCHOW GmbH (Bergen Germany). Candidate-based association mapping was performed fitting a linear mixed model correcting for relatedness using the centered kinship matrix in R (R Core Team, 2018). The Bonferroni correction was used for multiple testing correction to avoid false positives.

2.2.5.2 Phenotype-genotype association in a biparental population

Outliers' correction was performed on 'Apache x Biscay' and 'History x Rubens' data, and BLUEs were obtained. Markers located in candidate genes were checked for the association with FHB resistance in the 'Apache x Biscay' and 'History x Rubens' biparental populations using a nonparametric Mann-Whitney *U* test that does not require normal distributions of the data. The markers were considered significantly correlated with phenotype if $P \leq 0.05$.

2.2.6 Physical and genetic mapping, LD calculation

2.2.6.1 Physical mapping

The introduction of the new markers was done by both physical and genetic mapping. To find the exact position of the Ara6, DCL1(1), and DCL1(2) markers, the sequences of the markers were blasted to the reference genome of the wheat cultivar 'Chinese Spring' v.1.0 (IWGSC BLAST). As the sequence positions of the markers were known, the Triticeae Toolbox (T3) (Blake et al., 2016) was used to find the closest markers surrounding DCL1(1), DCL1(2), and Ara6 markers on the RefSeq v1.0 physical map. Depending on the markers' availability on the chromosome, the 10 Kbp sequence surrounding markers DCL1(1) and DCL1(2) and the 2 Mbp sequence surrounding marker Ara6 were checked. Moreover, the three markers were also checked for their distance to known FHB resistance QTL.

2.2.6.2 Linkage disequilibrium (LD) calculation

Markers that were monomorphic, or had a missing value above 20%, heterozygous in more than 20% of genotypes, or had minor allele frequency smaller than 1%, were discarded from the analysis. The LD was calculated using TASSEL 5 (Bradbury et al., 2007).

2.2.6.3 Genetic mapping

Since at the time of performing this work, the physical map of 'Chinese Spring' was still not fully available, the newly developed markers were introduced into genetic maps. What is more, genetic maps are still an important source of information for breeding companies. For this purpose, the markers were calculated *de novo* using JoinMap 4 in 'Apache x Biscay' population (treated as double haploids (DH)). A biparental population of 100 individuals was used for mapping. The population was checked for purity (cross-pollination). Heterozygous calls were changed for missing values. Among 15k SNP markers, obtained from KWS LOCHOW GmbH (Bergen Germany) tested on the parents, only polymorphic ones were taken further for analysis. Markers with more than 20% missing values were discarded, as well as genotypes with more than 20% missing values. A logarithm of odds (LOD) threshold of 6 was set for grouping. After the map computations, the inspections were made. The diagnostic was directed toward detecting erroneous observations and incorrect orderings. Post-mapping diagnostics include:

- Studying segregation distortion based on sudden changes may indicate errors caused by phenotypic observations of a locus. However, because of the linkage, segregation distortion that is caused by selection should be gradual.
- Estimating the number of recombination events in individuals under normal circumstances is in the normal range. For instance, a RIL population with 100 cM map length will show a range of up to ten recombinations per individual, while a backcross with the same map length will usually range from zero to four.
- Excluding singletons, which are phenotype observations, stand out from the other neighboring loci phenotypes on a map. Such an observation looks like it would be flanked by recombination events, which is an unlikely situation (van Ooijen & Jansen, 2013).

2.2.7 Selection of putative sRNA targets in Fusarium spp.

The list of sRNA molecules accumulating in *Fusarium graminearum* growing *in-vitro*, in FHB-infected and uninfected spikes of the barley genotype 'Morex', was obtained by small RNA sequencing by Dr. W. Chen, as a part of the "dsRNAguard" project coordinated by Dr. P. Schweizer (IPK, Gatersleben, Germany). The sRNA list served as a base for identifying potential candidate genes of *Fusarium* targeted by naturally present sRNA in the barley genome.

The sRNA candidates were selected by the following criteria:

- Present in 'Morex' (infected and uninfected) as they supposed to have barley origin
- sRNAs target *Fusarium* coding sequence with 1-2 mismatches
- At least 17 nt length to be able to initiate posttranscriptional gene silencing
- Candidate sRNAs present in a higher amount in FHB-infected barley in comparison to the healthy tissue as infection-related upregulation/induction of the candidate sRNAs in barley should be a plant response to the pathogen attack

The list of 50 candidate genes fulfilling these criteria was selected by Dr. P. Schweizer (IPK, Gatersleben, Germany). The putative function of the candidate genes was predicted by comparing the sequence similarity to functionally known proteins using X-BLAST in National Center for Biotechnology Information (NCBI) and by functional domain search using PROSITE (Sigrist et al., 2013). Out of the list of 50 candidates, eight sRNA targets in *Fusarium* were chosen based on literature information for a supposed role in pathogen development and/or virulence. The surrounding genomic regions of the selected sRNA sequences were further analysed for the presence of inverted sequences that may allow the formation of secondary structures as hairpins. The sRNA sequences were blasted against the barley 'Morex' genome using Ensembl Plants (Howe et al., 2020). The regions with 100% identity to the sRNA plus the surrounding 2000 nucleotides were defined and analysed for the presence of sequences complementary to the sRNA by using MultAlin (Corpet, 1988). Sequences carrying sRNA and the complementary sRNA sequence with not more than three mismatches or gaps were further checked.

RegRNA 2.0 (Chang et al., 2013) was used to identify functional RNA motifs in barley sequences like RNA structural patterns (Long Stems).

2.2.8 Software and databases

In this work, the following databases and software were used:

Databases:

- BLAST (Basic Local Alignment Search Tool) at NCBI (National Center for Biotechnology Information, 1988) https://blast.ncbi.nlm.nih.gov/Blast.cgi
- IWGSC BLAST (International Wheat Genome Sequencing Consortium) (Alaux et al., 2018) https://urgi.versailles.inrae.fr/blast/
- Ensembl Fungi (Cunningham et al., 2022) https://fungi.ensembl.org
- Ensembl Plants (Cunningham et al., 2022) http://plants.ensembl.org
- ViroBLAST (Deng et al., 2007) http://webblast.ipk-gatersleben.de/barley_ibsc/viroblast.php
- MultAlin (Corpet, 1988) for multiple sequence alignment http://multalin.toulouse.inra.fr/multalin/

Software:

- DNASTAR Lasergene7 (DNASTAR, Inc., Madison, USA) using SeqBuilder for sequence analysis and SeqMan for SNPs detection https://www.dnastar.com/
- Primer3 (Koressaar & Remm, 2007; Untergasser et al., 2012) - for primer design http://bioinfo.ut.ee/primer3-0.4.0/
- GraphPad version 7.00 - for statistical analysis and graphs creation (GraphPad Software, San Diego, California USA) www.graphpad.com
- Programm TASSEL5.2.31 - to create kinship matrix and evaluate linkage disequilibrium (Bradbury et al., 2007) http://www.maizegenetics.net/tassel
- Splign (Kapustin et al., 2008) - to compare cDNA-to-Genomic DNA https://www.ncbi.nlm.nih.gov/sutils/splign/splign.cgi?textpage=online&level=form
- JoinMap4 (Stam, 1993; Stam, 1995) - for genetic mapping https://www.kyazma.nl/index.php/JoinMap/
- The Triticeae Toolbox (T3) (Blake et al., 2016) - to check the marker sequence and their localization

https://triticeaetoolbox.org/wheat///genotyping/marker_selection.php

- GrainGenes (Yao et al. 2022) – to check the marker sequence and their localization
  https://wheat.pw.usda.gov/cgi-bin/GG3/browse.cgi?class=marker

- RegRNA 2.0 (Chang et al., 2013) - for identifying RNA motifs
  http://regrna2.mbc.nctu.edu.tw/detection.html

Programming environments:

- Python 3.8 - used for data analysis and graphs creation (Rossum & Drake, 2009), libraries: Matplotlib, seaborn, pandas, NumPy
  https://www.python.org/

- R 3.4.3 - used for candidate-based association mapping performed fitting a linear mixed model correcting for relatedness,
  ASReml-R Version 3 package

  https://www.R-project.org/

3. Results

Host Induced Gene Silencing is a relatively recent discovery, and several questions concerning the detailed mechanisms and whether it is a naturally occurring defense strategy of the plants remind widely open. This work aims to elucidate these questions by using different functional and genetic approaches.

3.1 Mechanism of HIGS

3.1.1 Work concept

Extensive literature studies revealed candidate genes from the plant silencing and secretory pathway putatively involved in HIGS. Silencing of the tested candidate genes is supposed to elucidate critical mechanisms of the HIGS process, such as which RNA molecules can be transported from the plant to the pathogen, which genes, and to what extent are taking part in the production and export of cross-kingdom trafficking RNA molecules. Since more than 150 genes were to be tested as putative candidate genes involved in HIGS, a transient-induced gene silencing (TIGS) method based on biolistic transgene delivery in *Bgh* – barley system was chosen. This method enables high-throughput gene function assessment and allows to address of gene functions in epidermal cells of barley (Douchkov et al., 2014; Douchkov et al., 2005), as well as it has been successfully employed to study the role of the fungal RNAi targets in *Bgh* – barley system (Nowara et al., 2010; Pliego et al., 2013). The experimental outline is presented in Figure R 1.

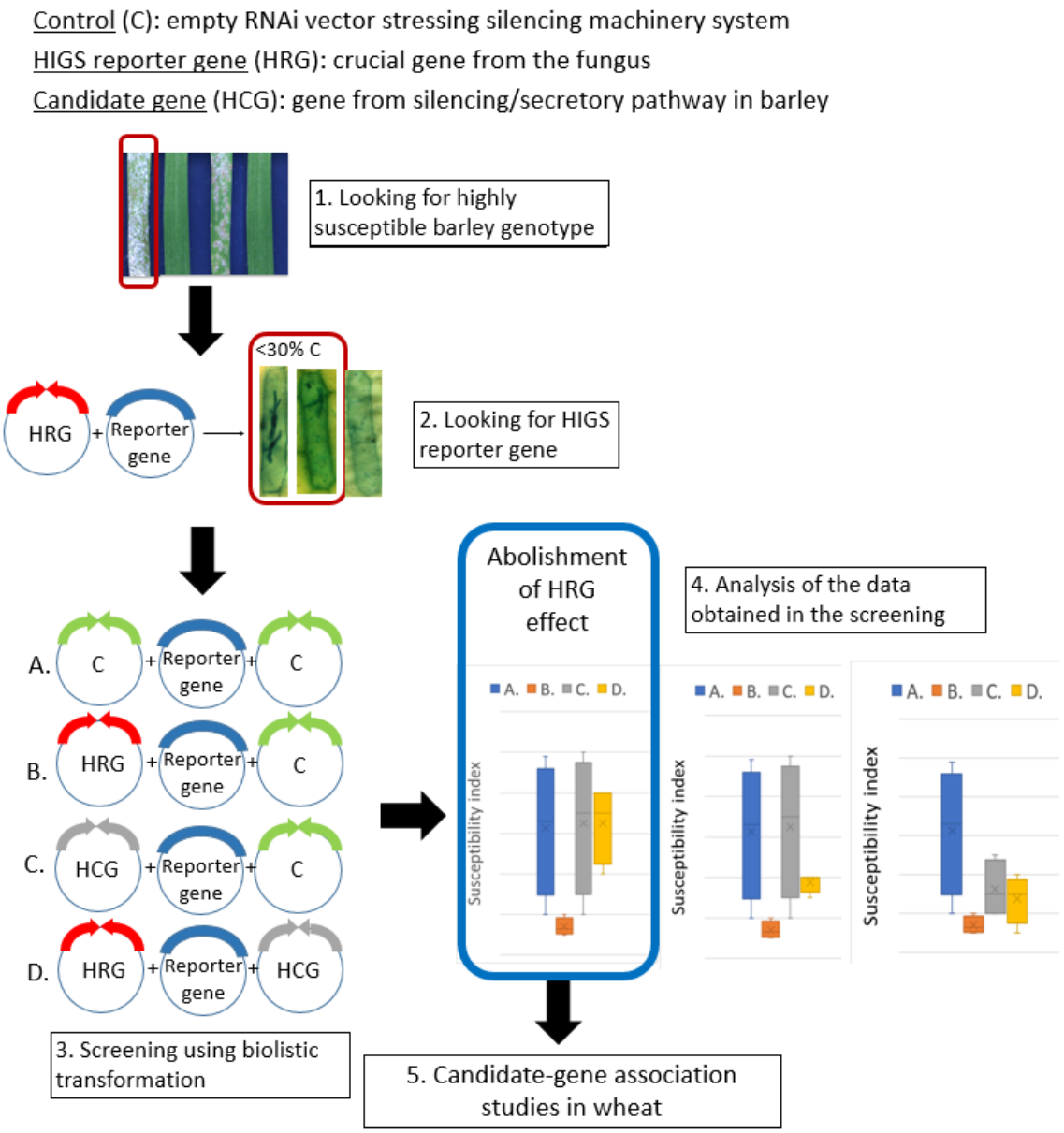

Figure R 1: Outline of planned experiments leading to understanding HIGS in plants mechanistically. Different barley genotypes are transiently transformed with control constructs to identify the highly susceptible genotype to powdery mildew, suitable for further experiments (1.). Later, a screen for a reliable HIGS reporter gene (HRG) was performed. Silencing of HRG should significantly affect the growth of Bgh on barley (2.). Four constructs combinations are used for screening the candidate genes (HCG) from silencing and secretory plant pathways (3.). The screening should allow the detection of candidate genes that abolish HRG activity, thereby are potentially involved in the HIGS process in plants (4.) The candidate—gene association studies in wheat with genes shown to be associated with HIGS mechanism in barley would be performed to find markers associated with wheat HIGS efficiency (5.).

An essential part of the experimental concept was to find a highly susceptible barley genotype that would allow straightforward observation of the changes in the susceptibility of barley to powdery mildew. The second component of the concept was to identify a crucial developmental or virulence gene of *Blumeria graminis* f.sp *hordei* (*Bgh*) and to use it as a HIGS reporter gene (HRG). Successful silencing of the expression of HRG should measurably impair the growth of *Bgh* on barley. The HIGS

candidate genes (HCG) were validated for their involvement in HIGS by Transient-Induced Gene-Silencing (TIGS) via biolistic transformation. To provide similar conditions, two silencing vectors were always co-bombarded (shown in Figure R 1) together with a reporter construct expressing beta-glucuronidase (GUS). Three different controls were included: 1) an empty RNAi vector to estimate the basal level of susceptibility of barley leaves to powdery mildew in each experiment (Figure R 1, 3:A); 2) an HCG silencing construct (RNAi: HCG) to control for the influence of the barley gene on the susceptibility (Figure R 1, 3:B); 3) an RNAi: HRG construct as a positive control and crucial 'marker' allowing to find barley genes involved in the RNA molecules generation or transport (Figure R 1, 3:C). The test combination includes RNAi constructs for both HCG and HRG plus the reporter construct (Figure R 1, 3:D). This combination should reveal whether the silenced HCG is required for silencing the HRG. If HCG is crucial for the transport of RNA molecules required for silencing of HRG, the effect of the silenced HRG will be minimized (Figure R 1, 4: blue rectangle). Based on the results obtained in *Bhg* – barley system, orthologs of genes potentially involved in HIGS are to be sought in wheat. The identified wheat orthologs should be used to investigate candidate-gene associations in the FHB - wheat system, using the germplasm and disease assessment described in Kollers et al. (2013) (Figure R 1, 5).

3.1.2 Reporter gene approach

Reporter gene approaches use a gene-silencing system to functionally assess plant silencing and secretory pathway-related genes in barley epidermal cells, together with a reporter gene to identify those involved in HIGS.

3.1.2.1 Selecting HIGS candidate gene orthologues in barley

Candidate genes potentially involved in cross-kingdom RNA trafficking were selected based on published references and grouped as follows:

- Genes encoding proteins directly processing RNA molecules like DICERs, which cleave dsRNA or RNA hairpins into short double-stranded RNA. A particular emphasis was put on both microRNA-generating DCL1, and small-interfering-RNA (hairpin-siRNA, natural-antisense siRNA, secondary siRNA and heterochromatic siRNA) generating DCL2, DCL3 and DCL4 (Bologna & Voinnet, 2014; Borges & Martienssen, 2015).
- Genes encoding core enzymes needed in sRNA production and function, such as Argonautes (AGOs) cleaving the siRNA complimentary transcript.
- Genes encoding the HUA ENHANCER 1 (HEN1) protein that stabilizes and protects sRNA from degradation (Bologna & Voinnet, 2014), and Cyclophilin 40 (CYP40) involved in the assembly of AGO1-containing RISC.

- Genes encoding RNA-dependent RNA polymerase (RdRp) and suppressor of gene silencing 3 (SGS3) necessary for secondary siRNA synthesis.
- Gene encoding F-BOX WITH WD-40 2 (FBW2). FBW2-mediated control of AGO1 loading/chaperoning involved in maintaining AGO1 steady-state levels to stay relatively constant under stress conditions (Bologna & Voinnet, 2014; Borges & Martienssen, 2015; Iki et al., 2012; Majumdar et al., 2017; Sinha, 2010).
- Genes encoding proteins with a putative function in the secretory pathway (RNA trafficking) like ESCRT proteins impotant for MVB development (Robinson et al., 2016; Scheuring et al., 2011) or exocyst subunits forming exocyst complex (Robinson et al., 2016).
- Genes encoding proteins needed for cytoskeleton functioning, e.g. MYOSIN XI K, actin-related proteins or RAC/ROP protein family (Park et al., 2018).
- Genes encoding SNAREs needed for fusing of the vesicles with the target membrane (Ding et al., 2014a).

In total, 24 genes of the RNAi pathway and 59 genes of the secretory pathway were found in the literature. These genes originated from *Arabidopsis thaliana*, *Zea mays,* and *Oryza sativa*. Candidate genes blasted against the barley genome, and the hits with E-value lower than 1E-35 were considered to be orthologues in barley. Based on this, 156 orthologues in barley were identified (Supplementary Data R11) and selected for validation.

3.1.2.2 Development of a TIGS test system to study the mechanism(s) of HIGS

Developing a TIGS system to validate candidate genes of plants' silencing or secretory pathway required a highly susceptible barley genotype that allows observing the reduction of SI caused by the HIGS reporter gene (HRG) and/or candidate gene (HCG). Furthermore, an HRG that reliably reduces the expression of a crucial *Bgh* gene and, thus, the SI of the leaves gene is required as a control.

3.1.2.2.1 Selecting a susceptible genotype for the TIGS test system

A set of barley genotypes was tested in a TIGS assay to select the most appropriate one for further experiments. Detached leaves of the cvs. ‘Manchuria’, ‘Hanna’, ‘Pallas’, ‘Ingrid’, ‘Golden Promise’, and the landrace HOR728 were transiently transformed via particle bombardment with an *Mlo* gene-silencing RNAi construct (pIPKTA36) and an empty vector (pIPKTA30N) (Figure R 2, Supplementary Data R1). Silencing of *Mlo* gene expression increases the *Bgh*-resistance of the barley leaves (Acevedo-Garcia et al., 2014).

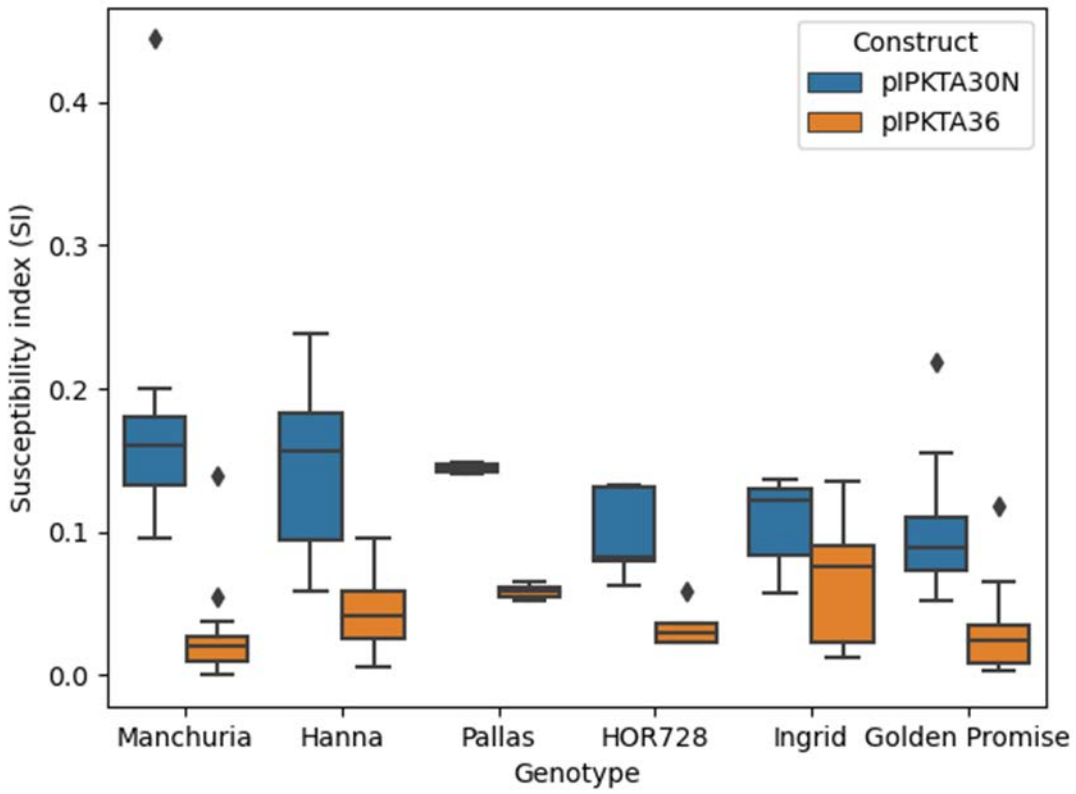

Figure R 2: Susceptibility index (SI) of chosen barley genotypes to *Bgh*.
Particle bombardment of six barley genotypes with an empty pIPKTA30N vector and positive control pIPKTA36. Experiments were performed to evaluate the susceptibility of genotypes to powdery mildew.

All cultivars when transformed with pIPKTA36 showed reduced SI in comparison to leaves transformed with an empty pIPKTA3N vector. At least five independent experiments (except for 'Pallas') have shown that none of the tested genotypes is susceptible at the range that is required for the screening (>0.4). Cv. 'Manchuria' showed the highest susceptibility index with a median of 0.161. The SI of 'Hanna' and 'Pallas' was 0.157 and 0.145, respectively. However, the calculated SI for 'Pallas' comes from only two experiments. The cultivar was technically difficult to handle because of the rolling leaves, which made 'Pallas' not suitable for screening on a large scale. The rest of the genotypes ('HOR728', 'Ingrid', and 'Golden Promise') exhibited higher resistance to powdery mildew and were not further considered. The cultivar 'Morex' was also considered a highly susceptible genotype, but previous tests (S. Lueck, IPK) demonstrated that its susceptibility in the TIGS system was not higher than that of cv. 'Manchuria'. Thus 'Manchuria' and 'Hanna' were chosen for the screening.

3.1.2.2.2 Failure to find reliable HIGS reporter gene

The HIGS reporter genes should have a distinct susceptibility phenotype upon silencing. HRG candidates were selected based on published works and tested on three different cultivars:

'Manchuria', 'Hanna', and 'Golden Promise'. The following fungal candidates genes were included in the tests (Table R 1):

- Gene encoding *Blumeria* effector candidate (BEC) 1011 (Pliego et al., 2013), showing similarity to microbial ribonuclease.
- Genes encoding 1,3-beta-glucanosyltransferases (GTFI and GTFII), known as virulence factors and involved in cell wall elongation (Nowara et al., 2010).
- Cytochrome P450 lanosterol C14 α-demethylase (*CYP51*) gene. Binding of CYP51 by ergosterol biosynthesis inhibitors disturbs fungal membrane integrity (Koch et al., 2013).
- β-1,3-Glucan Synthase (*GLS1*) gene. Deletion of *GLS1* gene is lethal for *Colletotrichum graminicola,* and RNAi:*GLS1* strains were unable to invade intact leaves when the wild-type strain caused disease symptoms on them (Oliveira-Garcia & Deising, 2013). Wheat plants transiently expressing HIGS transgene that target *F. culmorum GLS1* gene, showed reduced FHB disease symptoms (Chen et al., 2016).
- Gene encoding glycosylphosphatidylinositols (GPI) transamidase complex subunit. GPI are posttranslationally added to the C-terminus of secretory proteins as a common posttranslational modification of proteins in eukaryotic cells. The GPI synthesis gene *GPI8* is indispensable for the development and pathogenicity of the maize pathogen *C. graminicola* (Oliveira-Garcia & Deising, 2016).
- Gene encoding vacuolar serine protease that was shown to strongly reduce the haustorial index when tested in barley - powdery mildew system (Nowara et al., 2010).

The RNAi constructs for *GTF1*, *GTF1(1)* (targeting another region of *GTF1* gene), *GTF2*, *BEC1011*, *HO06F11* were kindly provided by Dr. D. Nowara and S. Lück (IPK), and for *CYP51*, *GLS1* and *GPI8* genes were created in this work.

Table R 1: HIGS reporter gene candidates tested by particle bombardment.
Genes' function and effects of their disruption or expression silencing on studied pathogens are shown below.
Haustorial index (HI) = haustoria inside transformed cells / total number of transformed cells per bombardment (Douchkov et al., 2005)

	Gene (EST ID)	Gene function	Effect	Pathogen	Literature
HIGS	BEC1011	*Blumeria* effector candidate 1011 (effector homolog to ribonuclease)	29.71% HI	*Blumeria graminis* sp. *hordei*	Pliego, Nowara et al. 2013
HIGS	CYP51	Cytochrome P450 lanosterol C14 α-demethylase (ergosterol biosynthesis inhibitor)	1.17%	*Fusarium graminearum*	Koch, Kumar et al. 2013
HIGS	(HO06F11)	Vacuolar serine protease	59.10% HI	*Blumeria graminis* sp. *hordei*	Nowara, Gay et al. 2010
HIGS	GTF1 (HO15J13)	1,3-beta-glucanosyltransferase	74.90% HI	*Blumeria graminis* sp. *hordei*	Nowara, Gay et al. 2010
HIGS	GTF2 (HO11N21)	1,3-beta-glucanosyltransferase	72.10% HI	*Blumeria graminis* sp. *hordei*	Nowara, Gay et al. 2010
RNAi fungal strain	GLS	β-1,3-Glucan Synthase	Unable to invade plant	*Colletotrichum graminicola*	Oliveira-Garcia and Deising 2013
RNAi fungal strain	GPI8	Cystein protease (component of the GPI transmidase complex)	Unable to invade plant	*Colletotrichum graminicola*	Oliveira-Garcia and Deising 2016

Transient silencing experiments were performed to find HRG. All values were normalized to the empty vector control pIPKTA30N, which was set as a baseline representing 100% susceptibility. The pIPKTA36 (Mlo silencing construct), used as a positive control, reduced the susceptibility to powdery mildew of cvs. 'Manchuria', 'Hanna' and 'Golden Promise' by 80%, 60%, and 70% compared to the control, respectively.

First, HRG's candidates (*GTF1*, *GTF2*, *BEC101*, *HO06F11*, and *GLS*) were evaluated in cv. 'Manchuria', as this barley genotype had the highest susceptibility index to powdery mildew. However, for all these candidates, the effect did not exceed 21% reduction of SI (for the *GTF1*) (Figure R 3, Supplementary Data R2), which renders them weak HRGs.

The same experiment was repeated in cv. 'Hanna' as the 2nd most susceptible genotype but with similar results. The constructs targeting the *GTF1(1)*, *GTF2*, and *HO06F11* were excluded from this and further

experiments since the effect of their silencing were reported as not as reliable as *GTF1* (Dr. D. Nowara, personal communication). The highest SI reduction was observed by silencing the gene encoding BEC1011, but still, the effect was much weaker than the one observed by Pliego et al. (2013).

The last tested genotype was 'Golden Promise', used for the experiments described by Pliego et al. (2013) and Nowara et al. (2010). Here, the reduction by 40% for *GTF1*, 30% for *CYP51*, and more than 20% for *BEC1011* of SI was observed compared to the negative control (empty vector (pIPKTA30N)) being 100%. However, none of the results was statistically significant due to the high variation of the effect of the constructs between the experiments.

The high variation and relatively weak effect on susceptibility did not allow the selection of a reliable HRG candidate; thus, this screening approach was not possible (Figure R 3, Supplementary Data R2).

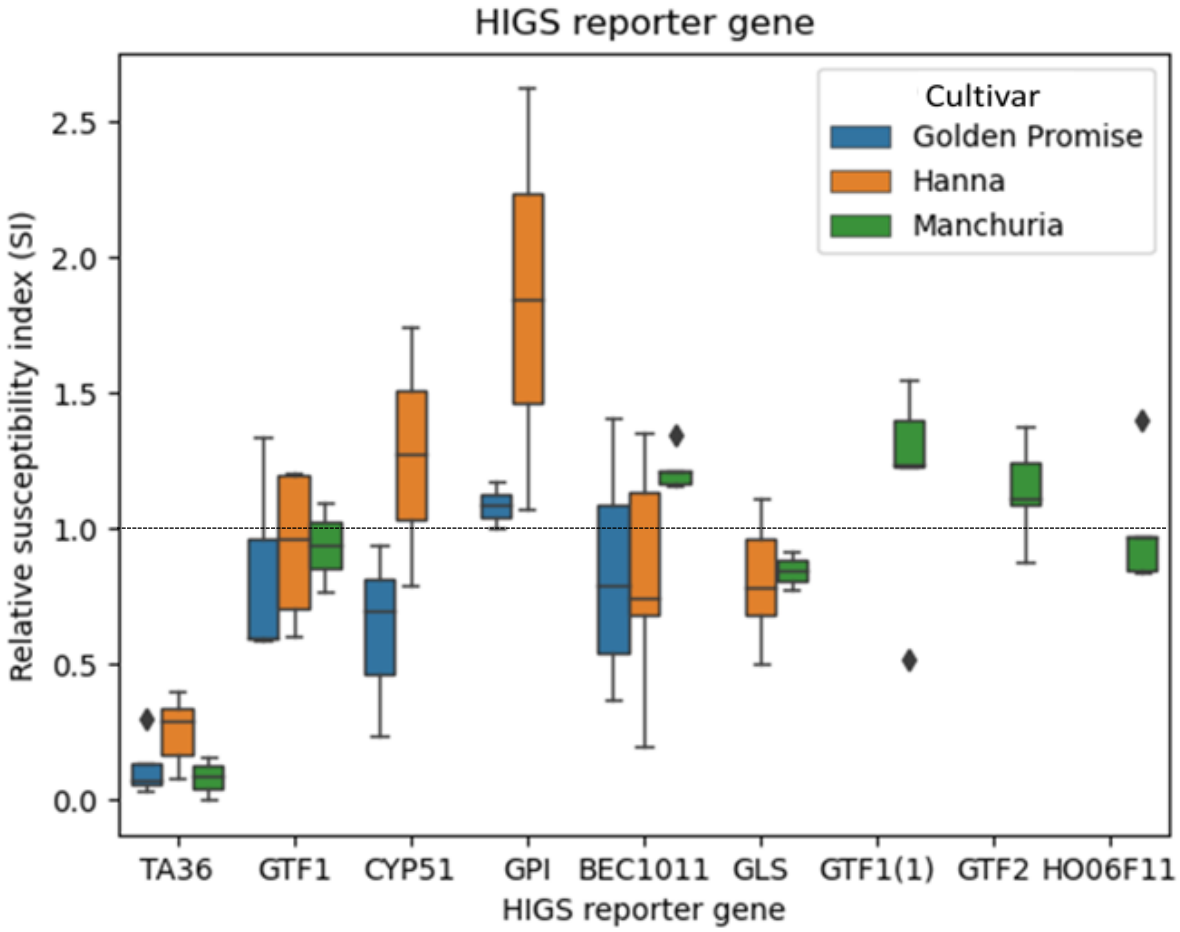

Figure R 3: The search for a reliable HIGS reporter gene among the eight gene candidates.
The graph shows the relative susceptibility index (SI) of the eight HIGS reporter gene candidates compared to the empty vector (pIPKTA30N) set to 1. Three barley cultivars, 'Manchuria', 'Hanna', and 'Golden Promise', were tested. The dotted line presents control bombarded with an empty pIPKTA30N vector. None of the candidate genes showed significant change in susceptibility; thus, none of them fulfilled the criteria for a HRG.

3.1.3 **Association approach**

The association approach was used to find the relationship between the natural genetic polymorphism in wheat genes from silencing and secretory plant pathways and FHB resistance between individuals. In addition, such gene products of the associated genes may be involved in the response of the plant to pathogens and additionally in cross-kingdom RNA trafficking efficiency. In the association approach, the previous *Bgh* - barley system, ideal for screening multiple genes, has been replaced by a destination system: wheat – FHB, for which FHB disease assessments were available in the GABI wheat population (Kollers et al., 2013), as well as in the biparental populations Apache x Biscay' and History x Rubens (Herter et al., 2018).

3.1.3.1 Selection of potential HIGS candidate genes orthologues in wheat

Thirty genes from barley putatively taking part in HIGS mechanism were used to find orthologues in wheat. These barley genes were single representatives selected from created gene families (Supplementary Data M10), characterized by the highest similarity to its orthologue in the plant of origin. Among them were eight genes from the plant silencing pathway and 22 from the secretory pathway. Most genes had three copies, one on each wheat genome (A, B, and D) (Supplementary Data M12). It resulted in the identification of 90 orthologues in wheat. The high similarity of the three wheat genomes entailed a primer design in the genes' intronic regions. Their intronic-exonic structure was analyzed using *Splign* program (Kapustin et al., 2004; Kapustin et al., 2008) and comparison of selected barley genes cDNA (A. *Dicer1*, B. *Exo70B2*, C. *VAMP721*, D. *LIP5*, E. *ESCRT*-III, F. *PEN3*, G. *Arp2/3*, H. *Ara6,* and I. *VPS25*) to wheat genomic DNA is presented in Figure R4.

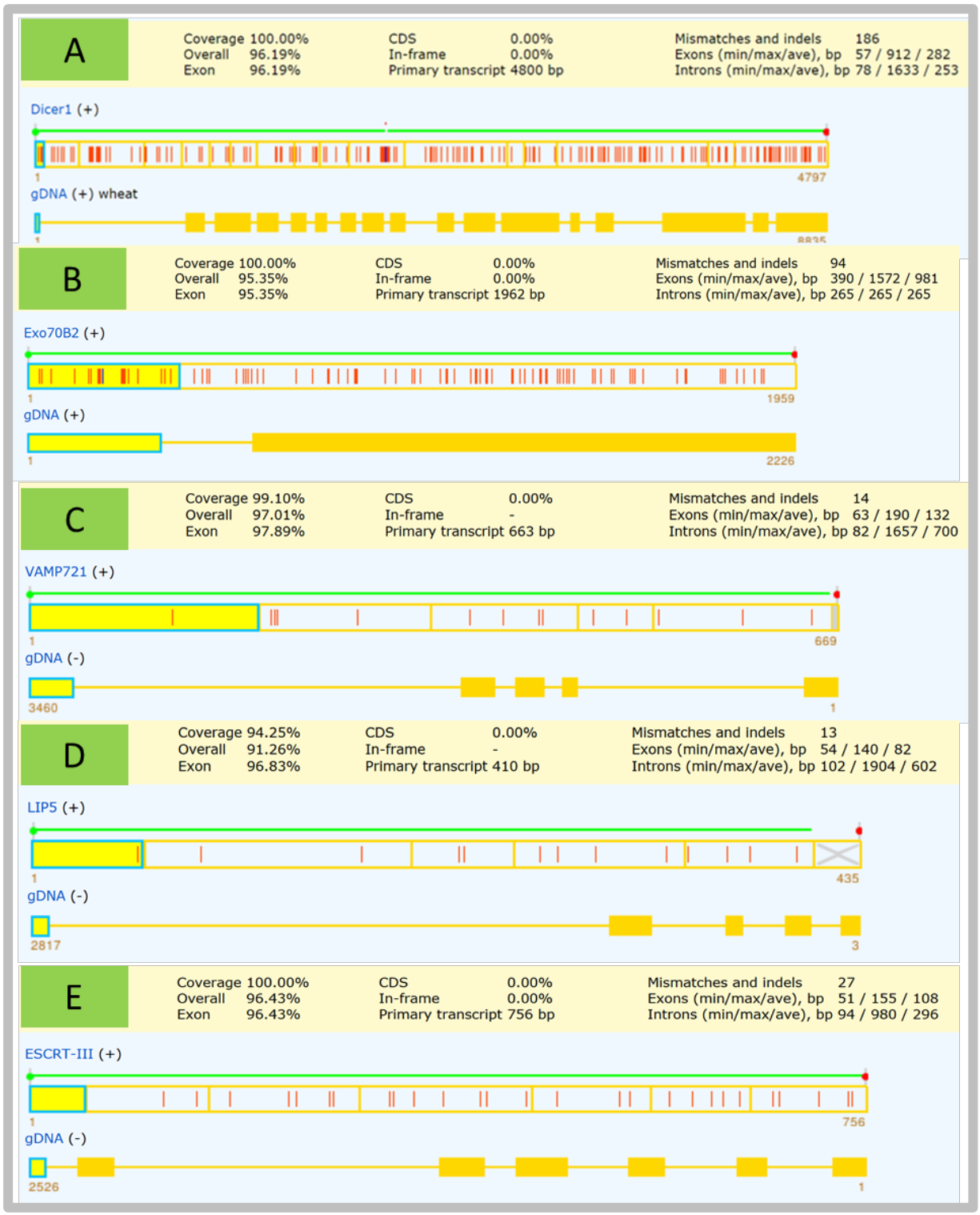
A
Coverage 100.00%
Overall 96.19%
Exon 96.19%
CDS 0.00%
In-frame 0.00%
Primary transcript 4800 bp
Mismatches and indels 186
Exons (min/max/ave), bp 57 / 912 / 282
Introns (min/max/ave), bp 78 / 1633 / 253
Dicer1 (+)
1
4797
gDNA (+) wheat
B
Coverage 100.00%
Overall 95.35%
Exon 95.35%
CDS 0.00%
In-frame 0.00%
Primary transcript 1962 bp
Mismatches and indels 94
Exons (min/max/ave), bp 390 / 1572 / 981
Introns (min/max/ave), bp 265 / 265 / 265
Exo70B2 (+)
1
1959
gDNA (+)
1
2226
C
Coverage 99.10%
Overall 97.01%
Exon 97.89%
CDS 0.00%
In-frame -
Primary transcript 663 bp
Mismatches and indels 14
Exons (min/max/ave), bp 63 / 190 / 132
Introns (min/max/ave), bp 82 / 1657 / 700
VAMP721 (+)
1
669
gDNA (-)
3460
1
D
Coverage 94.25%
Overall 91.26%
Exon 96.83%
CDS 0.00%
In-frame -
Primary transcript 410 bp
Mismatches and indels 13
Exons (min/max/ave), bp 54 / 140 / 82
Introns (min/max/ave), bp 102 / 1904 / 602
LIP5 (+)
1
435
gDNA (-)
2817
3
E
Coverage 100.00%
Overall 96.43%
Exon 96.43%
CDS 0.00%
In-frame 0.00%
Primary transcript 756 bp
Mismatches and indels 27
Exons (min/max/ave), bp 51 / 155 / 108
Introns (min/max/ave), bp 94 / 980 / 296
ESCRT-III (+)
1
756
gDNA (-)
2526
1

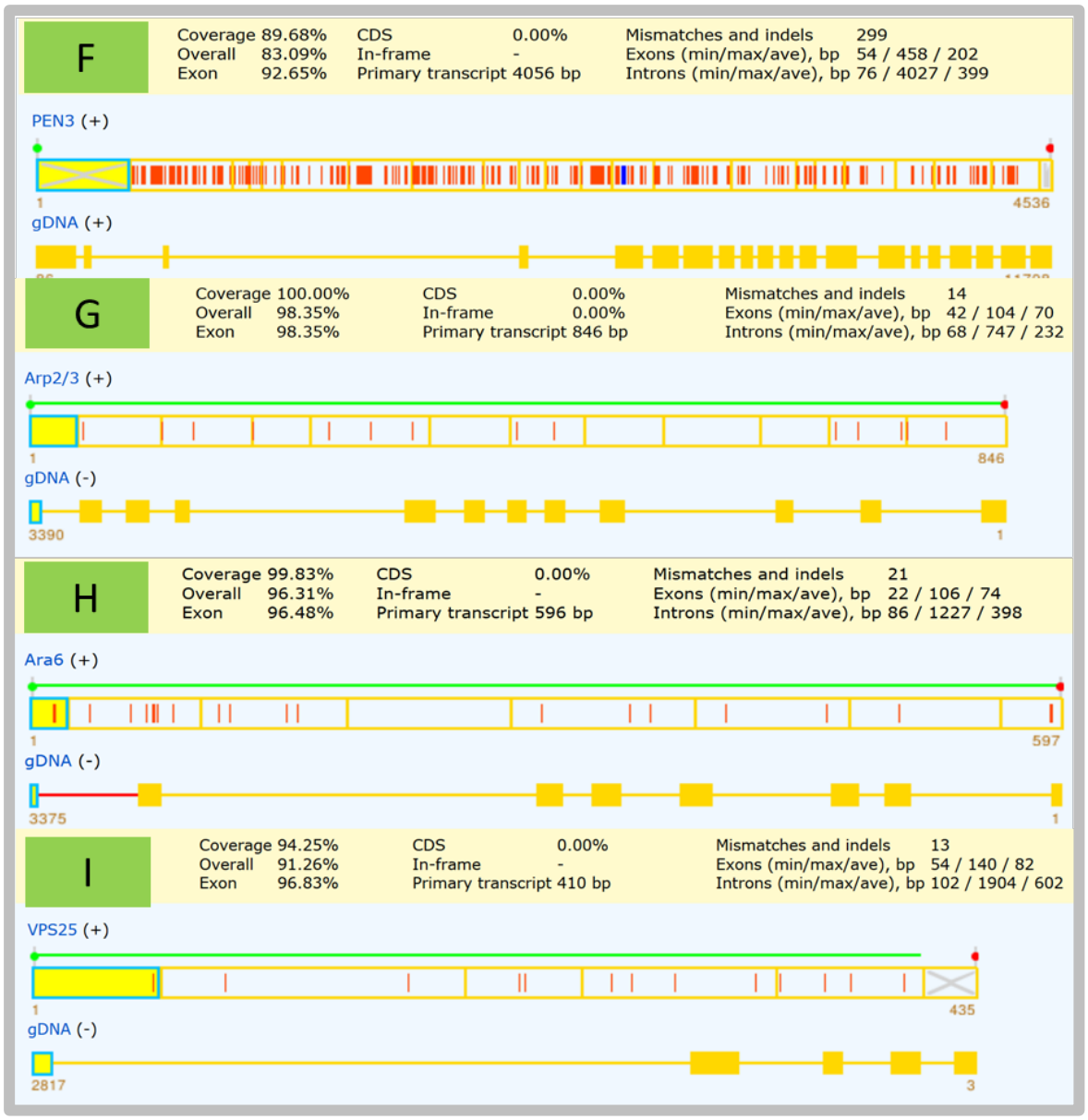

Figure R 4: Alignments of wheat genomic sequences to sequences of HIGS candidates of barley.
A) A 10Kbp wheat genomic sequence from chromosome 5A aligned to barley *Dicer1* cDNA (4800 bp) shows 17 exons with 96.19% identity to barley transcript. B) A 10Kbp wheat gDNA from chromosome 1A aligned to the barley *Exo70B2* gene (1962 bp) shows two exons with 95.35% similarity to barley cDNA. C) A 10Kbp wheat gDNA from chromosome 5D aligned to barley *VAMP721* cDNA (663 bp) shows five exons with 97.89% similarity to barley cDNA. D) A 10 Kbp wheat gDNA from chromosome 3D aligned to barley *LIP5* cDNA sequence (410 bp) shows five exons with 96.83% similarity to barley cDNA. E) A 10Kbp wheat gDNA from 5A chromosome aligned to barley *ESCRT-III* cDNA sequence (756 bp) shows seven exons with 96.43% identity to barley cDNA. F) A 10Kbp wheat gDNA from 5A chromosome aligned to the barley *PEN3* gene (4056 bp) shows 20 exons with 92.65% similarity to barley cDNA. G) A 10Kbp wheat gDNA from 3B chromosome aligned to barley *Arp2/3* gene cDNA (846 bp) shows 12 exons with 98.35% similarity to barley cDNA. H) A 10 Kbp wheat gDNA from 4D chromosome aligned to barley *Ara6* cDNA sequence (595 bp) shows eight exons with 96.48% similarity to barley cDNA. I) A 10Kbp wheat gDNA from 3D chromosome aligned to barley *VPS25* gene sequence (410 bp) shows five exons with 96.83% identity to barley cDNA.

The analysis allowing detection of SNPs was performed in SeqMan Pro DNASTAR Lasergene7 (DNASTAR, Inc., Madison, USA) and allele variant for each of the analyzed eight wheat genotypes are

shown in Table R 2. In nine genes, twelve polymorphisms were found. The genes were located on seven chromosomes (Table R 3) and were involved in both silencing (*Dicer1*) and secretory pathway (*Exo70B2*, *VAMP721*, *LIP5*, *ESCRT-III*, *VPS25*, *PEN3*, *Ara6*, *Arp2/3*). The functions of each of them are presented in Table R 3.

Table R 2: Polymorphisms found in nine genes among eight wheat genotypes (Slominska-Durdasiak et al., 2020).

	Ara6	Exo70B2	VAMP721	DCL(1)	DCL(2)	ESCRT-III	VPS25	Arp2/3	LIP5(1)	LIP5(3)	PEN3(1)	PEN3(2)
Arina	T	C	G	G	T	A	T	G	C	A	C	Del
Rubens	T	C	A	T	G	A	C	A	A	G	C	Del
Biscay	C	T	G	T	G	G	T	A	C	A	C	Del
Chinese Spring	T	C	G	T	G	A	C	A	A	G	C	Del
Florett	C	C	G	G	T	G	T	A	C	A	A	Ins
Apache	-	T	G	G	T	G	T	A	C	A	C	Del
History	T	C	G	G	T	G	T	A	C	A	C	Del
Julius	T	T	G	G	-	G	C	A	A	G	C	Del

Table R 3: Candidate genes potentially involved in HIGS with polymorphisms detected among the selected wheat genotypes.
Their ID, chromosome location and function (modified Slominska-Durdasiak et al. (2020)).

Gene	Gene ID	Chromosome	Function
Dicer1	TraesCS5A02G516000	5A	Involvement in miRNA biogenesis (Borges & Martienssen, 2015).
Exo70B2	TraesCS1A02G297800	1A	Encoding exocyst subunit, role in plant defense against pathogens (Zarsky et al., 2013).
VAMP721	TraesCS5D02G459900	5D	Encoding vesicle-associated membrane protein 721, linked directly with membrane vesicle trafficking (Zhang et al., 2015).
LIP5	TraesCS3D02G238800	3D	Encoding LIP5, regulator of MVB biogenesis (Robinson et al., 2016).
ESCRT-III	TraesCS5A02G316100	5A	Encoding endosomal sorting complexes required for transport (ESCRT) proteins, involved in MVBs formation (Robinson et al., 2016).
PEN3	TraesCS7A02G356100	7A	Encoding a plasma membrane ATP binding cassette (ABC) transporter (Hardham et al., 2007).
Arp2/3	TraesCS3B02G401300	3B	Encoding complex regulating actin dynamics (Frank et al., 2004).
Ara6	TraesCS4D02G267900	4D	Encoding a Rab5-like GTPase protein, labelling of MVBs (Ding et al., 2014a).
VPS25	TraesCS3D02G536400	3D	Involved in intraluminal vesicle formation in multivesicular bodies (Robinson et al., 2016; Scheuring et al., 2011).

3.1.3.2 Three markers associated with *Fusarium* infection in candidate-gene association studies

Twelve polymorphic markers were found in the nine genes located on seven different chromosomes. The CG approach performed on GABI wheat population revealed three significant marker-trait associations. These were two markers in the *Dicer1* gene: DCL1(1) and DCL1(2) with *P* values of 0.0001522 and 0.000009, respectively, and the marker Ara6 in the Rab5-like GTPase gene *Ara6* with a *P* value of 0.0002173. Two markers DCL1(1) and DCL1(2) are located in the 17th intron of the *Dicer1* gene (Supplementary Data R13), whereas marker Ara6 is located in the intronic region between 4th and 5th exon of the Rab5-like GTPase gene *Ara6* (Supplementary Data R12). The protein encoded by the *Dicer1* gene is crucial for miRNA biogenesis, while the protein encoded by the gene *Ara6* is labeling MVBs. Additionally, four markers showed significant interaction with the environment, that were Ara6, Exo80B2, VAMP721, and PEN2(3) (Table R 4); thus, the Ara6 marker is associated not only with *Fusarium* infection, but also its action depends on the environment.

Table R 4: Results of candidate-gene association mapping of polymorphic markers being located in the nine candidate genes.
The *P* value of their association with FHB severity and *P* value of their interaction with the environment.

	p-value (SNP main effect)	**p-value (SNP x env)**
Ara6	0.0002173**	0.0000488***
Exo70B2	0.6342757	0.0002264**
VAMP721	0.7527360	0.0008716*
DCL(1)	0.0001522**	0.0887238
DCL(2)	0.0000090***	0.1065772
ESCRT-III	0.3206665	0.7881132
Arp2/3	0.3957368	0.2856691
VPS25	0.4154120	0.3131183
LIP5(1)	0.6468704	0.5056728
LIP5(2)	0.1386782	0.0321115
PEN3(1)	0.1511683	0.2436707
PEN3(2)	0.0246802	0.0008306*

* Refers to P ≤ 0.05; ** Refers to P ≤ 0.01; ***Refers to P ≤ 0.001 applying Bonferroni correction for multiple

3.1.3.3 Validation of the marker-trait associations in the 'Apache x Biscay' and 'History x Rubens' populations

3.1.3.3.1 Confirmation of the marker-FHB infection associations in 'Apache x Biscay' population

A biparental population of 100 RILs, originating from the cross of the moderately resistant 'Apache' with FHB susceptible barley line 'Biscay' was used to validate data obtained in CG approach. Only four markers were polymorphic in 'Apache' and 'Biscay', among them were Ara6, DCL1(1), and DCL1(2), shown earlier to be significantly associated with the studied trait. Marker VAMP721, located on 5A chromosome, was neither associated with FHB resistance (Figure R 5) not with plant height (Figure R 6) or heading date (Figure R 7). Marker Ara6 was significantly associated ($P \leq 0.01$) with FHB resistance and resulted in 10% points difference between Ara6a and Ara6b alleles at the latest stage of FHB infection (Figure R 5). Marker Ara6 was also significantly associated with the plant height (on average 3.9% difference between the gene alleles) (Figure R 6), but not with wheat spike heading date (Figure R 7). Marker DCL1(1) was significantly associated with FHB infection at every stage of disease development (Figure R 5). Plants carrying the allelic variant DCL1(1)a, showed, on average, 9% points weaker FHB infection symptoms at the latest stage of disease development in comparison to the plants carrying allelic variant DCL1(1)b (Figure R 5). Marker DCL1(2) was only significantly associated at some stages of FHB infection. At the latest stage of the disease development, on average 8% points difference was observed between gene alleles (Figure R 5). Both markers, DCL1(1) and DCL1(2) did not show associations with plant height (Figure R 6) or spike heading date (Figure R 7). The effect of alleles of studied genes on the earlier FHB development stages are presented in Supplementary Data R3.

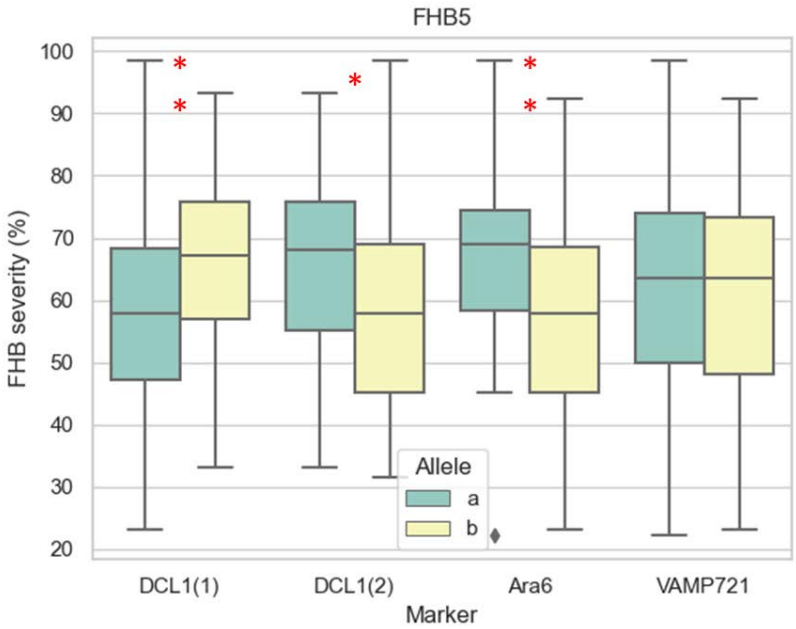

Figure R 5: Three markers shown to be associated with FHB infection at the latest stage of FHB disease development in 'Apache x Biscay' population.
Allelic variants are marked as a and b. Marker DCL1(1) and marker DCL1(1) are located in the *Dicer1* gene. Marker Ara6 is located in Rab5-like GTPase *Ara6* and marker VAMP721 in the *VAMP721* gene. *Refers to P ≤ 0.05; **Refers to P ≤ 0.01

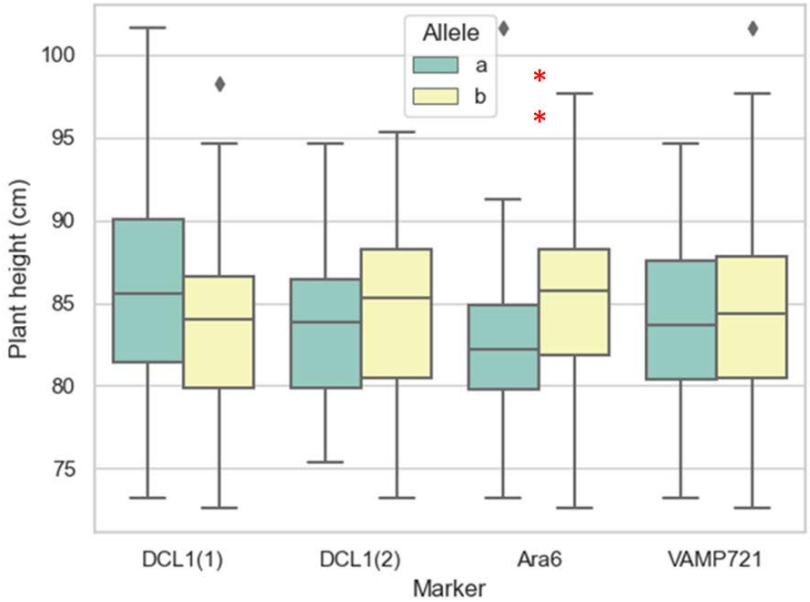

Figure R 6: Marker Ara6 associated with the plant height (PH) in 'Apache x Biscay' population.
Allelic variants are marked as a and b. Marker DCL1(1) and marker DCL1(1) are located in the *Dicer1* gene. Marker Ara6 is located in Rab5-like GTPase *Ara6* and marker VAMP721 in the *VAMP721* gene. *Refers to P ≤ 0.05; **Refers to P ≤ 0.01

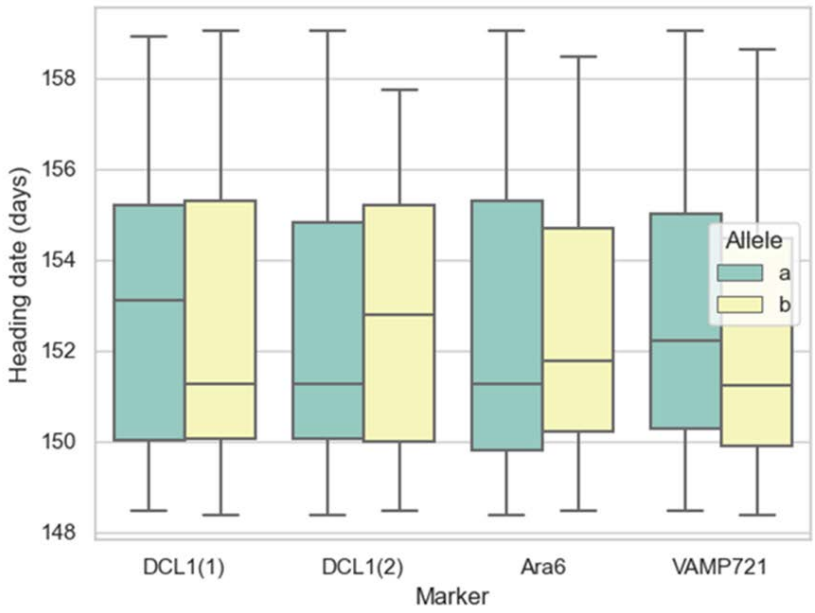

Figure R 7: No association of the heading date (days) and allelic variant of the markers located in the candidate genes.
Allelic variants are marked as a and b. Marker DCL1(1) and marker DCL1(1) are located in the *Dicer1* gene. Marker Ara6 is located in Rab5-like GTPase *Ara6* and marker VAMP721 in the *VAMP721* gene. *Refers to P ≤ 0.05; **Refers to P ≤ 0.01

3.1.3.3.2 Confirmation of marker DCL1(1) - FHB infection association in 'Rubens x History' population

A biparental population originating from the cross of FHB susceptible barley line 'Rubens' with the moderately resistant 'History' was used to validate data obtained in CG approach and in the biparental population 'Apache x Biscay'. The population counts 48 RILs. Only four markers were polymorphic in the population; among them was DCL1(1) which was earlier shown to be associated with FHB resistance. Markers VPS25 and VAMP721 were not associated with plant height (Figure R 10), heading date (Figure R 9), or FHB infection (Supplementary Data R4 and Supplementary Data R5). Marker ESCRT-III, located on chromosome 5A was significantly associated with both heading date (Figure R 9) and plant height (Figure R10) with an average of 2 days (HD) and 6.59 cm (PH) difference between the plants carrying ESCRT-IIIa and ESCRT-IIIb allele. Marker ESCRT-III was not associated with FHB infection (Supplementary Data R4 and Supplementary Data R5). Marker DCL1(1) was significantly associated with FHB infection at some stages of the disease (Figure R 8). Plants carrying the allelic variant DCL1(1)a show, on average stronger FHB infection symptoms at every stage of disease development in comparison to the plants carrying allelic variant DCL1(1)b (4.8% and 8% points for, respectively FHB2 and FHB3 stage). The trend disappeared at the latest (FHB5) stage of the infection. In contrast to the results obtained in 'Apache x Biscay' population, the DCL1(1) marker showed an association to the

wheat spike heading date in 'History x Rubens' population that differ 1.9 days between plants carrying different DCL1(1) alleles.

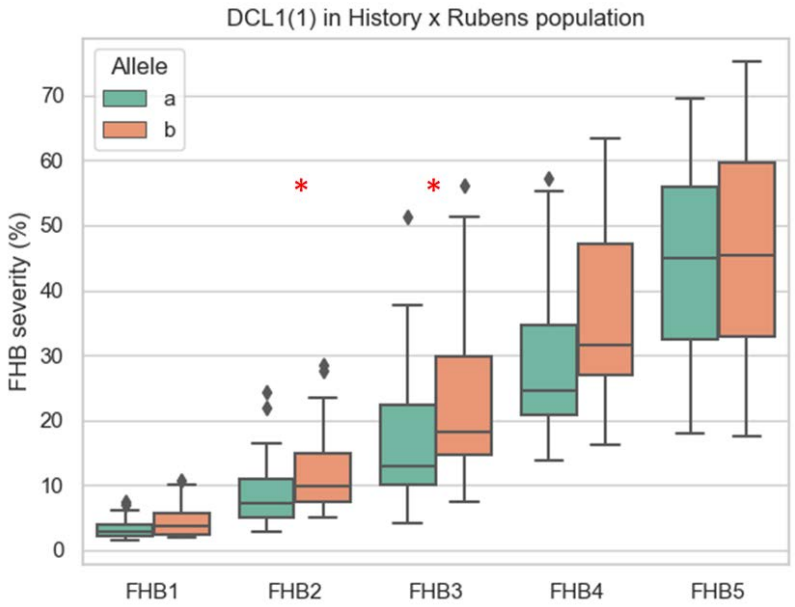

Figure R 8: Marker DCL1(1), located in *Dicer1* gene, associated with the FHB infection at some stages of FHB development in 'History x Rubens' population.
Allelic variants are marked as a and b. FHB1 – FHB5 are stage of infection. *Refers to $P \leq 0.05$; **Refers to $P \leq 0.01$

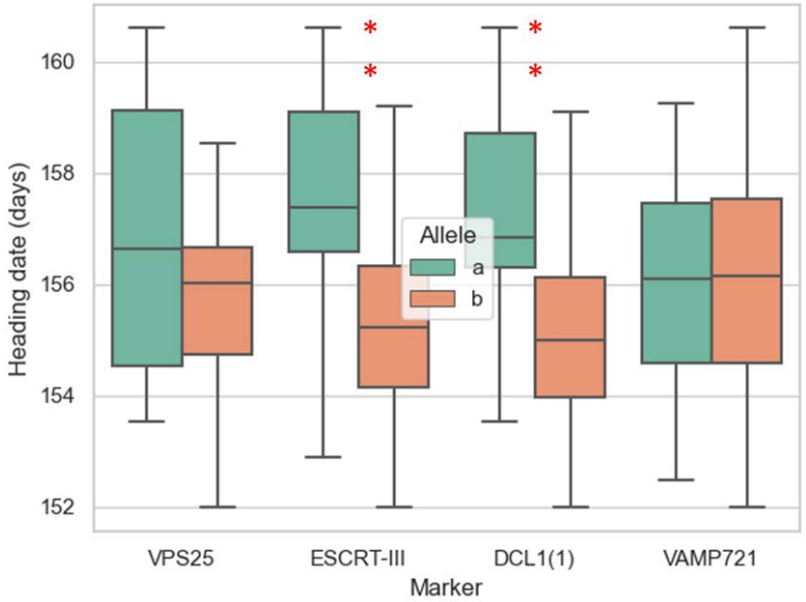

Figure R 9: DCL1(1) and ESCRT-III markers associated with the wheat spike heading date.
Allelic variants are marked as a and b. Marker DCL1(1) and marker DCL1(1) are located in the *Dicer1* gene. Marker Ara6 is located in Rab5-like GTPase *Ara6* and marker VAMP721 in the *VAMP721* gene. *Refers to $P \leq 0.05$; **Refers to $P \leq 0.01$*Refers to $P \leq 0.05$; **Refers to P ≤ 0.01

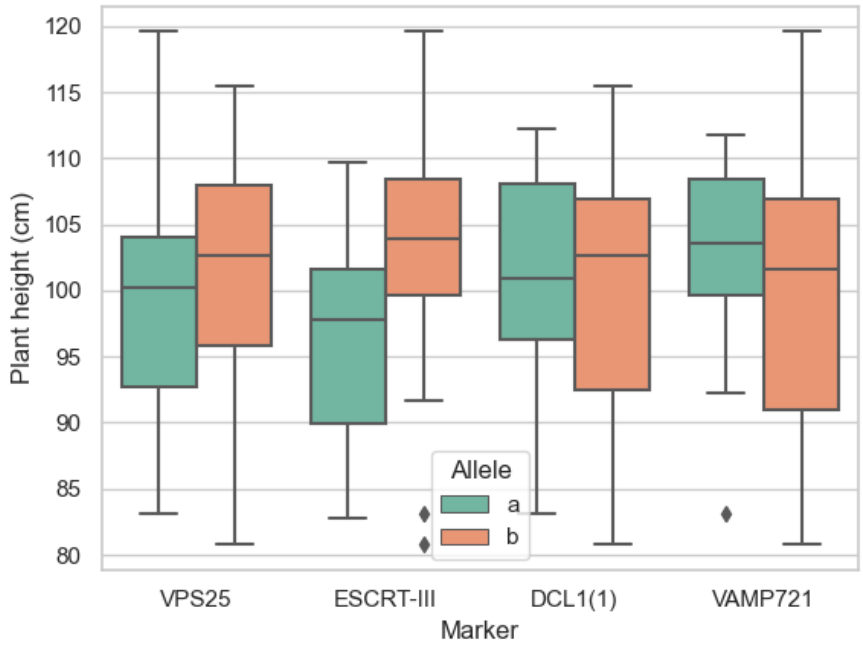

Figure R 10: No association of the wheat spike plant height and allelic variants of the four markers in 'History x Rubens' population.
Allelic variants are marked as a and b. Marker DCL1(1) and marker DCL1(1) are located in the *Dicer1* gene. Marker Ara6 is located in Rab5-like GTPase *Ara6* and marker VAMP721 in the *VAMP721* gene. *Refers to P ≤ 0.05; **Refers to P ≤ 0.01*Refers to P ≤ 0.05; **Refers to P ≤ 0.01

3.1.3.4 Analysis of the genes with DCL1(1), DCL1(2) and Ara6 markers

Three markers significantly associated with FHB resistance were located in two genes, *Dicer1* (TraesCS5A02G516000) and Rab5-like GTPase *Ara6* (TraesCS4D02G267900). The expression profiles of these two genes using a wheat expression browser *in situ* (Borrill et al., 2016; Ramirez-Gonzalez et al., 2018) were analyzed (Figure R 11). Wheat spikes infected with FHB were not showing higher expression of the gene *Dicer1* nor *Ara6* compared to healthy spikes. As the HIGS mechanism is supposed to influence wheat resistance, the gene expression of the two studied genes was also analyzed in wheat seedlings infected with Septoria tritici blotch, wheat yellow rust, or powdery mildew. In this case, the expression of the genes was higher in plants showing disease symptoms compared to the healthy seedlings.

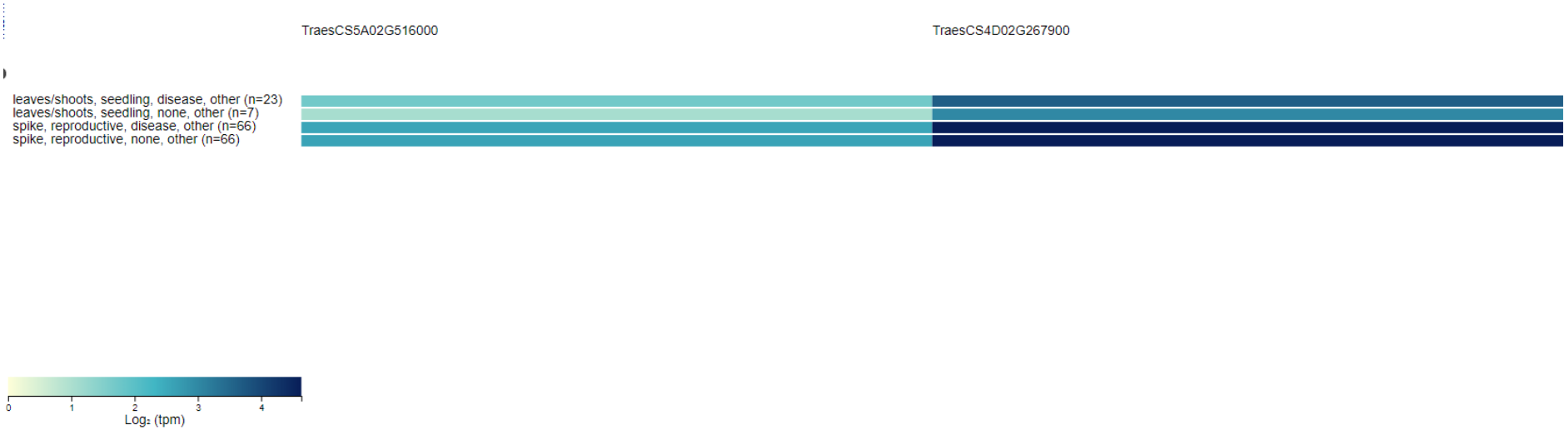

Figure R 11: Expression profiles of *Dicer1* and Rab5 GTPase *Ara6* genes. *Dicer1* (TraesCS5A02G516000) and *Ara6* (TraesCS4D02G267900) expression profiles show spikes infected with FHB and leaves, roots of seedlings infected with stripe rust, *Septroria tritici* and powdery mildew.

3.1.3.5 Physical mapping and analysis of linkage disequilibrium among the significant markers

RefSeq v1.0 physical map was used to find nearby laying markers to the DCL1(1), DCL1(2), and Ara6 markers. As many available markers is laying on the 5A chromosome, ~5k bp sequence from markers DCL1(1) and DCL1(2), located in the *Dicer1* gene were analyzed, and markers presented in the Table R 5 were found. Seven markers were discovered in the studied genomic region, the closest available marker WSNP_KU_REP_C71232_70948744 was located ~200 bp far from DCL1(2) marker and the marker IWA2840 ~900 bp far from the marker DCL1(1). Markers DCL1(1) and DCL1(2) are separated by around 165 nucleotides.

Table R 5: Markers surrounding DCL1(1) and DCL1(2) markers.
These markers are located in 10k bp wheat genomic DNA region, in the table also presented: version of the allele in GABI wheat population, chromosome localization and precise position of the marker on RefSeq v1.0 physical map.

Marker	alleles	chromosome	position
RAC875_C19949_2557	G	5A	679659572
WSNP_KU_REP_C71232_70948744	A/G	5A	679663686
DCL1(2)	G/T	5A	679663886
DCL1(1)	T/G	5A	679664051
IWA2840	-	5A	679664865
WSNP_EX_C23795_33033959	G/A	5A	679664943
EXCALIBUR_C23795_551	G	5A	679665883
WSNP_EX_C23795_33033150	G/A	5A	679665943
WSNP_EX_C23795_33033010	G/A	5A	679666083

As there is less known markers in 4D chromosome, 1 Mbp sequence from marker Ara6 was analyzed. 15 markers were discovered in the studied region. The closest markers to marker Ara6 are markers IACX749 and gbsHWWAMP48420 lying respectively 300 kbp and 535 kbp far from marker Ara6.

Table R 6: Markers surrounding Ara6 marker.
These markers are located in 2 Mbp wheat genomic DNA region. Table presents version of the allele in GABI wheat population, chromosome localization and precise position of the marker on RefSeq v1.0 physical map.

Marker	alleles	chromosome	position
synopGBS186	-	4D	438155104
D_GB5Y7FA02HBLTO_213	A/G	4D	438159053
WSNP_BF473052D_TA_2_1	A/G	4D	438257224
RAC875_C28230_772	A	4D	438257818
KUKRI_C62371_98	A	4D	438258347
BOBWHITE_REP_C64809_141	A	4D	438258355
KUKRI_C34453_332	A/C	4D	438790389
BOBWHITE_C29148_80	A	4D	438790422
WSNP_KU_REP_C108610_93615069	A	4D	438791150
wsnp_BE494848D_Ta_1_1	-	4D	438792830
IACX749	C	4D	438792830
Ara6	T/C	4D	439123105
gbsHWWAMP48420	-	4D	439658613
RAC875_C16405_84	G/A	4D	439771425
EX_C10897_540	A	4D	439778309
D_GDRF1KQ01EKNB6_159	A	4D	439825843

The linkage disequilibrum (LD) among the markers developed in this study and markers available for GABI wheat population was also studied. The LD plots shows developed markers in the performed here studies and their linkage to closely located markers from them that were present in the association study, on the RefSeq v1.0 physical map. We performed pairwise linkage disequilibrium analyses using a sliding window approach with window size 50. Every plot is divided into two parts. The lower part shows P-values for the two-sided Fisher's Exact test of each comparison and the upper part shows R squared, representing the correlation between alleles at two loci. R squared is used to measure the

strength of the association (https://bitbucket.org/tasseladmin/tassel-5-source/wiki/UserManual). Both are used to measure LD between pairs of markers.

Polymorphic markers in the association studies located 5 kbp far from markers DCL1(1) and DCL1(2) on the RefSeq v1.0 physical map were used to calculate LD. There were six markers located in the area (Table R 5). Four of them were polymorphic in the GABI wheat population (WSNP_KU_REP_C71232_70948744, WSNP_EX_C23795_33033959, WSNP_EX_C23795_33033150, WSNP_EX_C23795_33033010) and fulfilling criteria described in M&M. The LD plot showed strong linkage (R squared 100%) of the markers DCL1(1) and DCL1(2) with the surrounding markers except with the marker WSNP_EX_C23795_33033150 (Figure R 12).

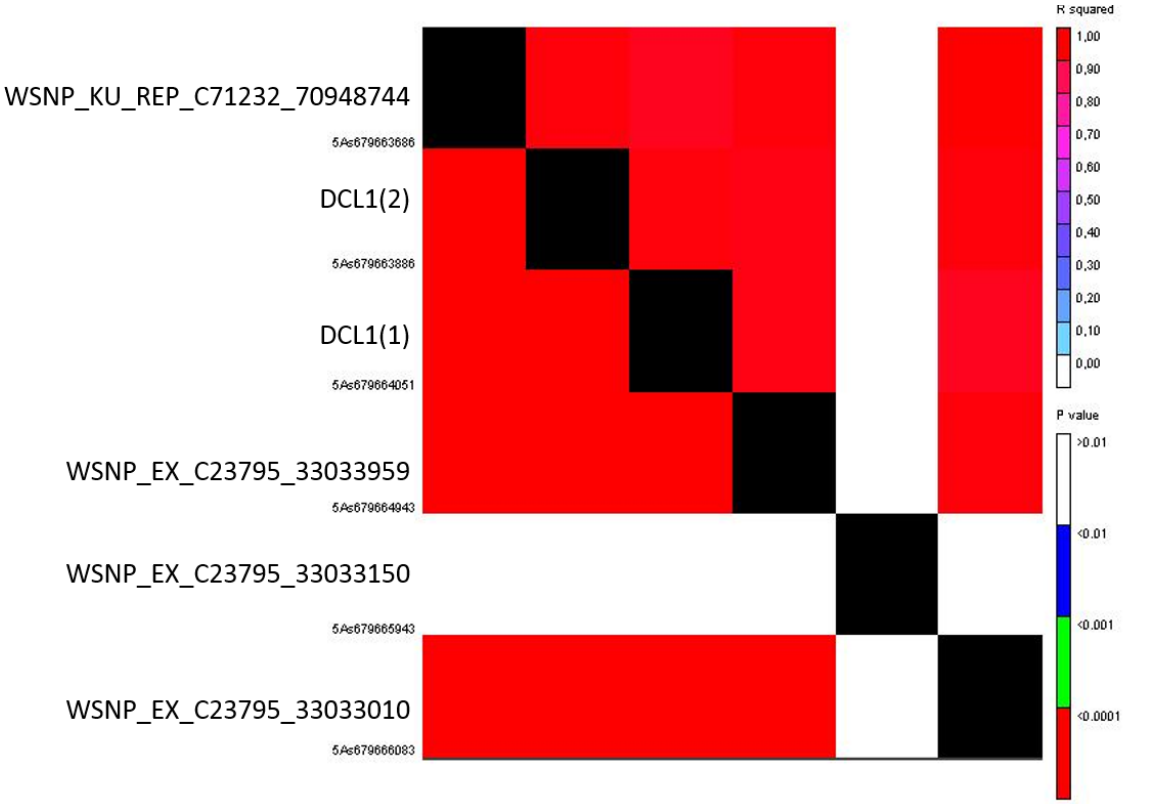

Figure R 12: LD plot of markers DL1(1), DCL1(2) and nearby lying markers on RefSeq v1.0 physical map. Pairwise LD as sliding window (window size 50). Above the diagonal, R squared values are displayed and the corresponding p-values for the two-sided Fisher's exact test displayed below the diagonal.

Polymorphic markers in the GABI wheat population located 1 Mbp distance from marker Ara6 on the RefSeq v1.0 physical map were used to check LD with closely lying markers. There were only 12 markers found in the 2 Mbp long sequence of the studied physical map (Table R 6). Four of them were polymorphic in the studied population (D_GB5Y7FA02HBLTO_213, WSNP_BF473052D_TA_2_1, KUKRI_C34453_332, RAC875_C16405_84) and fulfilling criteria described in M&M. None of the studied markers on the RefSeq v1.0 physical map was in LD with Ara6 (Figure R 13).

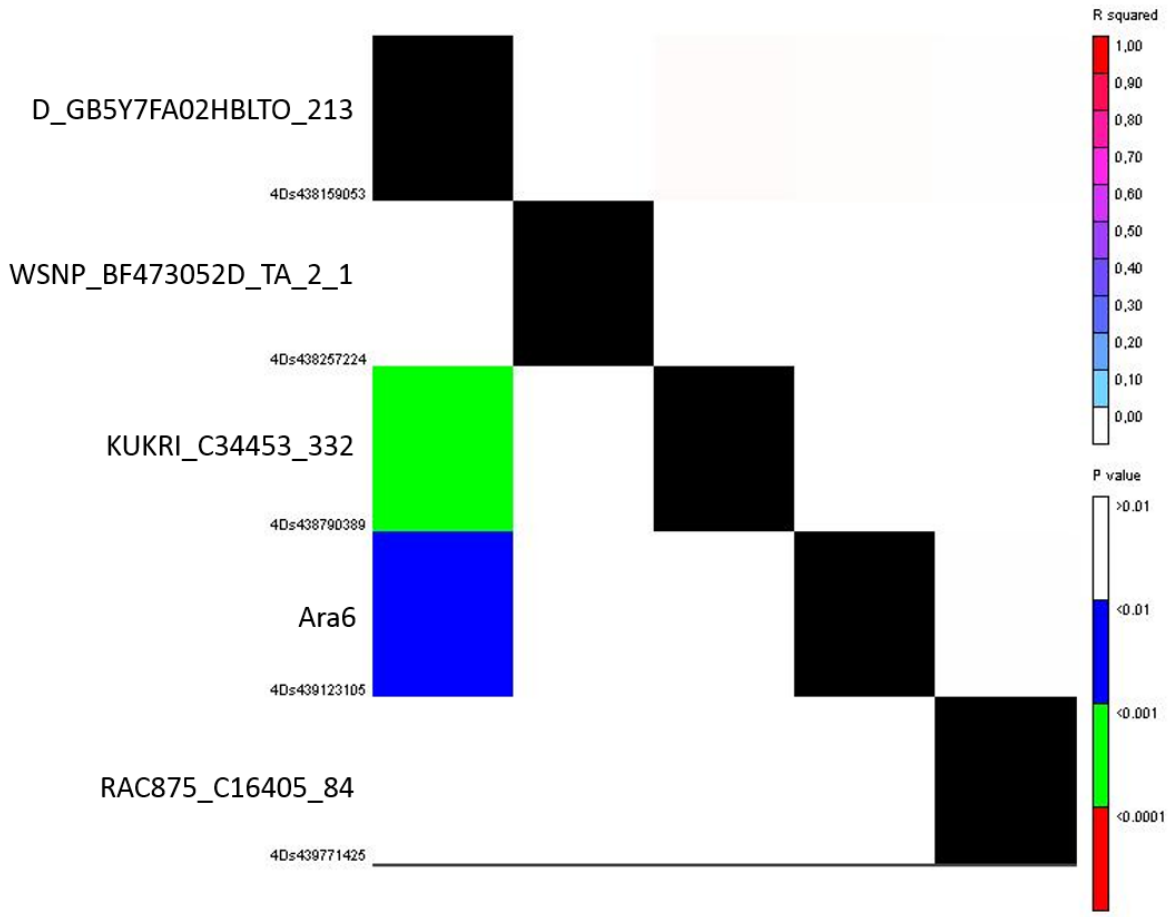

Figure R 13: LD plot of Ara6 marker and nearby lying markers on RefSeq v1.0 physical map.
Pairwise LD as sliding window (window size 50). Above the diagonal, R squered values are displayed and the corresponding p-values for the two-sided Fisher's exact test displayed below the diagonal.

3.1.3.6 Genetic mapping

Since genetic maps are still in use in breeding companies and they offer insight into different recombination rates at different genomic regions, we decided to introduce newly developed markers into genetic maps. Especially the Ara6 marker, influencing FHB severity in wheat, is located far away from other markers placed in the wheat RefSeq v1.0 physical map. The marker analysis was carried out with 100 individuals from the 'Apache x Biscay' population treated as double haploids. That was the only available population that could be used to map significantly associated markers with FHB. After quality control, 3,353 polymorphic markers were left. Markers were grouped with LOD=6 in JoinMap, and 32 linkage groups, containing at least 15 markers were obtained. Even though the RhtD1 marker was present in the study, it was linked with three markers (EXCALIBUR_C19647_294, internal KWS marker, and KUKRI_REP_C68594_530) but was not with the linkage group containing Ara6 marker. A linkage group containing 25 markers was used to create the map of 4D chromosome that presents location of 14 markers and is 53 cM long. The newly developed markers are marked in red. The Ara6 marker lays 11.9 cM away from the nearest marker (Figure R 14).

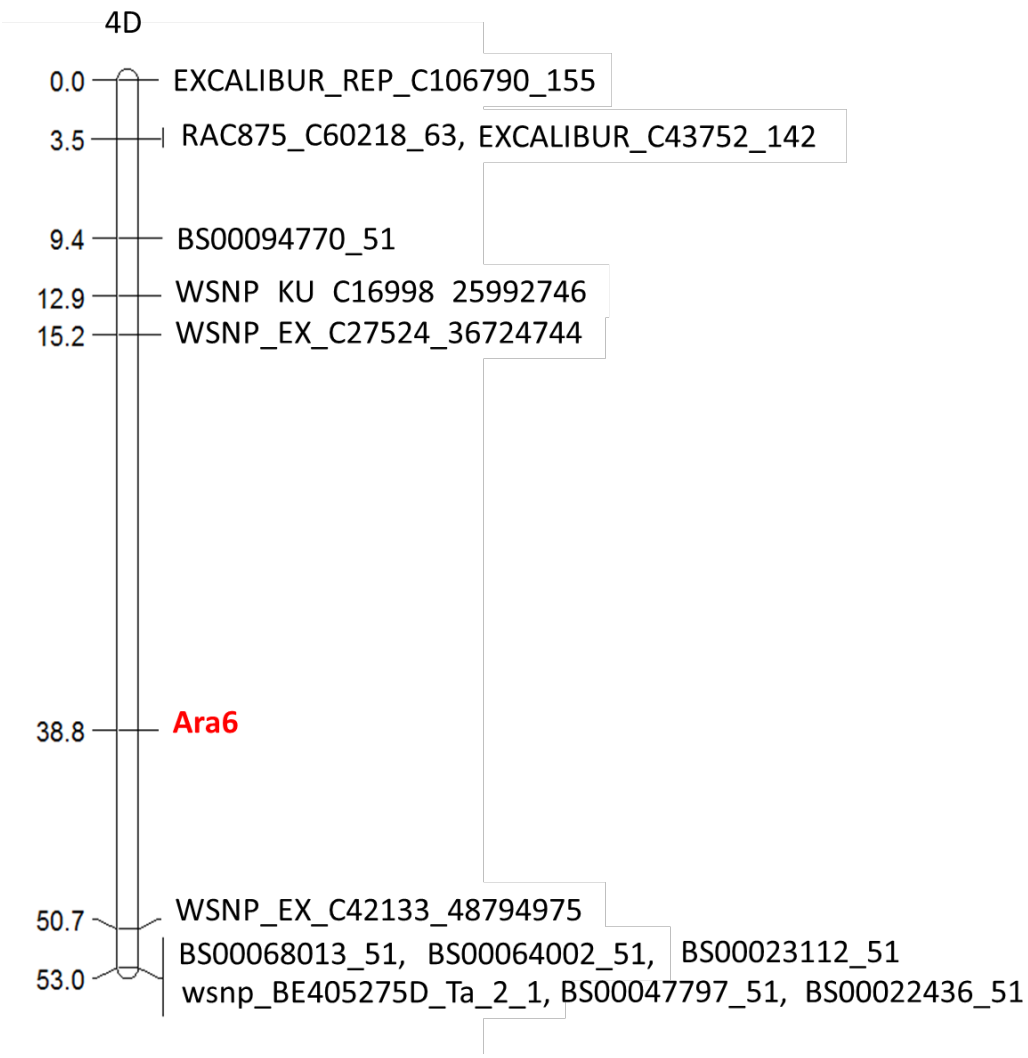

Figure R 14: Genetic map generated using 'Apache x Biscay' population, presenting relative distances of markers in the linkage to the Ara6 marker available for this population.

A linkage group containing 46 markers was used to create 5A chromosome genetic map. This map contains two newly developed markers here and is 121.5 cM long, showing the position of 40 markers. Markers DCL1(1) and DCL1(2) are in the same genetic position as markers KUKRI_C75091_154, WSNP_EX_C23795_33033010, RAC875_C32895_304 (Figure R 15).

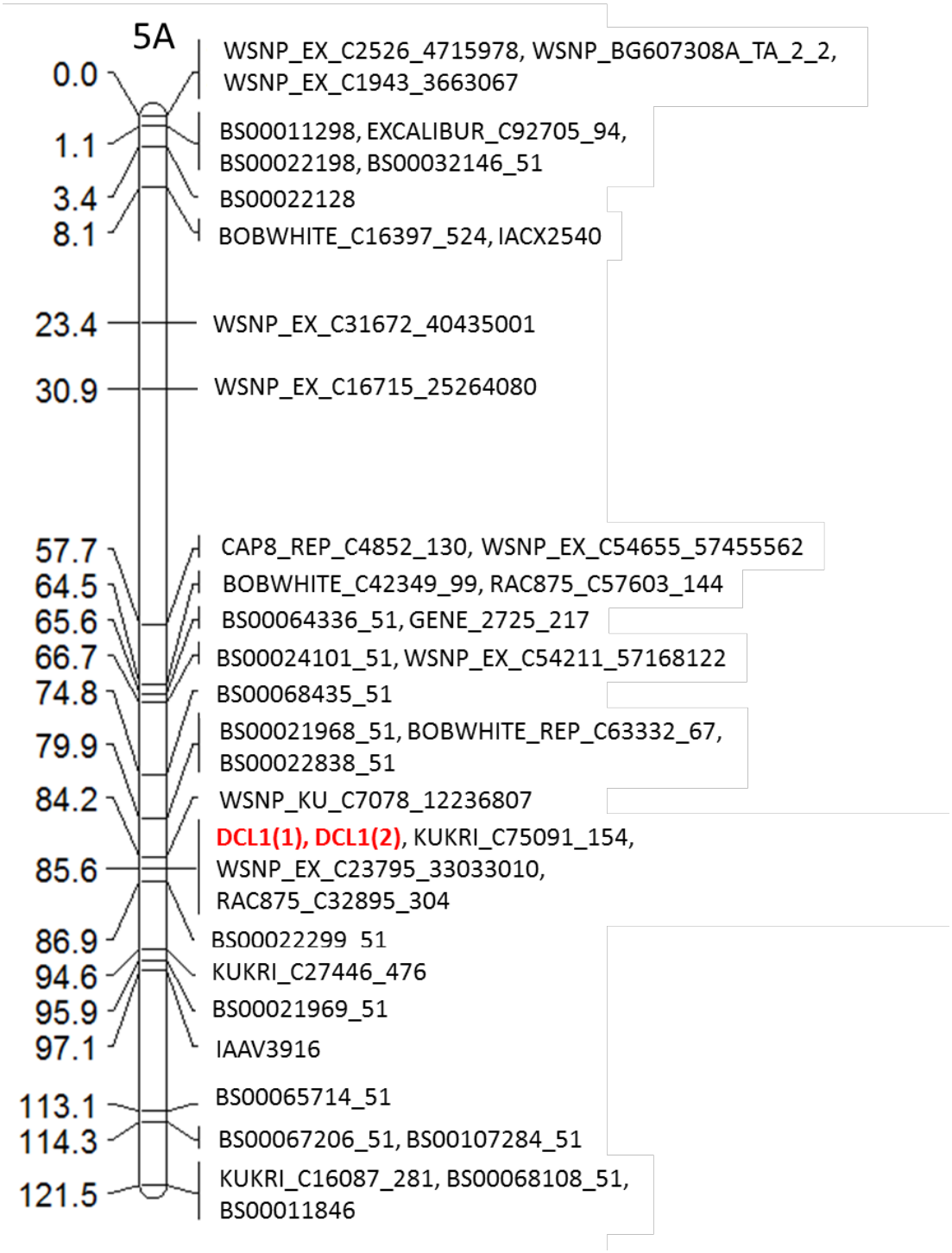

Figure R 15: Genetic map generated using 'Apache x Biscay' population, presenting relative distances of markers being in the linkage to the DCL1(1) and DCL1(2) markers, available for this population.

As the other markers were not associated with FHB resistance we did not introduce them into genetic maps.

3.2 Naturally occurring HIGS in barley against *Fusarium spp*.

The purpose of this part of the work was to demonstrate that the *Fusarium* genes, targets of natural barley sRNA, are essential for the fungus. The basis for further research was the RNAseq data from *Fusarium graminearum* and barley 'Morex' interaction generated in the frame of the dsRNAguard project (coordinated by Dr. Schweizcer). *Fusarium graminearum* and barley 'Morex' were chosen because of the availability of their genomes during the dsRNAguard project. These data were then used to select HIGS candidate genes in *Fusarium* based on the literature (Chacko & Gold, 2012; Cobessi et al., 2012; Ding et al., 2017; Kalidas et al., 2014; Liu et al., 2013; Staerkel et al., 2013; Sun et al., 2020; Zheng et al., 2013). In addition, sequences in barley that presumably could be responsible for the production of sRNAs targeting *Fusarium* genes were looked at. Validation analysis of selected HIGS candidate genes were conducted using VIGS, as a well-established method for such studies, in wheat – *Fusarium culmorum* system (this change was made feasible by the similarity of *Fusarium culmorum* and *Fusarium graminearum* genomes).

3.2.1 Selection of the HIGS candidate genes in *Fusarium*

Based on published evidence (Chacko & Gold, 2012; Cobessi et al., 2012; Ding et al., 2017; Kalidas et al., 2014; Liu et al., 2013; Staerkel et al., 2013; Sun et al., 2020; Zheng et al., 2013) and functional predictions, eight sequences were selected from a list of potential *Fusarium graminearum* targets of natural barley sRNA (sRNA samples were prepared by Dr. Chen and the list of 50 potential candidates was designed by Dr. P. Schweizer (personal communication)). The function of selected target-genes and the characteristics of the matching sRNA are summarized below (Supplementary Data R6):

1. The FGSG_09048 gene, potentially targeted by 13 detected sRNA, encodes a protein related to the bifunctional dethiobiotin synthetase. Inhibition of the biotin synthesis pathway's key enzymes is an attractive way for fungicide development (Cobessi et al., 2012). The expression of normalized amount of sRNA tags targeting *Fusarium* gene FGSG_09048 ranges from 3.5 to more than 100 times higher expression in FHB-infected barley cv. 'Morex' spikes in comparison to the healthy ones. The length of the sRNA sequences ranges from 20-30 nucleotides and hits 18 nucleotides of FGSG_09048 gene.
2. The FGSG_02471 was shown to be required for mating and full virulence of the plant pathogen *Ustilago maydis* (Chacko & Gold, 2012). Only a single sRNA sequence targeting the FGSG_02471 was detected in infected barley spikes. The transcript abundance of this sRNA was 4.4 fold higher in infected spikes compared to healthy ones. The sRNA counts 26 nucleotides, with 17 nucleotides identical to the FGSG_02471 gene.
3. The FGSG_10970 was also targeted by only one sRNA. The gene is involved in vegetative differentiation, asexual development, nuclear migration, and virulence in *F. graminearum*

(Zheng et al., 2013). The sRNA is 25 nucleotides long, where 21 nucleotides are identical to FGSG_10970 target. The sRNA transcript was increased 3.5 times in the infected tissue in comparison to the healthy one.

4. For the function of the fourth candidate - FGSG_01104, no information is available in fungi. However, the gene ortholog PheRSα knockdown resulted in notable effects in the parasite *Trypanosoma brucei*. It affected the cell cycle and cell morphology for PheRSα and led to a strong increase in the population of cells, suggesting a block in cytokinesis (Kalidas et al., 2014). Two sRNA tags were found to target the FGSG_01104 gene, counting 21 and 22 nucleotides and hitting 20 nucleotides sequence of the candidate gene. sRNA expression was induced more than 25 times for both sRNA tags in FHB-infected plants.
5. The FGSG_06175 gene, related to phospholipase d. Deletion of *FgPLD1* resulted in aberrant morphology, including reduced growth, defect in conidiation, and no perithecium formation during the *F. graminearum* sexual reproduction. It also reduced the production of DON and showed decreased virulence in wheat infection (Ding et al., 2017). The gene is targeted by two barley sRNAs of 26 and 27 nucleotides long and up-regulated upon infection of 7.5 and 19.3 times, respectively.
6. The FGSG_08039 gene encoding protein related to sugar transporter. Its orthologue, the glucose sensor-like protein Hxs1, is required for the virulence of *Cryptococcus neoformans* (Liu et al., 2013). The gene is targeted by one sRNA of 26 nucleotides length and induced 3.1 times in the FHB-infected spikes.
7. The FGSG_09183 gene, encoding protein related to o-methyltransferase that was shown to be involved in the pathogenicity of the fungal plant pathogen *Cercospora beticola* (Staerkel et al., 2013). Detected sRNA hitting this *Fusarium* candidate gene counts 31 nucleotides and it is 3.1 times more abundant in FHB infected spike of 'Morex' compared to the non-infected spike.
8. The FGSG_06195 is a gene encoding protein related to succinate dehydrogenase. Its inhibitors are used as fungicides to control FHB (Sun et al., 2020). The gene was targeted by 13 sRNA sequences with a length of 17 to 25 nucleotides and upregulation by the pathogen of 3.1 to 27.9 folds.

3.2.1.1 Analysis of putative barley sequences creating sRNA tags targeting *Fusarium* genes

A search in the barley 'Morex' genome for sequences potentially generating sRNA, like hairpins and inverted repeats, was performed (Table R 7). However, the obtained results should not necessarily cover all possible sRNA origins since many different sRNA biogenesis ways exist. The sequences flanking the studied sRNA in barley were downloaded and checked for the presence of inverted-repeats matching the sRNA sequences.

We did not find any barley sequence that would create sRNA targeting three *Fusarium* genes: FGSG_09048, FGSG_10970, and FGSG_01104 (Table R 7). Barley gene HORVU2Hr1G123570 is potentially able to generate three of the selected sRNA targeting *Fusarium* genes: Inverted repeats matching the sRNAtag883 are located in the nucleotide positions 275-300 and 929-904. Sequences matching the sRNAtag493 were found in positions 227-253 and 977-951 of the gene. And sequences matching sRNAtag1105 are located in positions 188-207 and 1016-997.

The barley HORVU6Hr1G024020 gene potentially creates the sRNAtag1323. Inverted repeats matching the sRNAtag1323 are located in the nucleotide positions 534-564 and 601-631.

A single barley gene that can create the sRNAtag599 was not found, although sRNA sequences in sense and antisense orientation were found in the barley genome. The barely sequences putatively producing sRNAs targeting *Fusarium* genes may be found in Supplementary Data R14.

Table R 7: Sequences in barley genome that may be responsible for sRNA targeting *Fusarium* genes creation.

Candidate	Sequence found in sense-antisense orientation in barley	Visualization of the sequence potentially creating sRNA in RegRNA 2.0
FGSG_09048	not found	-
FGSG_02471	>HORVU2Hr1G123570:HORVU2Hr1G123570.1 HORVU2Hr1G123570	
FGSG_10970	not found	-
FGSG_01104	not found	-
FGSG_06175	>HORVU2Hr1G123570:HORVU2Hr1G123570.1 HORVU2Hr1G123570	
FGSG_08039	>chr5H dna:chromosome chromosome:IBSC_v2:chr5H:59593881:59597909:1	
FGSG_09183	>HORVU6Hr1G024020:HORVU6Hr1G024020.1 HORVU6Hr1G024020	
FGSG_06195	>HORVU2Hr1G123570:HORVU2Hr1G123570.1 HORVU2Hr1G123570	

3.2.2 Stability of the BSMV

Virus-Induced Gene Silencing (VIGS) method was chosen as an efficient and well-established method for *Fusarium* genes functional analysis (Chen et al., 2016). Initially, the virus infection for VIGS was made via *in vitro* transcription and inoculation with the RNA by rubbing it into the leaves. However, this efficiency of the method was shown to be relatively low and not enough to achieve the minimal criteria of at least 7 BSMV positive plants per construct. Therefore an alternative method that uses an intermediate host (barley cv. 'Black Hulless') for the multiplication of the virus was selected. The intermediate host was infected via biolistic bombardment of microprojectiles coated with viral RNA-overexpressing DNA constructs. After the developing and multiplication of the virus, a leaf extract from the infected plants was used to infect the test plants. With this method, the infection efficiency significantly improved and exceeded 90%.

However, introducing an intermediate virus multiplication step also increases the risks of losing the transgenic insert, especially for larger inserts, as shown by Bruun-Rasmussen et al. (2007). To estimate the insert's optimal length that will allow efficient silencing and high stability, a series of constructs with different lengths was prepared and tested.

3.2.2.1 The stability of the virus in 'Black Hulless' is dependent on the length of the insert in the BSMV:γ vector

Different *Fusarium* sequences with various lengths were inserted into the BSMV:γ vector. The series included inserts of 104 nt, 164 nt, 180 nt, 233 nt (Figure R 16), 344 and 442 nt (Figure R 10). Figure R 16 and Figure R 17 show the products of PCR obtained by amplification of cDNA from the second leaf of 'Black Hulless' barley plants after particle bombardment with BSMV:α, BSMV:β, and BSMV:γ / recombinant BSMV:γ. Used primers are located in BSMV:γ, flanking the inserts (Figure R 16 and Figure R 17). Figure R 16 presents additional sequences that were amplified with insert-specific primers and a combination of insert-specific primer and BSMV:γ primer. The expected lengths of the PCR products are shown in Table R 8. BSMV:γ / recombinant BSMV:γ vectors used for microprojectile bombardment were used as a positive control (C+). Second leaves from 'Black Hulless' showing no BSMV symptoms were used as a negative control (C-). $BSMV_{FGSG_06175(495)}$ sample was a cDNA from the 'Black Hulless' plant that was particle bombarded with the appropriate set of vectors but did not show BSMV phenotype (Figure R 16)

Table R 8: Expected lengths of the PCR product:

	BSMV:γ specific primers (Figure R 16 and Figure R 17)	**Inserts specific primers (Figure R 16)**	**Combination of insert specific primer and BSMV:γ located primer (Figure R 16)**
BSMV:γ	147 nt	-	-
BSMV$_{FGSG_06175(190)}$	337 nt	-	-
BSMV$_{FGSG_10970(233)}$	380 nt	-	-
BSMV$_{FGSG_06195(164)}$	311 nt	-	-
BSMV$_{FGSG_06175(104)}$	327 nt	-	-
BSMV$_{FGSG_10970(442)}$	589 nt	442 nt	506 nt
BSMV$_{FGSG_01104(344)}$	491 nt	344 nt	408 nt
BSMV$_{FGSG_06175(495)}$	642 nt	495 nt	559 nt

Insert in BSMV$_{FGSG_06175(442)}$ is not detectable when amplified with BSMV:γ specific primers when majority of insert in BSMV$_{FGSG_01104(344)}$ is still intact. Inserts in both BSMV$_{FGSG_06175(442)}$ and BSMV$_{FGSG_01104(344)}$ are detectable when amplified with a combination of insert specific and BSMV:γ specific primers and with insert specific primers, but part of the insert in BSMV$_{FGSG_01104(344)}$ is lost (Figure R 16). Most of the insert in BSMV$_{FGSG_01104(344)}$ is intact, but partial deletions are observed when amplified with all tested here primer pairs (Figure R 16).

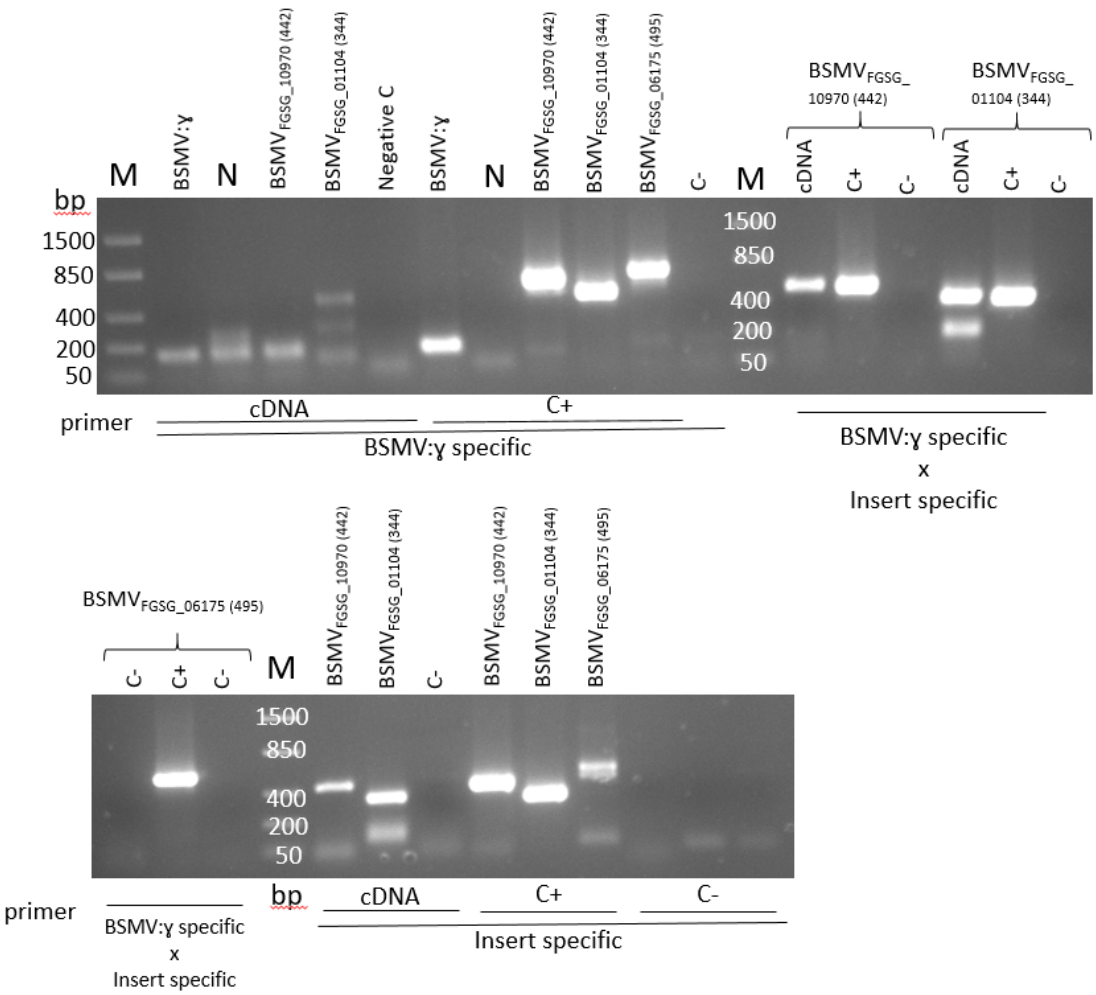

Figure R 16: Amplification of cDNA obtained from the second leaf of 'Black Hulless' barley plants after particle bombardment with BSMV:α, BSMV:β and BSMV:γ / recombinant BSMV:γ showed significant reduction / loss of inserts in BSMV:γ, having a length greated than or equal to 344 nt.
Primers used in RT-PCR are T7-gamma / T7-gamma 5' x insert specific 5' / insert specific (Supplementary Data M9). C+ is BSMV:γ / recombinant BSMV:γ vector used for microprojectile bombardment. C- is the second leaf of 'Black Hulless' not showing phenotypically BSMV symptoms. The expected lengths of the PCR product of $BSMV_{FGSG_10970(442)}$ is 589, $BSMV_{FGSG_01104(344)}$ is 491, $BSMV_{FGSG_06175(495)}$ is 642, when amplified with BSMV:γ specific primers. When amplified with combination of the primers (one located in the insert, one in BSMV:γ) it is: $BSMV_{FGSG_10970(442)}$ - 506 nt, $BSMV_{FGSG_01104(344)}$ - 408 nt, $BSMV_{FGSG_06175(495)}$ - 559 nt and when amplified with insert specific primers it is: $BSMV_{FGSG_10970(442)}$ - 442 nt, $BSMV_{FGSG_01104(344)}$ - 344 nt,, $BSMV_{FGSG_06175(495)}$ - 495 nt. N are unrelated samples. FastRuler Low Range DNA Ladder (Thermo Scientific) was used as a DNA size standard.

Figure R 17 presents the amplification of shorter inserts. $BSMV_{FGSG_06175(104)}$ (Figure R 17) was intact after the 8-day duration of the experiment when the rest of the recombinant vectors presented on Figure R 17 were stable, but a very slight reduction/losing of the insert can be observed.

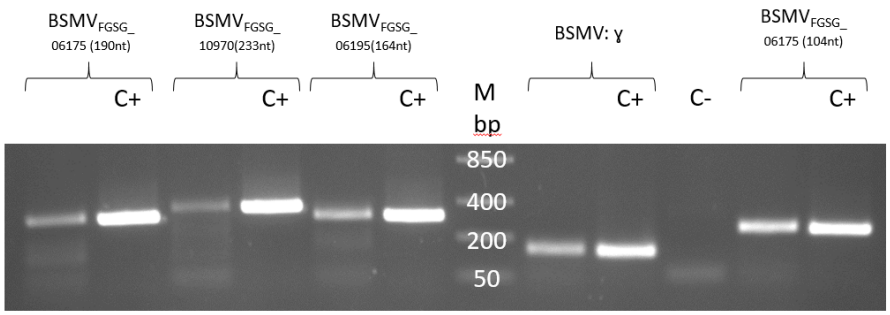

Figure R 17: Amplification of cDNA obtained from the second leaf of 'Black Hulless' barley plants after particle bombardment with BSMV:α, BSMV:β and BSMV:γ / recombinant BSMV:γ showed slight reduction/losing of the inserts in BSMV:γ, having a length greated than or equal to 164 nt. $BSMV_{FGSG_06175(104)}$ appears intact. Primers used in RT-PCR are T7-gamma (Supplementary Data M9). C+ is positive control that is BSMV:γ / recombinant BSMV:γ vector used for microprojectile bombardment. C- is a second leaf of 'Black Hulless' not showing phenotypically BSMV symptoms. Expected lengths of the PCR product of $BSMV_{FGSG_06175(190)}$ is 337 nt, $BSMV_{FGSG_10970(233)}$ is 380 nt, $BSMV_{FGSG_06195(164)}$ is 311 nt, BSMV:γ is 147, $BSMV_{FGSG_06175(104)}$ is 327 nt. FastRuler Low Range DNA Ladder (Thermo Scientific) was used as a DNA size standard.

The $BSMV_{FGSG_10970(442)}$ with the longest insert was the most unstable in 'Black Hulless'. The insert is not longer detectable after 8-days when amplifying by BSMV:γ specific primers, even though insert-specific primers can still amplify it. Therefore, we wanted to see if long inserts (344, 442, and 495 nt) are still detectable when the spikelet is inoculated with FHB (around 20 days of the experiment). Sequences of lengths 344 nt, 442 nt, and 495 nt were amplified from 'Apogee' spikelets cDNA with primers located in BSMV:γ (not shown here) and the combination of insert specific primer and BSMV:γ specific. None of the targets could be amplified with the combination of the primers (Supplementary Data R7). The 344 nt and 442 nt inserts were indetectable with BSMV:γ specific primers. The 495 nt insert was also nearly lost, with a very short part of the insert still left on the viral cDNA (Supplementary Data R7).

3.2.2.2 The 104 nt and 180 nt Inserts carried in BSMV:γ vectors were mainly stable over the entire VIGS experiment

The virus's stability in the bombardment-mediated VIGS experiments, which take around 30 days, was estimated by checking part of the samples. The experiments include inserts of size 104 nt, 180 nt, and 233 nt (Figure R 18 and R 19). Figures R 18 and R 19 show the PCR products obtained by primers flanking the inserts in the BSMV:γ using the 'Apogee' spikes cDNA template. BSMV:γ vectors used for microprojectile bombardment (recombinant and without insert) were used as positive controls (C+). The mock plants were infected with FHB but not with the BSMV. The expected lengths of the PCR product of $BSMV_{FGSG_06175(180)}$ is 337 nt, $BSMV_{FGSG_10970(233)}$ is 380 nt, and $BSMV_{FGSG_06175(104)}$ is 327 nt (Figure R 18 and R 19). Insert carried in $BSMV_{FGSG_06175(104)}$ (Figure R 18) was intact in most samples over the entire VIGS experiment, where some deletions or reductions of the insert in $BSMV_{FGSG_06175(180)}$ were observed (Figure R 18 and R 19). The longer insert of 233 nt was deleted in almost all samples in $BSMV_{FGSG_10970(233)}$ (Figure R 19). Part of the samples was tested for the presence of the BSMV using RT-

PCR with γ specific primers (Figure R 18 and R 19). The results confirmed that visual BSMV phenotyping is a reliable selection method. A discrepancy was found in only one sample phenotyped as BSMV negative, but virus RNA was detectable by the RT-PCR. Based on these results, the sorting to BSMV-positive and -negative plants was further done using only the phenotype.

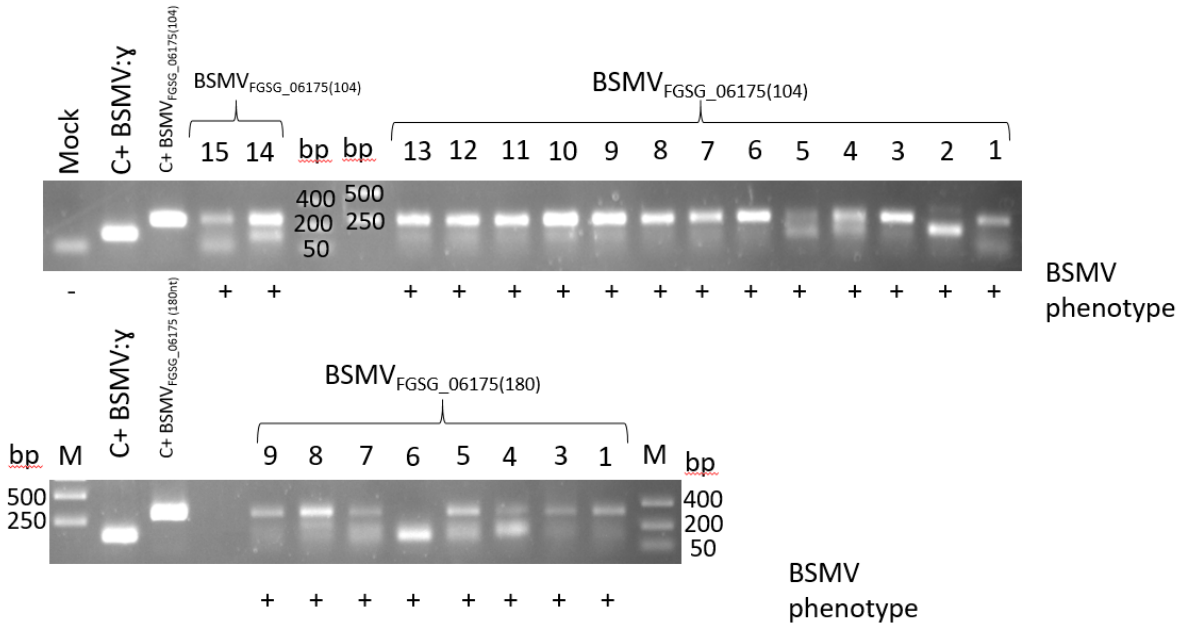

Figure R 18: Amplification of cDNA obtained from 'Apogee' wheat plants after the entire VIGS experiment showed that insert carried in BSMVFGSG_06175(104) was intact in most samples, where some deletions/reductions of the insert in BSMVFGSG_06175(180) were observed.
Primers used in RT-PCR are T7-gamma (Supplementary Data M9). The mock plants are wheat infected only with FHB but not BSMV in the same VIGS experiment. C+ BSMV:γ is a BSMV:γ vector also used for microprojectile bombardment. C+ $BSMV_{FGSG_06175(104)}$ is modified plasmid BSMV:γ, carrying 104 nt long sequences of FGSG_06175 gene. C+ $BSMV_{FGSG_06175(180)}$ is modified plasmid BSMV:γ, carrying 180 nt long sequence of FGSG_06175 gene. Expected product lengths of C+ BSMV:γ is 147 nt, C+ $BSMV_{FGSG_06175(104)}$ is 251 nt and C+ $BSMV_{FGSG_06175(180)}$ is 327 nt. + / - BSMV phenotype is plants BSMV phenotype observed during experiment. FastRuler Low Range DNA Ladder (Thermo Scientific) and GeneRuler 1 kb DNA Ladder (Thermo Scientific) were used as DNA size standard.

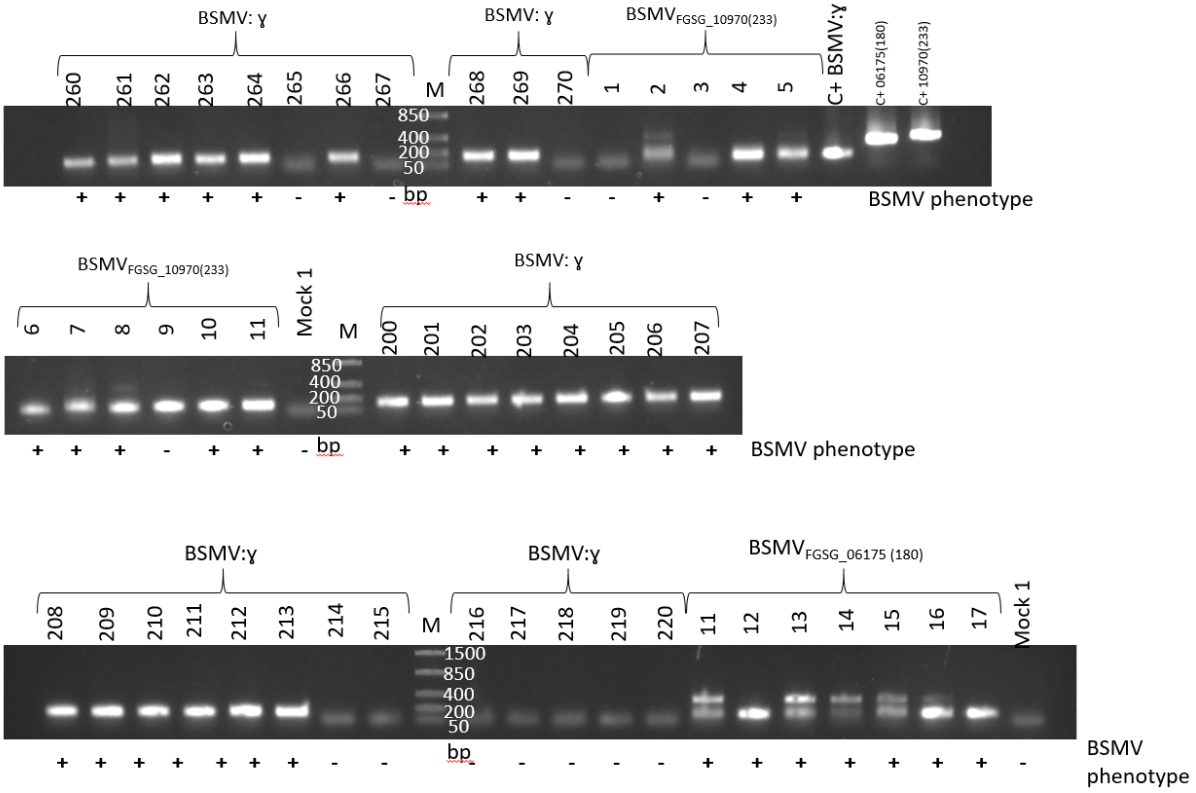

Figure R 19: Amplification of cDNA obtained from 'Apogee' wheat plants after the entire VIGS experiment showed some deletions/reductions of the 180 nt insert in BSMV$_{FGSG_06175(180)}$, where insert of 233 nt was deleted in almost all samples in BSMV$_{FGSG_10970(233)}$.
Primers used in RT-PCR are T7-gamma (Supplementary Data M9). Mock plant is a wheat plant not infected with BSMV, FHB infected being a part of the same VIGS experiment as the rest of the shown plants here. C+ BSMV:ɣ is a BSMV:ɣ vector also used for microprojectile bombardment. C+ BSMV$_{FGSG_10970(233)}$ is modified plasmid BSMV:ɣ, carrying 233 nt long sequence of FGSG_10970. C+ BSMV$_{FGSG_06175(180)}$ is a modified plasmid BSMV:ɣ, carrying 180 nt long sequence of FGSG_06175 gene. Expected product lengths of C+ BSMV:ɣ is 147 nt, C+ BSMV$_{FGSG_10970(233)}$ is 380 nt and C+ BSMV$_{FGSG_06175(180)}$ is 327 nt. + / - BSMV phenotype is plants BSMV phenotype observed during experiment. FastRuler Low Range DNA Ladder (Thermo Scientific) was used as a DNA size standard.

3.2.3 Two of the chosen candidate genes were shown to be essential for FHB development

VIGS *via* in vitro transcription method was used to test FGSG_09048, FGSG_06195, FGSG_01104, and FGSG_06175 genes. The cloning of the FGSG_08039 and FGSG_09183 sequences remained unsuccessful regardless of all efforts. Since the VIGS infection efficiency *via in vitro* transcription was very low, the bombardment-mediated VIGS replaced it, as explained above. Due to the change in the methodology and the time constraints, only four top candidates were finally tested (FGSG_10970, FGSG_01104, FGSG_06175, FGSG_06195). Various independent experiments were performed (1-5) depending on the candidate and the results (Table R 9). Additionally, two experiments combining two recombinant BSMV, namely BSMV$_{FGSG_06175(180)}$ and BSMV$_{FGSG_10970(233)}$ were performed. If no reduction of the FHB infection on virus-positive wheat spikes was observed, the candidates were excluded from further experiments.

Table R 9: The number of experiments with the number of BSMV-positive plants performed for each construct are shown in the table below. BSMV carrying different inserts were used to validate HIGS candidate genes in Fusarium.

Construct	No. of experiments	No. of recombinant BSMV+ plants	No. of BSMV:00+ plants
$BSMV_{FGSG_10970(233)}$	5	50	59
$BSMV_{FGSG_06175(104)}$	2	25	26
$BSMV_{FGSG_06175(180)}$	5	66	67
$BSMV_{FGSG_01104(107)}$	2	30	25
$BSMV_{FGSG_06195(164)}$	2	20	24
$BSMV_{FGSG_06175(180)+FGSG_10970(233)}$	2	28	26

Wheat spikes were point-inoculated with *Fusarium culmorum* macroconidia. The VIGS effects were always compared to the BSMV:00-infected plants and not the mock-treated controls. Samples that did not show FHB infection symptoms 20 days after FHB inoculation were removed from the analysis. The FHB infection analysis on the plants treated with the recombinant virus was performed using Wilcoxon Signed Rank Test. This test is nonparametric, and it does not require the normal distribution of the data. The results and FHB severity are presented in Supplementary Data R15.

Interestingly, FHB severity in plants carrying $BSMV_{FGSG_10970(233)}$ and $BSMV_{FGSG_06175(180)}$ was significantly reduced on some FHB developmental stages compared to plants carrying BSMV:00. Five independent experiments were performed for candidates FGSG_10970(233) and FGSG_06175(180). Plants carrying the $BSMV_{FGSG_10970(233)}$ virus showed less FHB disease symptoms than plants carrying BSMV:00 at every stage of FHB development. The plants carrying the recombinant virus showed significantly less disease symptoms after seven (on average 35%, *P*=0.0119) and ten days (on average 15%, *P*=0,0099) after the point inoculation in comparison to the plants carrying non-recombinant BSMV (Figure R 20, Supplementary Data R15).

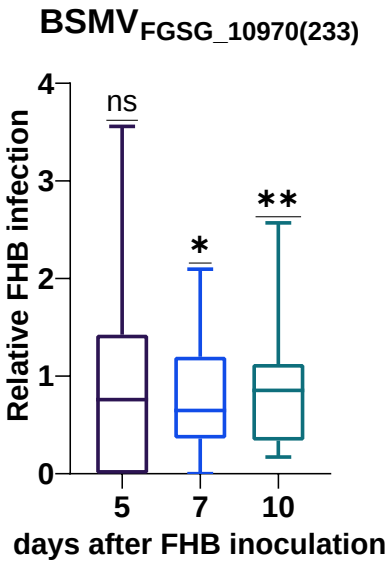

Figure R 20: Plants carrying the $BSMV_{FGSG_10970(233)}$ virus showed significantly less FHB disease symptoms than plants carrying BSMV:00 after seven and ten days after the point inoculation.
Relative FHB infection is shown for 'Apogee' wheat plants inoculated with recombinant BSMV, carrying FGSG_10970(233) insert. FHB severity was compared to the control plants carrying BSMV:00 and set as 1. Assessment of FHB severity was made five, seven and ten days after *Fusarium* inoculation of the wheat spike.

Moreover, plants carrying the $BSMV_{FGSG_06175}$ virus showed significantly less FHB disease symptoms than plants carrying non-recombinant vector, even though the effect disappeared after ten days and plants reached the severity of FHB infection of the BSMV:00 plants. This phenomenon was observed for plants treated with $BSMV_{FGSG_06175}$ carrying 104 nt and 180 nt insert. Five days after point inoculation with *Fusarium* macroconidia, plants inoculated with $BSMV_{FGSG_06175(180)}$ demonstrated on average 58% fewer disease symptoms than control (*P*= 0.0011). Seven days after point inoculation, wheat spikes showed on average 22% fewer FHB disease symptoms than control (*P*=0.0201). The effect disappeared after ten days, and plants were on average 3% less affected by FHB than control (Figure R 21, Supplementary Data R15). Similarly, five days after FHB inoculation, plants carrying $BSMV_{FGSG_06175(104)}$ showed 60% fewer FHB symptoms than plants carrying BSMV:00 (*P*=0.0015). Seven days post-FHB inoculation, the same effect was, although visible, not statistically significant. Ten days after FHB inoculation, the wheat plants carrying $BSMV_{FGSG_06175(104)}$ reached the same infection level as the BSMV:00 infected plants (Figure R 21, Supplementary Data R15).

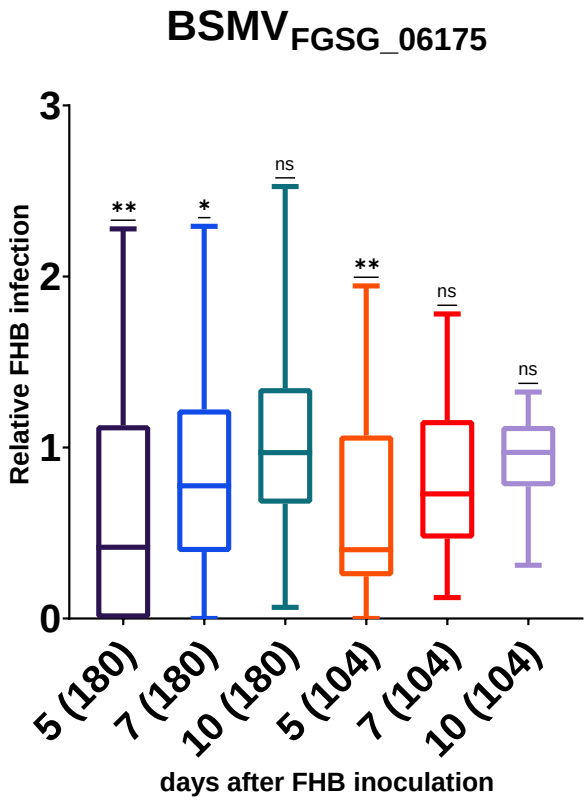

Figure R 21: Plants carrying the $BSMV_{FGSG_06175}$ virus showed less FHB disease symptoms than plants carrying a non-recombinant vector at some stage of FHB development.
Relative FHB infection is shown for 'Apogee' wheat plants inoculated with recombinant BSMVs, carrying FGSG_06175 inserts of two lengths (104 and 180 nt). FHB severity was compared to the control plants carrying BSMV:00 and set as 1. Assessment of FHB severity was made five, seven, and ten days after *Fusarium* inoculation of the wheat spike.

A combination of FGSG_10970(233) and FGSG_06175(180) constructs was tested as well. Plants carrying two recombinant viruses ($BSMV_{FGSG_06175(180)}$ and $BSMV_{FGSG_10970}$) showed significantly reduced FHB disease symptoms in comparison to the control. After five days post-FHB infection, the median calculated from 25 FHB-positive plants was 0 (P=0.0438). After seven days, plants carrying a combination of the recombinant BSMV showed on average 70% less FHB disease symptoms (P= <0.0001) and after ten days on average 34% fewer FHB symptoms (P=0.0386) than plants carrying BSMV:00 (Figure R 22, Supplementary Data R15).

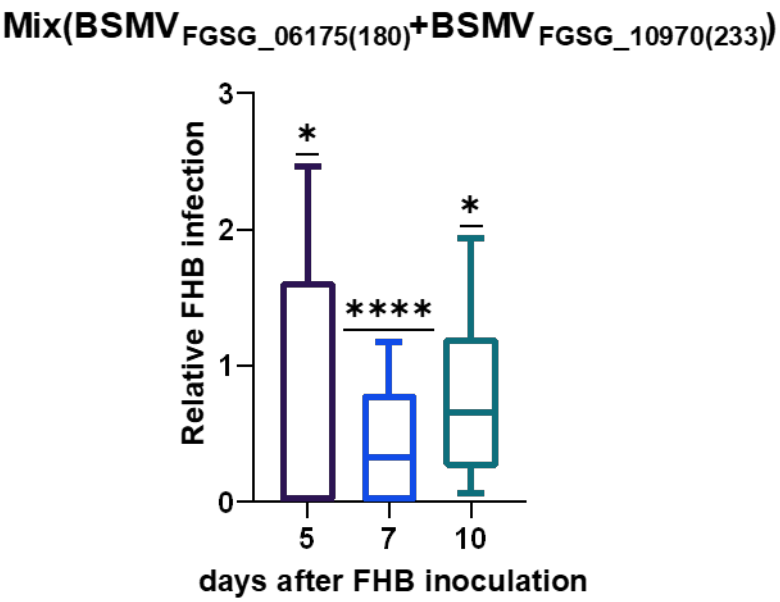

Figure R 22: Plants carrying two recombinant viruses ($BSMV_{FGSG_06175(180)}$ and $BSMV_{FGSG_10970}$) showed significantly reduced FHB disease symptoms compared to the control.
Relative FHB infection was shown for 'Apogee' wheat plants inoculated with recombinant BSMVs, carrying FGSG_10970(233) and FGSG_06175(180) inserts. FHB severity was compared to the control plants carrying BSMV:00 and set as 1. Assessment of FHB severity was made five, seven and ten days after *Fusarium* inoculation of the wheat spike.

Plants carrying $BSMV_{FGSG_06195(164)}$ did not show higher or lower resistance to FHB infection than the plants carrying BMSV:00 (Supplementary Data R15 and R8). Plants carrying $BSMV_{FGSG_01104(107)}$ were significantly more susceptible than control five and ten days after FHB inoculation (Supplementary Data R15 and R9).

Expression analyses were not performed on the entire set of samples with phenotypic data because the results of the partial data indicated a lack of silencing in most samples. Of 26 plants carrying $BSMV_{FGSG_06175(180)}$, only in five reduced transcript abundances were measured (<90% of the gene expression in BSMV:00). Nine out of 15 plants carrying $BSMV_{FGSG_06175(104)}$ and six out of 29 plants carrying $BSMV_{FGSG_10970(233)}$ had reduced transcript abundances (Supplementary Data R15 and R9).

3.2.4 Gene expression analysis vs. stability of the BSMV

Unlike in other similar studies (Brunn-Rasmussen et al., 2007) focusing on the silencing of host genes, the sRNA molecules produced in wheat have to be transferred to *Fusarium* to silence the expression of the fungal genes (HIGS). In addition, BSMV is passed over an intermediate host, so it was essential to check that the insert in the virus was stable throughout the experiment. This stability control enables examination of whether there was a link between the BSMV insert size, stability, and silencing efficiency. The expression of the VIGS targets was tested in the same pool of samples used to evaluate the stability of the BSMV. U. The relative quantity of transcript of the target gene was normalized to the gene encoding the translation elongation factor 1 of *Fusarium culmorum* (*Fc*EF1, accession no. JF740860.1) (Chen et al., 2016). The stability of the inserts in BSMV was visually estimated on electrophoresis gels, showing the amplicon sizes of the inserts from 'Apogee' cDNA isolated at the end of the VIGS experiment (Figure R 18 and 19). The intensity of the band corresponding to the full insert size was compared to the smaller size amplicons of the partially or fully aborted transgenic insert (the example in Figure R 23, Table R 10, and Supplementary Data R10):

Table R 10: The following relative criteria were used to assess recombinant BSMV stability of the insert after accomplishing the VIGS experiment.

Stability	Description	Example
1	The full-insert band is significantly stronger than the smaller bands suggesting that the insert in BSMV:ɣ is intact.	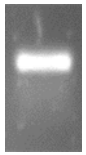 Band corresponding to the full insert size. Bands corresponding to the deteriorated insert and insert size of empty BSMV:ɣ are not visible.
0.6-0.9	The intensity of the full-insert band is reduced, and the lower bands are increased.	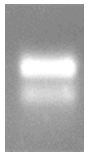 Band corresponding to the full insert size. Band corresponding to the insert size of empty BSMV:ɣ.
0.5	The complete- and deteriorated insert bands are in approximately equal intensity.	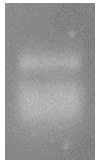 Band corresponding to the full insert size. Bands corresponding to the deteriorated insert and insert size of empty BSMV:ɣ.
0.1-0.4	The deteriorated insert bands are stronger than the full-insert band.	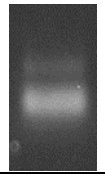 Band corresponding to the full insert size. Bands corresponding to the deteriorated insert and insert size of empty BSMV:ɣ.
0	Only amplicons with the size of empty BSMV:ɣ are present. The insert is completely lost.	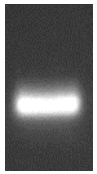 Band corresponding to the full insert size is not visible. Band corresponding to the insert size of empty BSMV:ɣ.

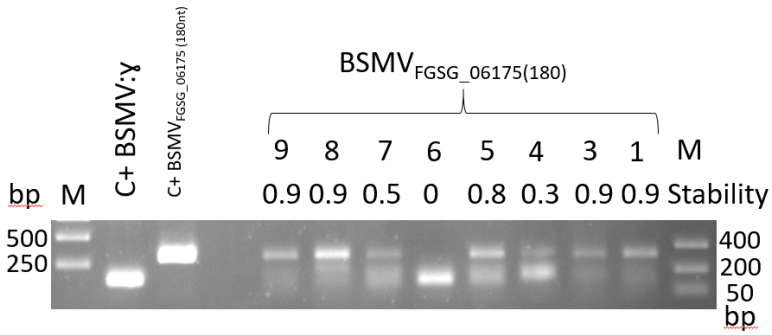

Figure R 23: Example of the visual assessment of the recombinant BSMV stability of the insert after accomplishing the VIGS experiment.
The stability was scored on a scale from 0 to 1, where 0 means that the insert is completely lost, and 1 means that the insert seems to be fully intact.

The correlation between gene expression of samples and inserts stability is 0.006 for BSMV$_{FGSG_06175(104)}$, 0.428 for BSMV$_{FGSG_06175(180)}$ and 0.372 for BSMV$_{FGSG_10970(233)}$. Thus there was no correlation between the stability of the virus and the target gene silencing for the smallest inserts, as the insert is generally stable. For the larger inserts, the correlation increases but remains low. Figure R 24 shows samples with their gene expression compared to the control (BSMV:00 infected plants) and the estimated insert stability in the corresponding samples (see Supplementary Data R15). The target silencing is the highest with the short insert (probably because of the better stability). Gene expression analysis was performed up to 10 days after the point inoculation with *Fusarium* when the FHB severity reached the levels of the BSMV:00 controls (Figure R 24).

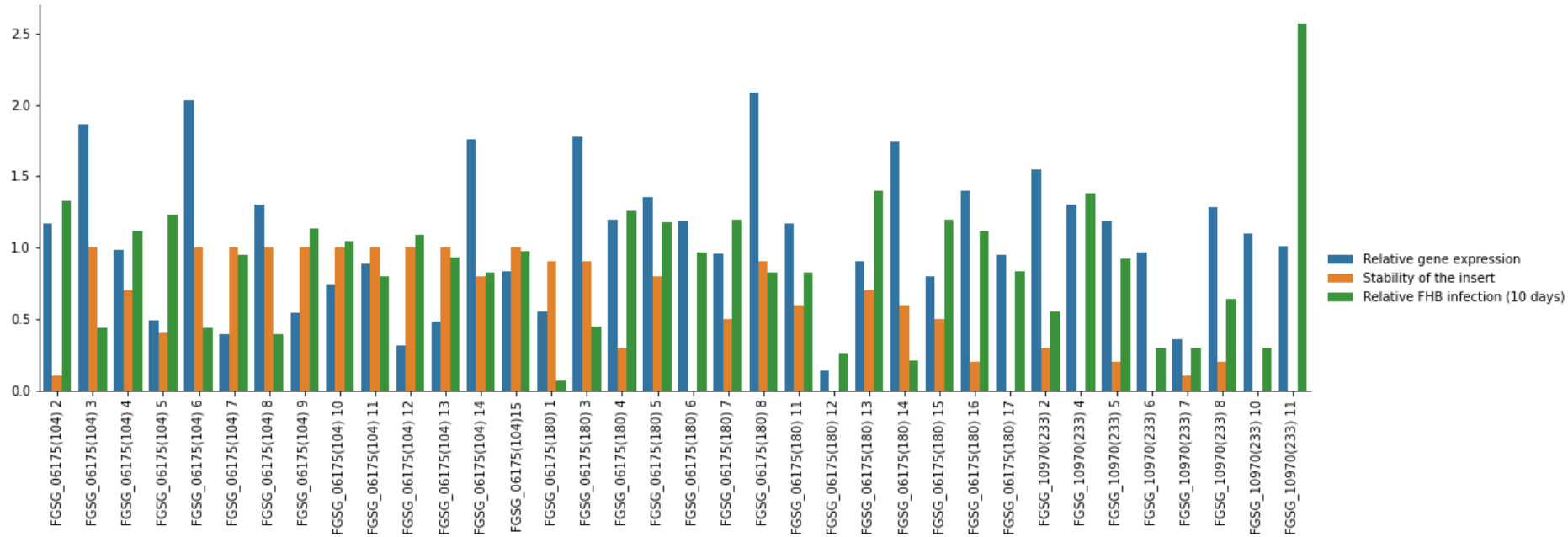

Figure R 24: Graph presenting samples with their gene expression paired with estimated insert stability (0 - insert is lost; 1 - insert is fully intact) and relative gene expression (10 days after *Fusarium* inoculation of the wheat spike).

4. Discussion

Host-induced gene silencing is an emerging approach for engineering crop disease resistance. A detailed understanding of this phenomenon will help developing efficient strategies for designing sustainable disease resistance and reducing the application of synthetic pesticides. This work studied the mechanism of HIGS using functional molecular and genetic approaches. In addition, the natural occurrence of HIGS, an important defense mechanism and a phenomenon that could potentially be exploited in breeding, was also investigated.

4.1.1 A critical view on the experimental design for functional validation and study of HIGS candidate genes

The genes and mechanisms involved in HIGS are poorly understood as it is a relatively newly discovered phenomenon. However, as typical for complex biological processes, many genes might be directly or indirectly involved in HIGS. Literature searches and educated guesses can provide several candidate genes, but confirming their involvement in HIGS requires validating their function in a suitable assay system. In this study, several approaches were evaluated. Typically, stably genetically transformed plants provide the most convincing evidence (Nowara et al., 2010). However, the stable transformation of plants is laborious and time-consuming and, therefore, hardly provides an option for screening many candidate genes (Chen et al., 2016).

A straightforward option for screening purposes is a method referred to as Virus-Induced Gene Silencing (VIGS) mediated by Barley Stripe Mosaic Virus (BSMV). VIGS is a powerful and efficient tool for analyzing gene function in cereals (Gunupuru et al., 2019). However, the presence of virus vectors can interfere with plant metabolism and affect interaction studies between plants and microbes (Dagnachew et al., 2019). Moreover, inserted genes in the VIGS vector can influence virus multiplication, and some viruses tend to delete the insert during multiplication (Dagnachew et al., 2019).

Another alternative is the transient-induced gene silencing (TIGS) method based on biolistic transgene delivery enabling high-throughput assessment of gene function. The method appropriately allows addressing gene functions in epidermal cells, resulting in a susceptible or resistant phenotype to the powdery mildew fungus. It allows addressing gene function on a large scale for both plant genes (Douchkov et al., 2014; Douchkov et al., 2005) and fungal RNAi targets (Nowara et al., 2010; Pliego et al., 2013). Because of the large number of candidate genes (156) selected in this study, the TIGS method was chosen as the most appropriate. However, this method has several limitations that should be considered when interpreting the results. As with all available methods for transient

transformation, TIGS is invasive, and the damage caused may trigger stress responses, altering the genes expression and potentially affecting the outcome of the experiments (Lacroix & Citovsky, 2020). Importantly, the method is most efficient in transforming epidermis cells, making it primarily suitable for epiphytic pathogens such as the powdery mildews. Also, the effect estimation is based on statistical methods, which are reliable only after reaching a relatively high number of transformation events. A high variation between the experiments is also often observed (Pliego et al., 2013), and multiple biological repetitions for achieving reliable results are unavoidable. Nevertheless, the TIGS method was chosen because of its efficiency, allowing for the screening of many candidate genes (Douchkov et al., 2014).

Besides selecting a test system, an essential requirement for establishing the HIGS test system is finding a highly susceptible genotype that would allow sensitive quantification of the alteration of the susceptibility. Some of the genotypes previously known to be highly susceptible like 'Manchuria' (Andersen & Torp, 1986), 'Pallas' (Andersen & Torp, 1986), 'Ingrid' (Saja et al., 2020), 'Golden Promise', 'Hanna', and the landrace 'HOR728' were tested and revealed significant differences between the genotypes. The cultivars 'Manchuria' and 'Hanna' were the most susceptible genotypes of the tested ones and were selected for the screen.

Douchkov et al. (2005) tested the possibility of co-silencing several barley genes. Co-bombardment of three additional RNAi constructs and a *Mlo* gene-silencing RNAi construct caused a decrease in the silencing efficiency for *Mlo*. However, RNAi constructs targeting the *Hv*GLP4 part of a *Hv*GLP:GFP fusion construct were still able to suppress the accumulation of the *Hv*GLP4:GFP fusion protein in the presence of up to twelve different RNAi constructs (Douchkov et al., 2005), which demonstrates that the silencing efficiency of multiple RNAi constructs strongly depends on the target. Therefore, we decided to co-bombard not more than two RNAi constructs simultaneously.

RNAi constructs for silencing fungal and host genes were planned to be co-bombarded in experiments, including three different controls. An empty vector control was used to estimate the basal level of susceptibility of barley leaves to powdery mildew in each experiment; a second control for the effect of the targeted candidate barley gene alone on susceptibility; and the third, positive control, using a preselected HIGS reporter gene, were included.

The selection of a HIGS reporter represented a particular challenge. The HIGS reporter should provide a readout for the influence of the candidate genes on HIGS efficiency. The first selected one, the ribonuclease-like effector BEC1011 obtained by Pliego et al. (2013) was chosen because in the original study a HIGS construct for this gene was able to reduce the number of powdery mildew-infected cells of cv. 'Golden Promise' by 70% compared to the controls. Although using a nearly identical experimental setup, the strong resistance phenotype of the BEC1011 HIGS construct tested in this work was hardly reproducible. In the cvs. 'Hanna' and 'Golden Promise', the susceptibility was only reduced

by 25% and 21%, respectively, and there was no effect in cv. 'Manchuria'. In none of the experimental series a significant reduction of susceptibility index (SI) was obtained by silencing the gene BEC1011, encoding *Blumeria* effector candidate 1011 (microbial effector homologous to ribonuclease). However, it is worth noticing that the standard deviation for cvs. 'Hanna' and 'Golden Promise' was very high and reached 38% and 45%, respectively. At least in some of the experiments, the effect was comparable to that described by Pliego et al. (2013). Silencing of the positive control gene *Mlo* of barley was successful, as indicated by the strongly reduced SI of barley, suggesting that the experiments were technically correct.

Another putative HIGS reporter was described by Nowara et al. (2010). An RNAi construct carrying a sequence from the EST clone H015J13, representing the β-1,3-glucanosyltransferase gene *GTF1* of *Blumeria graminis f. sp. hordei*, reduced the haustorial index (HI) on 'Golden Promise' by 25%. In the experiments performed in the current work, the median of SI was even 40% lower than the control. However, these effects were only observed in cv. 'Golden Promise' indicating the presence of genetic determinants of the HIGS efficiency.

The β-1,3-Glucan synthase gene (*GLS1*) was another promising HIGS candidate gene. It has been repeatedly shown to be a crucial fungal gene (Chen et al., 2016; Ha et al., 2006; Oliveira-Garcia & Deising, 2013). Its mutation was lethal in *C. graminicola* (Oliveira-Garcia & Deising, 2013), whereas cross-kingdom silencing in wheat caused severe hyphal cell wall defects in *F. culmorum* (Chen et al., 2016). RNAi-mediated transient silencing of the *GLS1* gene of *Bgh* altered the SI range from 50% to 111%, with a median of 80% in cv. 'Hanna' and 85% in cv. 'Manchuria'. The observed HIGS effect of *GLS1* on powdery mildew attacking barley was much smaller than the effect on FHB published by Chen et al. (2016), where 50-60% fewer FHB symptoms were observed on wheat when compared with control lines in a semi-open greenhouse trial. Finally, *GLS1* also failed to serve as an appropriate HIGS reporter. However, this result is not surprising since the two pathogens possess very different infection strategies. *Fusarium,* in its necrotrophic phase, is probably readily taking up sRNA among all other nutrients, whereas the obligate biotroph *B. graminis* has much more selective uptake. A deeper investigation of this hypothesis may answer whether the necrotrophic and hemibiotrophic pathogens are better targets for a HIGS approach than obligate biotrophs.

Another candidate gene was *cytochrome P450 lanosterol C14 α-demethylase* (*CYP51*). Silencing of *CYP51* gene expression using sprayed-induced gene silencing (SIGS) or HIGS was very effective (Koch et al., 2019; Koch et al., 2013). CYP51 inhibitors, that bind to the gene product, severely disturb the fungal membrane and are used as fungicides (Koch et al., 2013). *Blumeria graminis* is also sensitive to the demethylase inhibitor (DMI) class of fungicides that target the product of the *CYP51* gene (Zulak et al., 2018). Nevertheless, TIGS experiments in 'Hanna' resulted in a median SI of 127% with a standard deviation of 47%, representing an insignificant effect opposite expected. Targeting the same gene in

'Golden Promise' resulted in a median SI of 70%, ranging from 23% to 93%. Still, the effect is much smaller than that observed using SIGS against all 3 *CYP51 Fusarium* genes, where FHB infection in barley was reduced by 90%. SIGS of *CYP51A*, *CYP51B*, and *CYP51C* allowed reducing FHB symptoms by 80, 78, and 82%, respectively. HIGS targeting *CYP51A*, *CYP51B*, and *CYP51C* also caused a reduction of FHB symptoms in barley but only by 75, 40%, and 9%, respectively (Koch et al., 2019). These differences again indicate that cross-kingdom trafficking is probably more efficient in necrotrophic pathogens, where simple spraying of the leaf surface is the most straightforward way to introduce dsRNA and sRNAs into such organisms.

The last HIGS candidate gene was *GPI8*, indispensable for vegetative development and pathogenicity of *C. graminicola*. Deletion of this gene in *C. graminicola* is lethal (Oliveira-Garcia & Deising, 2016). The gene is a subunit of the glycosylphosphatidylinositol (GPI) transmidase complex and is responsible for the attachment of GPI to proteins and anchoring to the cell surface. However, in independent experiments performed in cvs. 'Hanna' and 'Golden Promise', the SI of these genotypes was 190% and 110%, respectively, compared to the control set to 100%, which excluded this candidate as a HIGS reporter. Thus, in the frame of this work, it was not possible to identify a suitable HIGS reporter gene for establishing a test system for HIGS candidate genes.

Evidence for cross-kingdom RNA trafficking to different fungi is also controversial. It was shown that HIGS is efficient against biotrophs (Qi et al., 2018; Nowara et al., 2010); hemibiotrophs (Zhang et al., 2016), and necrotrophs (Cai et. Al., 2018; McLoughlin et al., 2018). There are also examples of the lack of HIGS, such as between wheat and the hemibiotroph *Zymoseptoria tritici*. dsRNA targeting *Z. tritici* genes applied *in vitro* or generated in wheat did neither affect pathogen growth nor virulence. It was shown that *Z. tritici* did not take up dsRNA, and the RNAi pathway did not play a significant role in wheat infection by this pathogen, even though critical components of this pathway are encoded in the *Z. tritici* genome (Kettles et al., 2019). HIGS efficiency strongly depends on the ability of the pathogen to take up RNAi-triggering molecules such as long and/or short dsRNAs, but it seems that not all pathogens can efficiently take up small and/or long dsRNA. Biotrophic fungi take up RNA from the host cell, so such molecules must cross the plasma membranes (PMs) of the host and fungus. It is unclear how the passage of RNA takes place or whether biotrophic fungi take up only siRNAs or long dsRNAs. It is also unknown whether the fungal RNAi machinery responds to plant RNA molecule triggers (length, 5' nt, modifications) in the same way as they respond to their endogenous siRNAs. The compatibility of host and target RNAi machinery seems to play a crucial role in HIGS efficacy (Koch & Wassenegger, 2021).

As mentioned above, the effectiveness of cross-kingdom RNA trafficking might be genetically determined. Of the seven tested HRG candidates in cv. 'Manchuria', only three resulted in slightly reduced SI (by 6% - GTF1; 7% - CYP51 and 15% - BEC1011), when SI of the control Mlo RNAi construct

was reduced by 98%. In cv. 'Hanna', three of the five tested HRGs, reduced the SI (GTF1 by 3.5%; BEC1011 by 25%; GLS by 21%). Three of the four candidates tested in 'Golden Promise' resulted in SI reduction (GTF1 by 40%; CYP51 by 30%; BEC1011 by 21%). In total, the observed effect was the smallest in cv. 'Manchuria', and strongest in cv. 'Golden Promise'. Such genotype dependency of the HIGS efficiency is an interesting observation that certainly needs further investigation, for instance, by using larger genotype collections and performing genome-wide association studies (GWAS). Such studies were performed with some candidates, but GWAS may provide many more putative candidates.

In summary, the screening of the candidate genes using TIGS was technically not possible to establish because of the unavailability of reliable HIGS reporter genes. One option to overcome the problem would be to test other barley genotypes, which may respond better to HIGS. Alternatively, silencing methods other than biolistically delivering plasmids such as TIGS assay can be tested. One such method could be the approach presented by Lambertucci et al. (2019). These authors used short antisense phosphorothioate-modified oligodeoxyribonucleotides (PTOs) and scored *Bgh* disease by monitoring the proportion of conidia being able to produce secondary hyphae. Moreover, PTOs inhibit candidate gene transcription via RNase H degradation of targeted mRNA (omitting the RNAi machinery). This method would thus help to avoid the difficulty of silencing RNAi components by the RNAi machinery. However, the results of such experiments may still be challenging to interpret, lacking a reliable HRG control. It seems that cross-kingdom trafficking of RNA is probably more common in pathogens with a strong necrotrophic phase. For such pathogens, spraying the leaf surface might be the most efficient way to introduce RNAs into the fungus. However, employment of natural HIGS may offer a much more socially acceptable alternative for *Fusarium* protection than external RNA application.

4.1.2 Selection of genes potentially involved in the HIGS mechanism

Studies conducted on wheat and barley showed that HIGS can be successfully applied to control various diseases (Chen et al., 2016; Nowara et al., 2010; Pliego et al., 2013; Qi et al., 2019). Wheat creating RNA molecules silencing the expression of genes in *Meloidogyne incognita* and *Pratylenchus* spp. and weakened nematode reproduction. RNAi-based HIGS technology provided higher wheat and barley resistance towards the *Wheat streak mosaic* virus and *Wheat dwarf virus* (Qi et al., 2019). This approach was shown to be also useful against various fungi. *Blumeria graminis* was less efficient in attacking wheat and barley, transiently expressing RNA molecules against pathogen effectors (Nowara et al., 2010; Pliego et al., 2013; Qi et al., 2019). Employing HIGS, it was possible to obtain wheat with higher resistance to *Puccinia striiformis* f. sp. *tritici*, *Puccinia triticina, Fusarium graminearum* (Qi et al., 2019), and *Fusarium culmorum* (Chen et al., 2016; Qi et al., 2019) or barley coping better with *Fusarium* species (Koch et al., 2013; Qi et al., 2019). However, whether and how siRNAs or/and dsRNAs are transported from plant to pathogen is still poorly understood (Qi et al., 2019). Screening of genes

potentially involved in cross-kingdom RNA trafficking was supposed to provide answers or hints of the mechanism of HIGS and to validate candidate genes for further functional and genetic studies.

The extracellular vesicles (EVs) that transfer lipids, metabolites, proteins, and nucleic acids are involved in host-microbe interaction (Cai et al., 2019b). There are various possible sources of EVs in the plants. Among them are EVs originating from multivesicular bodies (MVBs), exocyst-positive organelles (EXPO) delivered EVs, or PENETRATION (PEN)1-associated EVs, the biogenesis pathway of which is still unclear (Cai et al., 2019a). EVs derived from MVBs contain plant-originating siRNAs, which can silence fungal virulence-related genes in *B. cinerea* (Cai et al., 2019a). PEN1-associated EVs carry 10-17 nt long sRNA, but their role in plant-pathogen interaction is still unclear. Whether EXPO-delivered EVs collect RNA molecules and are involved in HIGS remains unsolved (Cai et al., 2019a). The study considered genes that may be essential to cross-kingdom RNA trafficking and genes that have not previously been linked to this process but may play a role. The first group includes genes encoding SNARE complex proteins, a regulator involved in the fusion of transport vesicles with the target membrane (Cai et al., 2019b; Ding et al., 2014a). In response to *Blumeria graminis* f. sp. *hordei* attack, the plasma membrane located SNAREs PEN1, ROR2, and AtSNAP33 accumulated in the papillae of *Arabidopsis* and barley (Ding et al. 2014). PEN1 was shown to be associated with the exosomal EVs containing 11-17 nt RNAs (Baldrich et al., 2019; Cai et al., 2019a; Huang et al., 2019), and PEN1 activity depends on the ARF–guanine nucleotide exchange factor GNOM (Huang et al., 2019) that is also included in the research presented here. The plant tetraspanin genes *TET8* and *TET9* were shown to influence the transport of sRNA from *Arabidopsis* to *B*. *cinerea*, as tetraspanin (TET)-associated vesicles accumulate at fungal infection sites and are transported into the extracellular apoplastic area (Cai et al., 2018; Huang et al., 2019). However, in 2016, when the candidate genes were selected, no literature indicating the substantial role of TET8 and TET9 genes in cross-kingdom trafficking was available, and they were therefore not included in the screen reported in this thesis. The RAB5-like GTPase Ara6, detected in labeled MVBs, releases extracellular vesicles containing sRNAs (Cai et al., 2018). Since MVBs were shown to be involved in sRNA transport, genes so far not directly linked with the HIGS process but crucial in MVBs development, were included in the screening. Among them were the RAB5-like GTPase gene *Ara6*, genes encoding endosomal sorting complexes required for transport (ESCRT) proteins involved in the formation of MVBs, and a gene encoding a regulator of MVBs biogenesis, i.e., *LIP5* (Robinson et al., 2016). The genes shown to be important in the production and transport of extracellular sRNA included *RDR6* and *DCL*. The *Arabidopsis rdr6* mutant was impaired in the generation of siRNA, and plausibly, a dcl2/3/4 triple mutant was compromised in siRNAs biogenesis. These mutants were unable to downregulate the expression of target genes in *B. cinerea* during infection (Cai et al., 2018). Dicer1 generates miRNAs (Bologna & Voinnet, 2014; Borges & Martienssen, 2015) that are transported from plants to the pathogens, where they silence the source genes (Jiao & Peng, 2018; Zhang et al., 2016).

Many other genes (e.g. a secretory carrier membrane protein (SCAMP1), the vacuolar proton ATPase A1 (VHA-A1), or the coatomer beta subunit β'-COP Park and Jurgens (2011), were not linked to trans-kingdom sRNA trafficking, but their contribution cannot be excluded, so they also appear on the list of genes that would be tested. These are also genes crucial for the exocyst complex formation (Zarsky et al., 2013) and genes encoding PEN1, associated with EVs carrying 11-17 nt sRNA (Baldrich et al., 2019; Cai et al., 2019a; Huang et al., 2019). Moreover, genes encoding proteins involved in cytoskeleton organization, which may have a crucial role in the mechanism of HIGS, are also included in the potential list of gene candidates in this study. Collectively, the selected genes covered a broad spectrum of HIGS functions, including novel and not yet studied pathways.

4.2 Association studies

4.2.1 Reasons for choosing candidate-gene association mapping approach

The candidate-gene association mapping (CG) approach has not been a widely used method for identifying genetic markers associated with FHB severity, despite having some advantages over the commonly used GWAS. A major disadvantage of CG is that the detection of new genes and gene combinations will not be possible, as can happen with the GWAS approach (Amos et al., 2011). Additionally, CG mapping may be pointless for complex traits like yield, since many potential gene candidates are spread over the whole genome (Zhu et al., 2008). Moreover, GWAS allows for studying historical recombination events in a larger population of unrelated individuals, giving usually higher mapping resolution (Arruda et al., 2016). Nevertheless, also GWAS has limitations, such as weakness in identifying QTL with small effects (Burghardt et al., 2017) and difficulties identifying true SNP-trait associations caused by small phenotypic effect of rare allelic variants (Korte & Farlow, 2013). Furthermore, functional markers, with little frequency, have small impact on a whole populations and are difficult to detect (Myles et al., 2009). What is more, in GWAS with a high number of markers, the correction for multiple testing hampers the statistical power of the results. It has been shown that the CG approach tends to have greater statistical power than GWAS, regardless of the number of markers used in the study (Amos et al., 2011). Using the CG approach may allow us to find new marker associations with FHB which would be difficult to detect with the GWAS method.

4.2.2 Attempts to explore the mechanism of host-induced gene silencing

As cross-kingdom RNA silencing may be a relevant defense strategy of the plants against pathogens (Wang et al., 2017; Wang et al., 2016; Weiberg & Jin, 2015), candidate genes potentially involved in this process were selected and few of them could be assessed for their association with FHB severity in wheat. However, these genes may play an important role in wheat resistance to FHB, but potentially also in other pathogens. Additionally, it is possible that the CG approach performed here could explain an effect of some QTL previously shown to be associated with wheat resistance to FHB. Therefore,

identifying genes involved in resistance and potentially RNA trafficking is a prerequisite for the CG approach.

DNA polymorphisms required for the association study were found in nine candidate genes in eight genotypes (Figure D 1). However, the sequence similarity of the homeologs in the polyploid wheat genome prevented using the full-length sequences of the genes. Instead, only about 500 bp long genomic fragments, mostly intronic sequence, were used, which possibly do not cover the complete polymorphism of the gene.

The association studies on the nine candidate genes with polymorphic markers directed attention to two genes that may be key players in FHB–wheat interaction and cross-kingdom RNA trafficking. The gene encoding the RAB5-like GTPase Ara6, located on chromosome 4D, and *Dicer1* on chromosome 5A (Figure D 1).

Ara6 is associated with plant resistance to FHB and was shown to be involved in pathogen-induced vesicle transport (Ding et al., 2014a). Scientific reports show that only multivesicular bodies (MVBs) labeled with the Rab5-like GTPase Ara6 accumulate in the vicinity of *B. graminis* sp. *hordei* attack site, mediating membrane fusion between MVBs and the PM (Ding et al., 2014a; Nielsen et al., 2012). There is also evidence that the Rab5-like Ara6-labeled MVBs release extracellular vesicles carrying sRNAs but stay on MVB membranes fusing and remaining on the PM (Cai et al., 2018).

The second candidate gene significantly associated with FHB resistance, as indicated by two markers, was *Dicer1* known for its importance in miRNA production and the miRNA-based defense against fungal pathogens (Weiberg & Jin, 2015). The experiments performed with *dcl1 Arabidopsis* mutants almost entirely lacking miRNA accumulation, including miR393 required for first-line resistance, showed that *Dicer1* is highly needed to resist the bacterial pathogen *Pseudomonas syringae* (Mosher & Baulcombe, 2008). Furthermore, there are reports that miRNAs produced by plants may act in a cross-kingdom manner targeting transcripts of mammals, viruses (Han & Luan, 2015), or fungi (Jiao & Peng, 2018; Zhang et al., 2016). For example, cotton plants exporting miR166 and miR159 effectively silence the expression of *Verticillium dahlia* genes and reduce virulence of the pathogen (Zhang et al., 2016). Furthermore, wheat miR1023 represses *F. graminearum* infection by targeting and silencing the fungal *FGSG_03101* gene, encoding an alpha/beta hydrolase (Jiao & Peng, 2018). Thus, *Dicer1* is involved in plant resistance by participating in trans-kingdom RNA molecule trafficking (Jiao & Peng, 2018) and by having a role in pathogen defense pathways (Yang & Huang, 2014). However, the specific role of the two discovered genes in defense against FHB remains to be revealed.

Furthermore, there is a substantial possibility that the observed associations of the markers with FHB resistance are due to genetic linkage, and thus the genes in which the markers are located are not the causative factors of the resistance phenotype. Untill 2019, 556 QTL related to wheat FHB resistance were described in the literature (Venske et al., 2019). Venske at al. (2019) generated 65 meta-QTL,

based on literature information. Three meta-QTL were predicted in chromosome 4D, whereas five were in chromosome 5A. The markers shown to be in the linkage disequilibrium to the markers DCL1 and DCL2 (WSNP_KU_REP_C71232_70948744, WSNP_EX_C23795_33033959, WSNP_EX_C23795_33033150, WSNP_EX_C23795_33033010) are not present in any of the predicted meta-QTL generated by Venske et al. (2019). The major resistance QTL located on chromosome 5A, *Qfhi.nau-5A*, syn *Fhb5* (Xue et al., 2011), most likely lies in the meta-QTL2. That indicated an independent assort of this QTL and *Dicer1* gene.

Moreover, it is unlikely that *Fhb5* coming from Asian sources is present in the European wheat population (Slominska-Durdasiak et al., 2020). As marker Ara6 is not strongly linked to the other markers available in the GABI-wheat population, we were unable to check its position in relation to the described meta-QTL on chromosome 4D. Nevertheless, the physical position of the markers flanking meta-QTL on chromosome 4D excludes marker Ara6 in any of the predicted meta-QTL (Slominska-Durdasiak et al., 2020; Venske et al., 2019). Gene *(Rht)-D1*, lying in meta-QTL2 at the wheat chromosome 4D, having a severe impact on FHB resistance in wheat, lies at a great distance to the *Ara6* gene (approx. 420 Mbp apart from each other) (Slominska-Durdasiak et al., 2020). By creating a genetic map of wheat chromosome 4D, we excluded linkage between Ara6 and RhtD1 markers, even though a negative association of the wheat height and resistance to FHB would support linkage between these markers. So it appears that neither *Dicer1* nor *Ara6* lies in the already-known meta-QTL. However, definitive confirmation of the contribution of these two genes to the observed FHB phenotype will require the generation of wheat mutants or stable transgenic plants.

Nevertheless, the three markers identified in elite wheat lines can easily be used directly in a breeding program without problems like linkage drag associated with *Fhb1* QTL. The effect of the genes *Dicer1* and *Ara6* is weaker than the effect of the well-known *Fhb1*, explaining up to 40% phenotypic variance (Miedaner & Korzun, 2012) or *Qfhs.ifa-5A* explaining up to 60% of FHB severity and up to 58% of the FHB incidence (Steiner et al., 2017). However, the usage of the *Fhb1* QTL also entails adverse effects (Steiner et al., 2017), that various scientific groups are trying to overcome by characterization of the gene(s) responsible for the action of *Fhb1* (He et al., 2018; Jia et al., 2018; Li et al., 2019; Rawat et al., 2016; Su et al., 2019). DCL1(1), DCL1(2), and Ara6 markers explain about 10% FHB resistance variation in wheat, which is too little for breeding FHB resistance solely on these makers, but can provide a solid contribution to pyramiding FHB resistance together with other minor QTL.

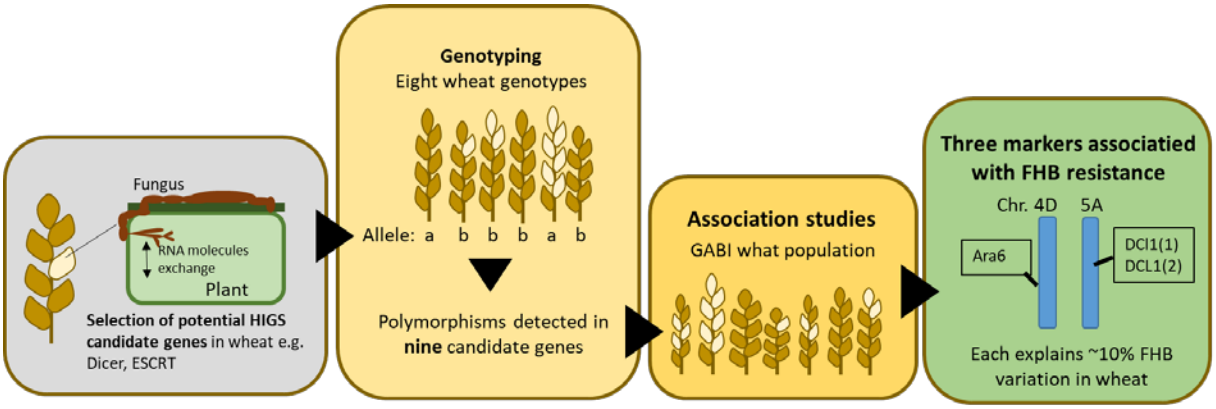

Figure D 1: Candidate genes potentially involved in cross-kingdom RNA silencing were selected in wheat.
Genotyping performed on eight wheat genotypes allowed the detection of polymorphisms in nine HIGS candidate genes. Association studies were carried out on the GABI wheat population and revealed three marker-FHB severity associations in two candidate genes. Each of the markers explains approx. 10% of the FHB severity variation in wheat.

4.2.3 Detected associations verified in RILs populations

Before routinely applying markers in marker-assisted breeding, validation of marker-trait associations is of central importance (Luders et al., 2016; Slominska-Durdasiak et al., 2020). Many of the QTL detected in approaches such as GWAS have not been helpful in breeding programs (Bernardo, 2008; Luders et al., 2016), which may be explained by the absence of associations' verification in the other environments or in other genetic backgrounds (Luders et al., 2016). There are not many examples of validations of marker-trait associations (Luders et al., 2016; Navara & Smith, 2014; Slominska-Durdasiak et al., 2020). Moreover, many of the identified associations obtained in association mapping studies could not later be confirmed (Luders et al., 2016; Navara & Smith, 2014). Therefore it is so important to verify obtained results by other methods. The study presented here validated the markers associated with FHB resistance in the CG approach in two bi-parental populations (Figure D 2). Four markers out of 14 available were polymorphic in the 'Apache x Biscay' population of 100 individuals. All associations observed in previously performed CG mapping were validated. The three markers associated with the studied trait in the GABI wheat population also influenced FHB severity in the 'Apache x Biscay' RIL population.

Furthermore, it was confirmed that markers with no effect on wheat resistance in the CG approach were also not associated with the severity of FHB in the studied biparental population. Moreover, the other four markers were assessed for their association with wheat FHB resistance in a smaller 'History x Rubens' RILs population of 48 individuals. Only one marker, DCL1(1), which was earlier found to be associated with the studied trait in CG mapping, was polymorphic in a smaller RIL population. This marker has also proven to be associated with FHB severity at some stages of FHB development in the 'History x Rubens' population, confirming the results obtained in the CG approach. The rest of the

markers were not shown to be associated with wheat resistance to FHB. The association of DCL1(2) and Ara6 markers with the studied trait were not studied because they were not polymorphic in the 'History x Rubens' population. Nevertheless, the validation of the markers DCL1(1), DCL1(2), and Ara6 in the 'Apache x Biscay' population and DCL1(1) additionally in the 'History x Rubens' population allows their use in wheat breeding programs.

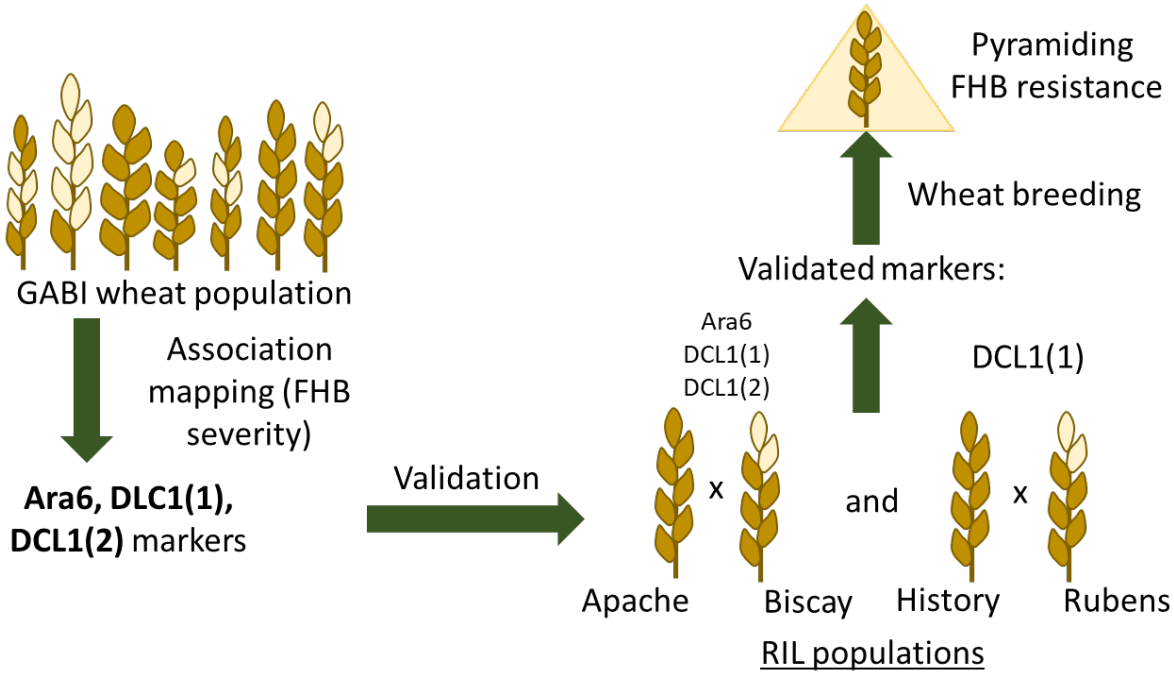

Figure D 2: Three polymorphic markers (Ara6, DCL1(1), and DCL1(2)) out of twelve detected in the GABI wheat population were found to be associated with the FHB severity.
These three markers were polymorphic in the 'Apache x Biscay' population and were shown to be as well-associated with the studied trait. Validation of the marker DCL1(1) in 'History x Rubens' population confirmed the association of the marker with FHB resistance. These markers can contribute to pyramiding FHB resistance together with other minor QTL.

4.2.4 Ara6 marker associated with plant height

Besides the FHB resistance association, the studies performed on the 'Apache x Biscay' population also revealed an association of the marker Ara6 with plant height. As this marker was not polymorphic in the 'History x Rubens' population, the association of the marker in the second population was not studied. However, the association of plant height and FHB resistance is a known phenomenon (Herter et al., 2018). The allele (Rht)-D1b, also located on 4D chromosome, is widely used in wheat breeding to obtain semidwarf plants that are better yielding but are more susceptible to FHB (Buerstmayr & Buerstmayr, 2016). One theory explaining such association is a passive resistance mechanism of the tall plants having e.g. larger distances between spikelets and different microclimate than semidwarf plants (Buerstmayr et al., 2000). However, such an explanation is unlikely as the second known dwarfing allele, Rht-B1b, has a comparable effect on wheat height but a minor impact on FHB severity

(Buerstmayr & Buerstmayr, 2016). In our study, the divergence between the heights of plants carrying different gene alleles was, on average 3.9%. Plants of the 'History x Rubens' population differ in height on average by 11.2% depending on the (Rht)-D1 gene allele they are carrying (Herter et al., 2018). In the last stage of FHB infection, plants carrying the Ara6b allele were on average about 10% points more resistant than the Ara6a carriers. This difference is nearly the same as that reported for plants carrying Rht-D1-a or Rht-D1-b (10.05% points) (Herter et al., 2018). Thus, the Ara6 marker does not affect the height of the wheat as strongly, while having a similar effect on its resistance to FHB. This finding would suggest a different substrate for FHB resistance than *Rht-D1* gene-dependent plant height. Thus it may be the Rab5-like GTPase gene *Ara6* itself or a gene closely located, although we cannot draw any conclusion without further testing. Nevertheless, the Ara6 marker is a good candidate for being used in wheat breeding, improving FHB resistance without having a large effect on plant height.

4.2.5 The association of candidate genes putatively involved in trans-kingdom RNA trafficking and heading date

The 'History x Rubens' population study revealed an association between the endosomal sorting complexes marker ESCRT-III and DCL1(1) with the wheat spike heading date (HD). In the larger 'Apache x Biscay' population, a DCL1(1) association with the HD was not detected, and the ESCRT-III marker was not polymorphic. Therefore, we were unable to validate the results obtained in the smaller 'History x Rubens' population for the ESCRT-III marker. Both DCL1(1) and ESCRT-III markers are located on 5A chromosome. Interestingly, two other genes that influence the wheat HD are also located in chromosome 5A. One of them is a gene *Vrn-A2* that delays flowering untill plants are vernalized, and it is one of the major genes impacting wheat HD architecture (Zanke et al., 2014). Second, the gene *Vrn-A1* is known to regulate flowering and heading time. Moreover, QTL for FHB was detected at the *Vrn-A1* locus (Buerstmayr et al., 2020; He et al., 2016). Markers of these genes were missing in these studies, so the linkage of the ESCRT-III or DCL1(1) markers and *Vrn* genes cannot be excluded. Plants carrying different alleles of ESCRT-III differ in spike HD with two days on average. Cardona-Lopez et al. (2015) presented studies on alix-1 *Arbidopsis* mutants. ALIX proteins likely act as a part of ESCRT-III complexes, and mutation of the gene leads to reduced plant growth and late flowering in *Arabidopsis,* indicating the connection between the *ESCRT-III* gene with wheat heading date and plant growth (Cardona-Lopez et al., 2015). The ESCRT-III gene may be responsible for the observed association with HD, but may also be another linked gene. The distance between ESCRT-III and the *Vrn-1A* gene is almost 61 Mbp, and the distance to *Vrn-2A* (Loukoianov et al., 2005) is more than 171 Mbp. An association of ESCRT-III with FHB severity was not observed, so the results obtained here do not indicate the importance of this gene in plant FHB resistance or trans-kingdom RNA trafficking.

Carriers of different DCL1(1) alleles were, on average, 1.9 days difference in HD. DCL1(1) marker was shown to be associated with both HD and FHB resistance in the small 'History x Rubens' population, although its association with HD was not detected in the larger 'Apache x Biscay' population. Several publications identified the association between flowering time and FHB resistance (Buestmayr et al., 2019, He et al., 2016). However, when a multi-environment evaluation of European winter wheat lines was performed, no systematic association was found between FHB severity and wheat flowering date (Buerstmayr et al., 2008; Buestmayr et al., 2019). As already mentioned, the two genes *Vrn-A1* and *Vrn-A2* are present on 5A wheat chromosome. The distances measured using physical map IWGSC RefSeq v.1.0 between the gene *Dicer1* and genes *Vrn-1A* and *Vrn-2A* were 92 Mbp and 18.5 Mbp, respectively. A QTL reported for both HD and FHB resistance contains the *Vrn-A1* gene (Buestmayr et al., 2019). As markers for the *Vrn* genes were not available in this study, a linkage between these genes cannot be excluded, but considering the distance, it is implausible.

4.3 Naturally occurring HIGS

4.3.1 Selection of the HIGS candidate genes in *Fusarium*

Employing natural genetic resources for crop protection is considered the most sustainable option to improve plant health. Plants have evolved different mechanisms to defend themselves from pathogens, and HIGS seems to be one of them. Recently it was discovered that the plant genomes contain sequences potentially able to generate sRNA that target fungal genes. One of the tasks of this work was to investigate the natural HIGS phenomenon and to validate the function of these putative sequences found in the barley genome. Studying naturally occurring HIGS between *Fusarium* and barley was initiated by Dr. P. Schweizer (IPK), who prepared a list of candidate genes in *Fusarium* that have close sequences matches in the 'Morex' genome, which was the only available sequenced barley genome at that time. Since the genes were selected when a complete gene model of *Fusarium* was not available, the putative function of the candidates was identified via homology to annotated genes from other organisms. The initial selection of 50 candidate genes was further reduced to eight, based on the published information. For some of them, the studies indicated their importance for development or virulence of this fungus (FGSG_06175, FGSG_10970) (Ding et al., 2017; Zheng et al., 2013). The studies were performed in other organisms for the rest of the candidates. Unfortunately, two sequences were not successfully cloned, so the final list was six candidates.

Naturally occurring sRNA exchange was shown to occur between many different organisms (Jian & Liang, 2019; Jiao & Peng, 2018; Weiberg et al., 2013; Zhang et al., 2016). Furthermore, cross-kingdom sRNA trafficking was also observed between wheat and *Fusarium graminearum* (Jian & Liang, 2019; Jiao & Peng, 2018). However, so far, there is no evidence for naturally occurring sRNA exchange

between barley and *Fusarium*, even though cross-kingdom gene silencing in the *Fusarium* - barley interaction is possible (Koch et al., 2019; Werner et al., 2020).

The first aim of this work was to demonstrate that the putatively targeted *Fusarium* genes are essential for the fungus. Spray-induced gene-silencing (SIGS) (Werner et al., 2020), which would be one of the most accessible options to validate target genes, was not established when the experiments of this thesis were designed. Furthermore, generating stable *Fusarium* mutants was not considered an option since it was expected that a complete KO mutation for some of the targeted genes could be lethal for the fungus. Furthermore, generating barley mutants deficient in sRNA production, besides being time-consuming, is too complex since several different sRNA pathways may be involved (Borges & Martienssen, 2015). Finally, the method of choice was VIGS as a well-established method for such studies (Chen et al., 2016; Jiao & Peng, 2018).

Since the aim was to confirm that the targeted genes are essential for the fungus, it was decided to use optimal *Fusarium* genome-derived sRNA design instead of the putative natural HIGS sequences of barley, targeting the same fungal gene. The barley sequences were predicted to have too many off-targets in wheat. Therefore, the *Fusarium*-derived constructs were designed to have no off-targets in the wheat and *Fusarium* genome, providing more precise results. Although this approach will not directly confirm the function of the natural HIGS sequences, it aims to validate their targets. Targets shown to be relevant for FHB development would be further tested as natural HIGS targets (preferentially taking an approach using sRNA molecules perfectly matching the barley genome). Moreover, such genes could be used in the future as natural targets for pathogen control using GM plants.

4.3.2 VIGS – stability of the insert and validation analysis

VIGS is a powerful method for functional genomics studies in plants. However, there are several concerns about using this technology. Bruun-Rasmussen et al. (2007) have shown that the insert length influences the stability of recombinant viruses. BSMV vectors carrying inserts ranging from 128 to 584 nucleotides were studied. Using VIGS via *in vitro* transcription, photobleaching, and *Phytoene desaturase* (PDS) gene silencing was strongest, with the constructs carrying 400 and 275 nt sequences two weeks after the BSMV inoculation. Plants with a virus carrying 585 nt insert caused less photobleaching, while those carrying 128 nt insert rarely showed any typical PDS symptoms.

Interestingly, the phenotype did not correlate with mRNA quantity. Downregulation of PDS transcripts was highest with the 128nt insert (84%) and ranged from 68-78% for the other constructs. The shortest insert was intact after 14 days and the 584 nt construct was the most unstable. Two other inserts had partial deletions, but most were present in the virus (Bruun-Rasmussen et al., 2007). Chen et al. (2016),

studying *Fusarium culmorum* genes in wheat, using VIGS via *in vitro* transcription, used inserts of 300-461 nt. Reduced transcript abundances were observed with all constructs. However, the highest correlation between phenotype and mRNA level was shown for the virus-carrying insert of 461 nt.

Initially, VIGS via *in vitro* transcription was a method planned to be used for functional validation of *Fusarium* genes. With this method, the BSMV virus replicated in the plant about 25 days before the collection of samples. Nevertheless, the method was not very efficient, and the number of BSMV-positive plants did not allow reliable conclusions. Therefore, an alternative method, based on VIGS *via* particle bombardment (Meng et al., 2009), was selected as more amenable to high-throughput studies. VIGS via bombardment was used to study the role of the genes *Importin α-1b* (Contig3615_at) and *Sec61 γ* in barley-powdery mildew interactions (Xu et al., 2015). Inserts of 319 nt incorporated into the BSMV vector were shown to influence the powdery mildew development, and qRT-PCR confirmed that transcript accumulation for the target genes was suppressed. Nevertheless, most studies on BSMV-mediated host-induced gene silencing were performed using VIGS via *in vitro* transcription (Chen et al., 2016; Qi et al., 2019) or with *Agrobacterium*-mediated transformation (Jiao & Peng, 2018).

Since the *Fusarium* – wheat interactions take longer than the *Bgh* – barley interaction described in Meng et al. (2009), and the virus is passed over the intermediate host barley, it was important to check the stability of different lengths of BSMV:γ-inserts over time. As expected, the longer the insert, the less stable it was. Inserts longer than 344 nucleotides were mostly lost during virus replication in barley cv. 'Black Hulless', preventing their use for the secondary BSMV infection in wheat. Although it was described that even when the insert is undetectable, silencing of the target gene is still possible (Bruun-Rasmussen et al., 2007), to stay on the safe side, I decided to perform validation experiments with shorter inserts (100-200 nt).

The same constructs designed to check stability of the inserts were examined for their silencing efficiency of the HIGS target. There was no correlation between stability of the virus and the transcript amount for the shortest insert, since the stability of the insert was constant. However, there was a weak but positive correlation between the insert stability and targeted gene expression for the longer constructs.

Besides the previously described (Bruun-Rasmussen et al., 2007) possibility for silencing even when the insert is undetectable, the opposite situation was also observed. Although the insert was presented, the targeted genes were not silenced in some cases.

In general, silencing of the studied *Fusarium* genes was most efficient for the shortest insert $BSMV_{FGSG_06175(104)}$, where 60% of the plants showed reduced levels of the targeted transcript. On the other hand, the transcript reduction observed for the $BSMV_{FGSG_06175(180)}$ and $BSMV_{FGSG_10970(233)}$ constructs was only 20% and 21 %, respectively.

Yin et al. (2011) tested different time points of *P. striiformis* f. sp. *tritici* inoculation after BSMV infection, showing that the timing of the experiment is crucial for the ability to reduce mRNA levels in the pathogen by HIGS. The *PSTha12J12* mRNA abundance was assessed by qRT-PCR in infected wheat leaves for up to seven days after stripe rust inoculation. When rust inoculation was performed ten days after virus infection, more than 80% of the plants infected with rust showed a substantial reduction of gene expression. A fifteen-day interval was also suitable for reducing target gene expression in 80% of the samples but to a lower level than the ten-day interval. Finally, a twenty-day interval between virus and rust infections reduced the expression of the target gene in only 33% of the samples to a level similar to the fifteen-day interval plants. Other factors, such as the targeted genes (Yin et al., 2011) or the length of the experiment (Chen et al., 2016) may also strongly influence the VIGS efficiency.

Plants carrying $BSMV_{FGSG_06175(180)}$ or $BSMV_{FGSG_06175(104)}$, targeting a gene encoding phospholipase d, showed strong and similar protection of the wheat against FHB, 5 days post-FHB inoculation. It is in line with previous studies on a non-lethal *FgPld1* mutant of *Fusarium* (FGSG_06175) that showed reduced deoxynivalenol (DON) production and virulence in flowering wheat spikes (Ding et al., 2017). Nevertheless, the gene-expression analysis showed no reduction of the target gene at the end of the experiment. A possible explanation might be that the target gene was efficiently silenced in the initial stages of the infection, but later the silencing effect was eroded due to the insert instability discussed above. Another explanation was suggested by Chen et al. (2016), who also observed a quantitative reduction of FHB disease symptoms in transgenic wheat lines silencing *GLS1* without target transcript reduction. Since the silencing of *GLS1* has a lethal phenotype (Chen et al., 2016; Oliveira-Garcia & Deising, 2013), this observation was explained by a positive selection for *Fusarium* cells escaping the lethal HIGS effect and, therefore, delivering the majority of the fungal transcripts for analysis.

The non-lethal deletion mutant of *FgApsB* (FGSG_10970), incapable of producing anucleate primary sterigmata B (ApsB) protein, showed reduced conidiation, mycelial growth, and virulence on flowering wheat spikes (Zheng et al., 2013). Similar to previous studies (Zheng et al. 2013), also in here, gene FGSG_10970 occurred to be essential for *Fusarium* virulence, although gene expression analysis did not show a reduction of the transcript abundance of *FgApsB* gene at the end of the experiment.

Gene FGSG_06195 was not shown to be associated with FHB severity on wheat spikes. It is a gene that was chosen as a fungal housekeeping gene based on its similarity to succinate dehydrogenase (SDH) from *Purpureocillium lilacinum*. However, four other genes were annotated as the genes encoding four SDH subunits in *Fusarium* (Sun et al., 2020), and thus the role of the gene FGSG_06195 remains unknown.

The gene FGSG_01104 encodes phenylalanyl-tRNA synthetase alpha chain. Studies revealing its importance in *Fusarium* have been unavailable so far (11.10.2020), although deletion of its ortholog in *Trypanosoma brucei* resulted in an affected cell cycle (Kalidas et al., 2014). Wheat plants carrying BSMV

targeting the FGSG_01104 gene were significantly more affected by FHB than the BSMV:00 infected plants after 5 and 10 days post-FHB inoculation, indicating silencing of a gene FGSG_01104 is required for the pathogen recognition.

Two genes encoding phospholipase d and the anucleate primary sterigmata protein were shown to be important targets in *Fusarium*, not only based on literature describing *Fusarium* mutants but also when tested in a cross-kingdom system using the VIGS method. Most likely, gene expression analyses should be performed earlier and with the shortest constructs that give the highest stability and most effective silencing of the target gene. It would make sense to prepare barley mutants unable to produce sRNAs targeting genes FGSG_06175 and FGSG_10970, which could be a direct confirmation of the naturally occurring phenomenon between barley and *Fusarium*.

5. Summary

Fusarium head blight (FHB) is a wheat disease that leads to yield losses and reduced grain quality by producing mycotoxins. Combining FHB control strategies like breeding for resistance and a recently developed technique called **host-induced gene silencing (HIGS)** may open new ways to control FHB and other diseases. Therefore, the primary aims of this doctoral thesis were: a) to better understand the HIGS phenomenon; b) to identify candidate genes or genome regions of wheat that contribute to FHB resistance by using allelic association studies with selected potential HIGS genes.

Production and transport of small interfering RNAs are two processes that are very likely to be central to the HIGS mechanisms. Candidate genes from these two categories were selected based on published evidence. The validation strategy was to transiently silence candidate genes and quantify the effect on the resistance against powdery mildew. However, critical to this approach is that a reliable HIGS-reporter gene could not be identified, making the method inapplicable. Nevertheless, the selected candidate genes of barley were used to find orthologues in wheat and perform candidate-gene **association mapping** in a wheat population. This approach revealed three **significant marker-FHB resistance associations** in two genes: *Dicer1* and the *Rab5-like GTPase* gene *Ara6*. *Dicer1* influences gene expression to prevent pathogen development. The second gene, encoding *Ara6*, participates in vesicle trafficking important for response to biotic and abiotic stresses and plant development. Thus, both genes are strongly suspected to be involved in the HIGS process. Detected associations were validated in 'Apache x Biscay' and 'History x Rubens' biparental populations. Three markers associated with FHB severity detected in candidate-gene studies were also significantly associated with the studied trait in the 'Apache x Biscay' population. Only one marker in the *Dicer1* gene was polymorphic in the other biparental population and confirmed earlier results. Still, detailed studies on wheat mutants are needed to exclude linkage drag effects and confirm the causative genes. Nevertheless, the **markers are ready for use in wheat breeding programs** for plants with higher FHB resistance and HIGS efficiency.

Naturally occurring HIGS is a fascinating phenomenon of great importance for plant protection and the evolution of plant-pathogen interactions. Barley cv. 'Morex' and *Fusarium spp.* were selected as model system to study the natural HIGS phenomenon. Regions potentially able to generate **antifungal sRNA** were discovered in the barley genome. Fungal genes predicted to be natural targets of barley sRNA were silenced via Virus-induced gene silencing (VIGS). Furthermore, two fungal genes encoding *phospholipase d* and the *anucleate primary sterigmata protein b,* predicted to be targeted by barley sRNA, showed to **efficiently reduce the FHB symptoms** upon silencing in a cross-kingdom manner. These results strongly suggest that the HIGS phenomenon might be essential natural disease resistance mechanisms of plants.

References

Acevedo-Garcia, J., Kusch, S., & Panstruga, R. (2014). Magical mystery tour: MLO proteins in plant immunity and beyond. The New Phytologist 204(2), 273–281. https://doi.org/10.1111/nph.12889

Alaux, M., Rogers, J., Letellier, T., Flores, R., Alfama, F., Pommier, C., Mohellibi, N., Durand, S., Kimmel, E., Michotey, C., Guerche, C., Loaec, M., Laine, M., Steinbach, D., Choulet, F., Rimbert, H., Leroy, P., Guilhot, N., Salse, J., . . . Quesneville, H. (2018). Linking the International Wheat Genome Sequencing Consortium bread wheat reference genome sequence to wheat genetic and phenomic data. Genome Biology 19(1), 111. https://doi.org/10.1186/s13059-018-1491-4

Amos, W., Driscoll, E., & Hoffman, J. I. (2011). Candidate genes versus genome-wide associations: which are better for detecting genetic susceptibility to infectious disease? Proceedings of the Royal Society B-Biological Sciences 278(1709), 1183-1188. https://doi.org/10.1098/rspb.2010.1920

Andersen, E. J., Ali, S., Byamukama, E., Yen, Y., & Nepal, M. P. (2018). Disease resistance mechanisms in plants. Genes 9(7), 339. https://doi.org/10.3390/genes9070339

Andersen, J. B., & Torp, J. (1986). Quantitative-analysis of the early powdery mildew infection stages on resistant barley genotypes. Journal of Phytopathology-Phytopathologische Zeitschrift 115(2), 173-186. https://doi.org/DOI 10.1111/j.1439-0434.1986.tb00875.x

Arruda, M. P., Brown, P., Brown-Guedira, G., Krill, A. M., Thurber, C., Merrill, K. R., Foresman, B. J., & Kolb, F. L. (2016). Genome-wide association mapping of Fusarium head blight resistance in wheat using genotyping-by-sequencing. The Plant Genome 9(1), 1-14. https://doi.org/10.3835/plantgenome2015.04.0028

Azevedo, C., Sadanandom, A., Kitagawa, K., Freialdenhoven, A., Shirasu, K., & Schulze-Lefert, P. (2002). The RAR1 interactor SGT1, an essential component of R gene-triggered disease resistance. Science 295(5562), 2073-2076. https://doi.org/10.1126/science.1067554

Baldrich, P., Rutter, B. D., Karimi, H. Z., Podicheti, R., Meyers, B. C., & Innes, R. W. (2019). Plant extracellular vesicles contain diverse small RNA species and are enriched in 10-to 17-nucleotide "tiny" RNAs. The Plant Cell 31(2), 315-324. https://doi.org/10.1105/tpc.18.00872

Bentham, A. R., De la Concepcion, J. C., Mukhi, N., Zdrzalek, R., Draeger, M., Gorenkin, D., Hughes, R. K., & Banfield, M. J. (2020). A molecular roadmap to the plant immune system. The Journal of Biological Chemistry 295(44), 14916-14935. https://doi.org/10.1074/jbc.REV120.010852

Bernardo, R. (2008). Molecular markers and selection for complex traits in plants: Learning from the last 20 years. Crop Science 48(5), 1649-1664. https://doi.org/10.2135/cropsci2008.03.0131

Bi, G., Su, M., Li, N., Liang, Y., Dang, S., Xu, J., Hu, M., Wang, J., Zou, M., Deng, Y., Li, Q., Huang, S., Li, J., Chai, J., He, K., Chen, Y. H., & Zhou, J. M. (2021). The ZAR1 resistosome is a calcium-permeable channel triggering plant immune signaling. Cell 184(13), 3528-3541 e3512. https://doi.org/10.1016/j.cell.2021.05.003

Blake, V. C., Birkett, C., Matthews, D. E., Hane, D. L., Bradbury, P., & Jannink, J. L. (2016). The Triticeae toolbox: combining phenotype and genotype data to advance small-grains breeding. The Plant Genome 9(2), 1-10. https://doi.org/10.3835/plantgenome2014.12.0099

Bohlenius, H., Morch, S. M., Godfrey, D., Nielsen, M. E., & Thordal-Christensen, H. (2010). The multivesicular body-localized GTPase ARFA1b/1c is important for callose deposition and ROR2 syntaxin-dependent preinvasive basal defense in barley. The Plant Cell 22(11), 3831-3844. https://doi.org/10.1105/tpc.110.078063

Bologna, N. G., & Voinnet, O. (2014). The diversity, biogenesis, and activities of endogenous silencing small RNAs in *Arabidopsis*. Annual Review of Plant Biology 65, 473-503. https://doi.org/10.1146/annurev-arplant-050213-035728

Borges, F., & Martienssen, R. A. (2015). The expanding world of small RNAs in plants. Nature reviews. Molecular Cell Biology 16(12), 727-741. https://doi.org/10.1038/nrm4085

Borrill, P., Ramirez-Gonzalez, R., & Uauy, C. (2016). expVIP: a customizable RNA-seq data analysis and

visualization platform. Plant Physiology 170(4), 2172-2186. https://doi.org/10.1104/pp.15.01667

Boyd, L. A., Ridout, C., O'Sullivan, D. M., Leach, J. E., & Leung, H. (2013). Plant-pathogen interactions: disease resistance in modern agriculture. Trends in Genetics : TIG 29(4), 233-240. https://doi.org/10.1016/j.tig.2012.10.011

Bozkurt, T. O., Richardson, A., Dagdas, Y. F., Mongrand, S., Kamoun, S., & Raffaele, S. (2014). The plant membrane-associated REMORIN1.3 accumulates in discrete perihaustorial domains and enhances susceptibility to *Phytophthora infestans*. Plant Physiology 165(3), 1005-1018. https://doi.org/10.1104/pp.114.235804

Bradbury, P. J., Zhang, Z., Kroon, D. E., Casstevens, T. M., Ramdoss, Y., & Buckler, E. S. (2007). TASSEL: software for association mapping of complex traits in diverse samples. Bioinformatics 23(19), 2633-2635. https://doi.org/10.1093/bioinformatics/btm308

Bruun-Rasmussen, M., Madsen, C. T., Jessing, S., & Albrechtsen, M. (2007). Stability of Barley stripe mosaic virus-induced gene silencing in barley. Molecular Plant-Microbe Interactions : MPMI 20(11), 1323-1331. https://doi.org/10.1094/MPMI-20-11-1323

Buck, A. H., Coakley, G., Simbari, F., McSorley, H. J., Quintana, J. F., Le Bihan, T., Kumar, S., Abreu-Goodger, C., Lear, M., Harcus, Y., Ceroni, A., Babayan, S. A., Blaxter, M., Ivens, A., & Maizels, R. M. (2014). Exosomes secreted by nematode parasites transfer small RNAs to mammalian cells and modulate innate immunity. Nature Communications 5, 5488. https://doi.org/10.1038/ncomms6488

Buerstmayr, H., Ban, T., & Anderson, J. A. (2009). QTL mapping and marker-assisted selection for Fusarium head blight resistance in wheat: a review. Plant Breeding 128(1), 1-26. https://doi.org/10.1111/j.1439-0523.2008.01550.x

Buerstmayr, H., Steiner, B., Lemmens, M., & Ruckenbauer, P. (2000). Resistance to Fusarium head blight in winter wheat: Heritability and trait associations. Crop Science 40(4), 1012-1018. https://doi.org/DOI 10.2135/cropsci2000.4041012x

Buerstmayr, M., & Buerstmayr, H. (2016). The semidwarfing alleles Rht-D1b and Rht-B1b show marked differences in their associations with anther-retention in wheat heads and with Fusarium head blight susceptibility. Phytopathology 106(12), 1544-1552. https://doi.org/10.1094/Phyto-05-16-0200-R

Buerstmayr, M., Steiner, B., & Buerstmayr, H. (2020). Breeding for Fusarium head blight resistance in wheat-Progress and challenges. Plant Breeding 139(3), 429-454. https://doi.org/10.1111/pbr.12797

Burghardt, L. T., Young, N. D., & Tiffin, P. (2017). A guide to genome-wide association mapping in plants. Current protocols in plant biology, 2(1), 22-38. https://doi.org/10.1002/cppb.20041

Buschges, R., Hollricher, K., Panstruga, R., Simons, G., Wolter, M., Frijters, A., vanDaelen, R., vanderLee, T., Diergaarde, P., Groenendijk, J., Topsch, S., Vos, P., Salamini, F., & Schulze-Lefert, P. (1997). The barley *mlo* gene: A novel control element of plant pathogen resistance. Cell 88(5), 695-705. https://doi.org/Doi 10.1016/S0092-8674(00)81912-1

Cai, Q., He, B., Weiberg, A., Buck, A. H., & Jin, H. (2019a). Small RNAs and extracellular vesicles: New mechanisms of cross-species communication and innovative tools for disease control. PLoS pathogens, 15(12), e1008090. https://doi.org/10.1371/journal.ppat.1008090

Cai, Q., He, B. Y., & Jin, H. L. (2019b). A safe ride in extracellular vesicles - small RNA trafficking between plant hosts and pathogens. Current Opinion in Plant Biology 52, 140-148. https://doi.org/10.1016/j.pbi.2019.09.001

Cai, Q., Qiao, L., Wang, M., He, B., Lin, F. M., Palmquist, J., Huang, S. D., & Jin, H. (2018). Plants send small RNAs in extracellular vesicles to fungal pathogen to silence virulence genes. Science 360(6393), 1126-1129. https://doi.org/10.1126/science.aar4142

Cardona-Lopez, X., Cuyas, L., Marin, E., Rajulu, C., Irigoyen, M. L., Gil, E., Puga, M. I., Bligny, R., Nussaume, L., Geldner, N., Paz-Ares, J., & Rubio, V. (2015). ESCRT-III-associated protein ALIX mediates high-affinity phosphate transporter trafficking to maintain phosphate homeostasis in *Arabidopsis*. The Plant Cell 27(9), 2560-2581. https://doi.org/10.1105/tpc.15.00393

Chacko, N., & Gold, S. (2012). Deletion of the *Ustilago maydis* ortholog of the *Aspergillus* sporulation regulator *medA* affects mating and virulence through pheromone response. Fungal Genetics and Biology: FG & B 49(6), 426-432. https://doi.org/10.1016/j.fgb.2012.04.002

Chang, T. H., Huang, H. Y., Hsu, J. B. K., Weng, S. L., Horng, J. T., & Huang, H. D. (2013). An enhanced computational platform for investigating the roles of regulatory RNA and for identifying functional RNA motifs. Bmc Bioinformatics 14(Suppl 2):S4. https://doi.org/10.1186/1471-2105-14-S2-S4

Chen, W., Kastner, C., Nowara, D., Oliveira-Garcia, E., Rutten, T., Zhao, Y., Deising, H. B., Kumlehn, J., & Schweizer, P. (2016). Host-induced silencing of Fusarium culmorum genes protects wheat from infection. Journal of Experimental Botany 67(17), 4979-4991. https://doi.org/10.1093/jxb/erw263

Cobessi, D., Dumas, R., Pautre, V., Meinguet, C., Ferrer, J. L., & Alban, C. (2012). Biochemical and structural characterization of the *Arabidopsis* bifunctional enzyme dethiobiotin synthetase-diaminopelargonic acid aminotransferase: evidence for substrate channeling in biotin synthesis. The Plant Cell 24(4), 1608-1625. https://doi.org/10.1105/tpc.112.097675

Corpet, F. (1988). Multiple sequence alignment with hierarchical-clustering. Nucleic Acids Research 16(22), 10881-10890. https://doi.org/DOI 10.1093/nar/16.22.10881

Cunningham, F., Allen, J. E., Allen, J., Alvarez-Jarreta, J., Amode, M. R., Armean, I. M., Austine-Orimoloye, O., Azov, A. G., Barnes, I., Bennett, R., Berry, A., Bhai, J., Bignell, A., Billis, K., Boddu, S., Brooks, L., Charkhchi, M., Cummins, C., Da Rin Fioretto, L., . . . Flicek, P. (2022). Ensembl 2022. Nucleic Acids Research 50(D1), D988-D995. https://doi.org/10.1093/nar/gkab1049

Dagnachew, B., Kassahun, T., & Asnake, F. (2019). Applications of virus induced gene silencing (VIGS) in plant functional genomics studies. Journal of Plant Biochemistry & Physiology, 7(1), 1-7.

Deng, W., Nickle, D. C., Learn, G. H., Maust, B., & Mullins, J. I. (2007). ViroBLAST: a stand-alone BLAST web server for flexible queries of multiple databases and user's datasets. Bioinformatics 23(17), 2334-2336. https://doi.org/10.1093/bioinformatics/btm331

Ding, M., Zhu, Q., Liang, Y., Li, J., Fan, X., Yu, X., He, F., Xu, H., Liang, Y., & Yu, J. (2017). Differential roles of three FgPLD genes in regulating development and pathogenicity in *Fusarium graminearum*. Fungal Genetics and Biology : FG & B 109, 46-52. https://doi.org/10.1016/j.fgb.2017.10.007

Ding, Y., Robinson, D. G., & Jiang, L. (2014a). Unconventional protein secretion (UPS) pathways in plants. Current opinion in cell biology 29, 107-115. https://doi.org/10.1016/j.ceb.2014.05.008

Ding, Y., Wang, J., Lai, J. H. C., Chan, V. H. L., Wang, X. F., Cai, Y., Tan, X. Y., Bao, Y. Q., Xia, J., Robinson, D. G., & Jiang, L. W. (2014b). Exo70E2 is essential for exocyst subunit recruitment and EXPO formation in both plants and animals. Molecular Biology of the Cell 25(3), 412-426. https://doi.org/10.1091/mbc.E13-10-0586

Dodds, P. N., Lawrence, G. J., Catanzariti, A. M., Teh, T., Wang, C. I., Ayliffe, M. A., Kobe, B., & Ellis, J. G. (2006). Direct protein interaction underlies gene-for-gene specificity and coevolution of the flax resistance genes and flax rust avirulence genes. Proceedings of the National Academy of Sciences of the United States of America 103(23), 8888-8893. https://doi.org/10.1073/pnas.0602577103

Douchkov, D., Luck, S., Johrde, A., Nowara, D., Himmelbach, A., Rajaraman, J., Stein, N., Sharma, R., Kilian, B., & Schweizer, P. (2014). Discovery of genes affecting resistance of barley to adapted and non-adapted powdery mildew fungi. Genome Biology 15(12), 518. https://doi.org/10.1186/s13059-014-0518-8

Douchkov, D., Nowara, D., Zierold, U., & Schweizer, P. (2005). A high-throughput gene-silencing system for the functional assessment of defense-related genes in barley epidermal cells. Molecular Plant-Microbe Interactions : MPMI 18(8), 755-761. https://doi.org/10.1094/MPMI-18-0755

Du, Y., Overdijk, E. J. R., Berg, J. A., Govers, F., & Bouwrneester, K. (2018). Solanaceous exocyst subunits are involved in immunity to diverse plant pathogens. Journal of Experimental Botany 69(3), 655-666. https://doi.org/10.1093/jxb/erx442

Fan, J., Urban, M., Parker, J. E., Brewer, H. C., Kelly, S. L., Hammond-Kosack, K. E., Fraaije, B. A., Liu, X., & Cools, H. J. (2013). Characterization of the sterol 14alpha-demethylases of *Fusarium*

graminearum identifies a novel genus-specific CYP51 function. The New Phytologist 198(3), 821-835. https://doi.org/10.1111/nph.12193

Food and Agriculture Organization of the United Nations. (2017). The future of food and agriculture : trends and challenges. Food and Agriculture Organization of the United Nations.

Food and Agriculture Organization of the United Nations. (2019). State of Food and Agriculture 2019. Moving forward on food loss and waste reduction.

Forderer, A., Li, E., Lawson, A. W., Deng, Y. N., Sun, Y., Logemann, E., Zhang, X., Wen, J., Han, Z., Chang, J., Chen, Y., Schulze-Lefert, P., & Chai, J. (2022). A wheat resistosome defines common principles of immune receptor channels. Nature 610(7932), 532-539. https://doi.org/10.1038/s41586-022-05231-w

Frank, M., Egile, C., Dyachok, J., Djakovic, S., Nolasco, M., Li, R., & Smith, L. G. (2004). Activation of Arp2/3 complex-dependent actin polymerization by plant proteins distantly related to Scar/WAVE. Proceedings of the National Academy of Sciences of the United States of America 101(46), 16379-16384. https://doi.org/10.1073/pnas.0407392101

Freeman, B. C., & Beattie, G. A. (2008). An overview of plant defenses against pathogens and herbivores. The Plant Health Instructor. Retrieved 22.02.221 from https://www.apsnet.org/edcenter/disimpactmngmnt/topc/Pages/OverviewOfPlantDiseases.aspx

Gill, U. S., Lee, S., & Mysore, K. S. (2015). Host versus nonhost resistance: distinct wars with similar arsenals. Phytopathology 105(5), 580-587. https://doi.org/10.1094/PHYTO-11-14-0298-RVW

Glawe, D. A. (2008). The powdery mildews: a review of the world's most familiar (yet poorly known) plant pathogens. Annual review of phytopathology, 46, 27-51. https://doi.org/10.1146/annurev.phyto.46.081407.104740

Guilfoyle, T. J., & Dietrich, M. A. (1987). Plant RNA polymerases: structures, regulation, and genes. Basic Life Sciences 41, 87-100. https://doi.org/10.1007/978-1-4684-5329-4_8

Gunupuru, L. R., Perochon, A., Ali, S. S., Scofield, S. R., & Doohan, F. M. (2019). Virus-Induced Gene Silencing (VIGS) for functional characterization of disease resistance genes in barley seedlings. Methods in Molecular Biology (Clifton, N.J.) 1900, 95-114. https://doi.org/10.1007/978-1-4939-8944-7_7

Gupta, R., Lee, S. E., Agrawal, G. K., Rakwal, R., Park, S., Wang, Y. M., & Kim, S. T. (2015). Understanding the plant-pathogen interactions in the context of proteomics-generated apoplastic proteins inventory. Frontiers in plant science, 6, 352. https://doi.org/10.3389/fpls.2015.00352

Ha, Y. S., Covert, S. F., & Momany, M. (2006). *FsFKS1*, the 1,3-beta-glucan synthase from the caspofungin-resistant fungus *Fusarium solani*. Eukaryotic Cell 5(7), 1036-1042. https://doi.org/10.1128/EC.00030-06

Han, L., & Luan, Y. S. (2015). Horizontal transfer of small RNAs to and from plants. Frontiers in Plant Science 6, 1113. https://doi.org/10.3389/fpls.2015.01113

Han, Q., Wang, Z. Z., He, Y. X., Xiong, Y. H., Lv, S., Li, S. P., Zhang, Z. G., Qiu, D. W., & Zeng, H. M. (2017). Transgenic cotton plants expressing the *HaHR3* gene conferred enhanced resistance to *Helicoverpa armigera* and improved cotton yield. International Journal of Molecular Sciences 18(9), 1874. https://doi.org/10.3390/ijms18091874

Hanahan, D. (1983). Studies on transformation of *Escherichia coli* with plasmids. Journal of Molecular Biology 166(4), 557-580. https://doi.org/10.1016/s0022-2836(83)80284-8

Hao, C., Wang, Y., Hou, J., Feuillet, C., Balfourier, F., & Zhang, X. (2012). Association mapping and haplotype analysis of a 3.1-Mb genomic region involved in Fusarium head blight resistance on wheat chromosome 3BS. PLoS One 7(10), e46444. https://doi.org/10.1371/journal.pone.0046444

Hardham, A. R., Jones, D. A., & Takemoto, D. (2007). Cytoskeleton and cell wall function in penetration resistance. Current Opinion in Plant Biology 10(4), 342-348. https://doi.org/10.1016/j.pbi.2007.05.001

He, X. Y., Lillemo, M., Shi, J. R., Wu, J. R., Bjornstad, A., Belova, T., Dreisigacker, S., Duveiller, E., & Singh, P. (2016). QTL characterization of Fusarium head blight resistance in CIMMYT bread wheat line

Soru#1. PloS One 11(6), e0158052. https://doi.org/10.1371/journal.pone.0158052
He, Y., Zhang, X., Zhang, Y., Ahmad, D., Wu, L., Jiang, P., & Ma, H. X. (2018). Molecular characterization and expression of PFT, an FHB resistance gene at the Fhb1 QTL in wheat. Phytopathology 108(6), 730-736. https://doi.org/10.1094/Phyto-11-17-0383-R
Herter, C. P., Ebmeyer, E., Kollers, S., Korzun, V., Leiser, W. L., Wurschum, T., & Miedaner, T. (2018). *Rht24* reduces height in the winter wheat population 'Solitar x Bussard' without adverse effects on Fusarium head blight infection. TAG. Theoretical and Applied Genetics. Theoretische und Angewandte Genetik 131(6), 1263–1272. https://doi.org/10.1007/s00122-018-3076-8
Hou, Y. N., Zhai, Y., Feng, L., Karimi, H. Z., Rutter, B. D., Zeng, L. P., Choi, D. S., Zhang, B. L., Gu, W. F., Chen, X. M., Ye, W. W., Innes, R. W., Zhai, J. X., & Ma, W. B. (2019). A *Phytophthora* effector suppresses trans-kingdom RNAi to promote disease susceptibility. Cell Host & Microbe 25(1), 153-+. https://doi.org/10.1016/j.chom.2018.11.007
Howe, K. L., Contreras-Moreira, B., De Silva, N., Maslen, G., Akanni, W., Allen, J., Alvarez-Jarreta, J., Barba, M., Bolser, D. M., Cambell, L., Carbajo, M., Chakiachvili, M., Christensen, M., Cummins, C., Cuzick, A., Davis, P., Fexova, S., Gall, A., George, N., . . . Flicek, P. (2020). Ensembl Genomes 2020-enabling non-vertebrate genomic research. Nucleic Acids Research 48(D1), D689-D695. https://doi.org/10.1093/nar/gkz890
Huang, C. Y., Wang, H., Hu, P., Hamby, R., & Jin, H. (2019). Small RNAs - big players in plant-microbe interactions. Cell Host Microbe, 26(2), 173-182. https://doi.org/10.1016/j.chom.2019.07.021
Huang, G. Z., Allen, R., Davis, E. L., Baum, T. J., & Hussey, R. S. (2006). Engineering broad root-knot resistance in transgenic plants by RNAi silencing of a conserved and essential root-knot nematode parasitism gene. Proceedings of the National Academy of Sciences of the United States of America 103(39), 14302-14306. https://doi.org/10.1073/pnas.0604698103
Huckelhoven, R. (2007). Transport and secretion in plant-microbe interactions. Current Opinion in Plant Biology 10(6), 573-579. https://doi.org/10.1016/j.pbi.2007.08.002
Hudzik, C., Hou, Y., Ma, W., & Axtell, M. J. (2020). Exchange of small regulatory RNAs between plants and their pests. Plant Physiology 182(1), 51-62. https://doi.org/10.1104/pp.19.00931
Ibrahim, A. K., Zhang, L. W., Niyitanga, S., Afzal, M. Z., Xu, Y., Zhang, L. L., Zhang, L. M., & Qi, J. M. (2020). Principles and approaches of association mapping in plant breeding. Tropical Plant Biology 13(3), 212-224. https://doi.org/10.1007/s12042-020-09261-4
Iki, T., Yoshikawa, M., Meshi, T., & Ishikawa, M. (2012). Cyclophilin 40 facilitates HSP90-mediated RISC assembly in plants. The EMBO Journal 31(2), 267-278. https://doi.org/10.1038/emboj.2011.395
Jia, H. Y., Zhou, J. Y., Xue, S. L., Li, G. Q., Yan, H. S., Ran, C. F., Zhang, Y. D., Shi, J. X., Jia, L., Wang, X., Luo, J., & Ma, Z. Q. (2018). A journey to understand wheat Fusarium head blight resistance in the Chinese wheat landrace Wangshuibai. Crop Journal 6(1), 48-59. https://doi.org/10.1016/j.cj.2017.09.006
Jian, J., & Liang, X. (2019). One small RNA of *Fusarium graminearum* targets and silences *CEBiP* gene in common wheat. Microorganisms 7(10). https://doi.org/10.3390/microorganisms7100425
Jiang, Y., Zhao, Y., Rodemann, B., Plieske, J., Kollers, S., Korzun, V., Ebmeyer, E., Argillier, O., Hinze, M., Ling, J., Roder, M. S., Ganal, M. W., Mette, M. F., & Reif, J. C. (2015). Potential and limits to unravel the genetic architecture and predict the variation of Fusarium head blight resistance in European winter wheat (*Triticum aestivum* L.). Heredity 114(3), 318-326. https://doi.org/10.1038/hdy.2014.104
Jiao, J., & Peng, D. (2018). Wheat microRNA1023 suppresses invasion of *Fusarium graminearum* via targeting and silencing *FGSG_03101*. Journal of Plant Interactions 13(1), 514-521. https://doi.org/10.1080/17429145.2018.1528512
Jones, J. D. G., & Dangl, J. L. (2006). The plant immune system. Nature 444(7117), 323-329. https://doi.org/10.1038/nature05286
Kalidas, S., Cestari, I., Monnerat, S., Li, Q., Regmi, S., Hasle, N., Labaied, M., Parsons, M., Stuart, K., & Phillips, M. A. (2014). Genetic validation of aminoacyl-tRNA synthetases as drug targets in *Trypanosoma brucei*. Eukaryotic Cell 13(4), 504-516. https://doi.org/10.1128/EC.00017-14

Kanyuka, K., & Rudd, J. J. (2019). Cell surface immune receptors: the guardians of the plant's extracellular spaces. Current Opinion in Plant Biology 50, 1-8. https://doi.org/10.1016/j.pbi.2019.02.005

Kapustin, Y., Souvorov, A., & Tatusova, T. (2004). Splign - a hybrid approach to spliced alignments. Currents in Computational Molecular Biology.

Kapustin, Y., Souvorov, A., Tatusova, T., & Lipman, D. (2008). Splign: algorithms for computing spliced alignments with identification of paralogs. Biology Direct 3, 20. https://doi.org/10.1186/1745-6150-3-20

Kettles, G. J., Hofinger, B. J., Hu, P. S., Bayon, C., Rudd, J. J., Balmer, D., Courbot, M., Hammond-Kosack, K. E., Scalliet, G., & Kanyuka, K. (2019). sRNA profiling combined with gene function analysis reveals a lack of evidence for cross-kingdom RNAi in the wheat - *Zymoseptoria tritici* pathosystem. Frontiers in Plant Science 10. https://doi.org/ARTN 892 10.3389/fpls.2019.00892

Koch, A., Biedenkopf, D., Furch, A., Weber, L., Rossbach, O., Abdellatef, E., Linicus, L., Johannsmeier, J., Jelonek, L., Goesmann, A., Cardoza, V., McMillan, J., Mentzel, T., & Kogel, K. H. (2016). An RNAi-based control of *Fusarium graminearum* infections through spraying of long dsRNAs Involves a plant passage and is controlled by the fungal silencing machinery. PloS Pathogens 12(10), e1005901. https://doi.org/10.1371/journal.ppat.1005901

Koch, A., Hofle, L., Werner, B. T., Imani, J., Schmidt, A., Jelonek, L., & Kogel, K. H. (2019). SIGS vs HIGS: a study on the efficacy of two dsRNA delivery strategies to silence *Fusarium FgCYP51* genes in infected host and non-host plants. Molecular Plant Pathology 20(12), 1636-1644. https://doi.org/10.1111/mpp.12866

Koch, A., Kumar, N., Weber, L., Keller, H., Imani, J., & Kogel, K. H. (2013). Host-induced gene silencing of cytochrome P450 lanosterol C14alpha-demethylase-encoding genes confers strong resistance to *Fusarium* species. Proceedings of the National Academy of Sciences of the United States of America 110(48), 19324-19329. https://doi.org/10.1073/pnas.1306373110

Koch, A., & Wassenegger, M. (2021). Host-induced gene silencing - mechanisms and applications. The New Phytologist 231(1), 54–59. https://doi.org/10.1111/nph.17364

Kollers, S., Rodemann, B., Ling, J., Korzun, V., Ebmeyer, E., Argillier, O., Hinze, M., Plieske, J., Kulosa, D., Ganal, M. W., & Roder, M. S. (2013). Whole genome association mapping of Fusarium head blight resistance in european winter wheat (*Triticum aestivum* L.). PloS One 8(2), e57500. https://doi.org/10.1371/journal.pone.0057500

Koressaar, T., & Remm, M. (2007). Enhancements and modifications of primer design program Primer3. Bioinformatics 23(10), 1289-1291. https://doi.org/10.1093/bioinformatics/btm091

Korte, A., & Farlow, A. (2013). The advantages and limitations of trait analysis with GWAS: a review. Plant Methods 9. 29. https://doi.org/10.1186/1746-4811-9-29

Kosova, K., Chrpova, J., & Sip, V. (2009). Cereal resistance to Fusarium head blight and possibilities of its improvement through breeding. Czech Journal of Genetics and Plant Breeding 45(3), 87-105. https://doi.org/10.17221/63/2009-Cjgpb

Lacroix, B., & Citovsky, V. (2020). Biolistic approach for transient gene expression studies in plants. Methods in Molecular Biology (Clifton, N.J.) 2124, 125-139. https://doi.org/10.1007/978-1-0716-0356-7_6

Lambertucci, S., Orman, K. M., Das Gupta, S., Fisher, J. P., Gazal, S., Williamson, R. J., Cramer, R., & Bindschedler, L. V. (2019). Analysis of barley leaf epidermis and extrahaustorial proteomes during powdery mildew infection reveals that the PR5 thaumatin-like protein TLP5 is required for susceptibility towards *Blumeria graminis* f. sp. *hordei*. Frontiers in Plant Science 10, 1138. https://doi.org/10.3389/fpls.2019.01138

Landy, A. (1989). Dynamic, structural, and regulatory aspects of lambda site-specific recombination. Annual Review of Biochemistry 58, 913-949. https://doi.org/10.1146/annurev.bi.58.070189.004405

Lee, W. S., Hammond-Kosack, K. E., & Kanyuka, K. (2012). Barley stripe mosaic virus-mediated tools for investigating gene function in cereal plants and their pathogens: virus-induced gene silencing,

host-mediated gene silencing, and virus-mediated overexpression of heterologous protein. Plant Physiology 160(2), 582-590. https://doi.org/10.1104/pp.112.203489

Lemmens, M., Scholz, U., Berthiller, F., Dall'Asta, C., Koutnik, A., Schuhmacher, R., Adam, G., Buerstmayr, H., Mesterhazy, A., Krska, R., & Ruckenbauer, P. (2005). The ability to detoxify the mycotoxin deoxynivalenol colocalizes with a major quantitative trait locus for fusarium head blight resistance in wheat. Molecular Plant-Microbe Interactions : MPMI 18(12), 1318-1324. https://doi.org/10.1094/Mpmi-18-1318

LGC Biosearch Technologies: How does KASP work.
URL: https://www.biosearchtech.com/how-does-kasp-work (Accessed 01.10.2019)

Li, G. Q., Zhou, J. Y., Jia, H. Y., Gao, Z. X., Fan, M., Luo, Y. J., Zhao, P. T., Xue, S. L., Li, N., Yuan, Y., Ma, S. W., Kong, Z. X., Jia, L., An, X., Jiang, G., Liu, W. X., Cao, W. J., Zhang, R. R., Fan, J. C., . . . Ma, Z. Q. (2019). Mutation of a histidine-rich calcium-binding-protein gene in wheat confers resistance to Fusarium head blight. Nature Genetics 51(7), 1106-1112. https://doi.org/10.1038/s41588-019-0426-7

Li, W., Deng, Y., Ning, Y., He, Z., & Wang, G. L. (2020). Exploiting broad-spectrum disease resistance in crops: from molecular dissection to breeding. Annual Review of Plant Biology 71, 575-603. https://doi.org/10.1146/annurev-arplant-010720-022215

Li, Y. H., Sorefan, K., Hemmann, G., & Bevan, M. W. (2004). *Arabidopsis* NAP and PIR regulate actin-based cell morphogenesis and multiple developmental processes. Plant Physiology 136(3), 3616-3627. https://doi.org/10.1104/pp.104.053173

Liu, T. B., Wang, Y. N., Baker, G. M., Fahmy, H., Jiang, L. H., & Xue, C. Y. (2013). The glucose sensor-like protein Hxs1 is a high-affinity glucose transporter and required for virulence in *Cryptococcus neoformans*. PloS One 8(5). https://doi.org/10.1371/journal.pone.0064239

Loukoianov, A., Yan, L., Blechl, A., Sanchez, A., & Dubcovsky, J. (2005). Regulation of *VRN-1* vernalization genes in normal and transgenic polyploid wheat. Plant Physiology 138(4), 2364-2373. https://doi.org/10.1104/pp.105.064287

Luck, S., Kreszies, T., Strickert, M., Schweizer, P., Kuhlmann, M., & Douchkov, D. (2019). siRNA-finder (si-Fi) software for RNAi-target design and off-target prediction. Frontiers in Plant Science 10, 1023. https://doi.org/10.3389/fpls.2019.01023

Lueck, S.,
URL: http://www.snowformatics.com/primer-factory.html (Accessed on 01.07.2016)

Luders, T., Ahlemeyer, J., Forster, J., Weyen, J., Rossa, E., Korzun, V., Lex, J., Friedt, W., & Ordon, F. (2016). Verification of marker-trait associations in biparental winter barley (*Hordeum vulgare* L.) DH populations. Molecular Breeding 36, 14. https://doi.org/10.1007/s11032-016-0438-2

Machado, A. K., Brown, N. A., Urban, M., Kanyuka, K., & Hammond-Kosack, K. E. (2018). RNAi as an emerging approach to control Fusarium head blight disease and mycotoxin contamination in cereals. Pest Management Science 74(4), 790-799. https://doi.org/10.1002/ps.4748

Mackintosh, C. A., Lewis, J., Radmer, L. E., Shin, S., Heinen, S. J., Smith, L. A., Wyckoff, M. N., Dill-Macky, R., Evans, C. K., Kravchenko, S., Baldridge, G. D., Zeyen, R. J., & Muehlbauer, G. J. (2007). Overexpression of defense response genes in transgenic wheat enhances resistance to Fusarium head blight. Plant Cell Reports 26(4), 479-488. https://doi.org/10.1007/s00299-006-0265-8

Majumdar, R., Rajasekaran, K., & Cary, J. W. (2017). RNA interference (RNAi) as a potential tool for control of mycotoxin contamination in crop plants: concepts and considerations. Frontiers in Plant Science 8, 200. https://doi.org/10.3389/fpls.2017.00200

Makandar, R., Essig, J. S., Schapaugh, M. A., Trick, H. N., & Shah, J. (2006). Genetically engineered resistance to Fusarium head blight in wheat by expression of *Arabidopsis* NPR1. Molecular Plant-Microbe Interactions : MPMI 19(2), 123-129. https://doi.org/10.1094/MPMI-19-0123

Massman, J., Cooper, B., Horsley, R., Neate, S., Dill-Macky, R., Chao, S., Dong, Y., Schwarz, P., Muehlbauer, G. J., & Smith, K. P. (2011). Genome-wide association mapping of Fusarium head blight resistance in contemporary barley breeding germplasm. Molecular Breeding 27(4), 439-454. https://doi.org/10.1007/s11032-010-9442-0

McLoughlin, A. G., Wytinck, N., Walker, P. L., Girard, I. J., Rashid, K. Y., de Kievit, T., Fernando, W. G. D., Whyard, S., & Belmonte, M. F. (2018). Identification and application of exogenous dsRNA confers plant protection against *Sclerotinia sclerotiorum* and *Botrytis cinerea*. Scientific Reports 8(1), 7320. https://doi.org/10.1038/s41598-018-25434-4

Meng, Y., Moscou, M. J., & Wise, R. P. (2009). Blufensin1 negatively impacts basal defense in response to barley powdery mildew. Plant Physiology 149(1), 271-285. https://doi.org/10.1104/pp.108.129031

Miedaner, T., & Korzun, V. (2012). Marker-assisted selection for disease resistance in wheat and barley breeding. Phytopathology 102(6), 560-566. https://doi.org/10.1094/Phyto-05-11-0157

Miedaner, T., Risser, P., Paillard, S., Schnurbusch, T., Keller, B., Hartl, L., Holzapfel, J., Korzun, V., Ebmeyer, E., & Utz, H. F. (2012). Broad-spectrum resistance loci for three quantitatively inherited diseases in two winter wheat populations. Molecular Breeding 29(3), 731-742. https://doi.org/10.1007/s11032-011-9586-6

Miedaner, T., Würschum, T., Maurer, H.P., Korzun V., Ebmeyer E., Reif J.C. (2011) Association mapping for Fusarium head blight resistance in European soft winter wheat. Molecular Breeding 28, 647–655. https://doi.org/10.1007/s11032-010-9516-z

Mirdita, V., Liu, G., Zhao, Y., Miedaner, T., Longin, C. F., Gowda, M., Mette, M. F., & Reif, J. C. (2015). Genetic architecture is more complex for resistance to Septoria tritici blotch than to Fusarium head blight in Central European winter wheat. BMC Genomics 16(1), 430. https://doi.org/10.1186/s12864-015-1628-8

Mitter, N., Worrall, E. A., Robinson, K. E., Li, P., Jain, R. G., Taochy, C., Fletcher, S. J., Carroll, B. J., Lu, G. Q., & Xu, Z. P. (2017). Clay nanosheets for topical delivery of RNAi for sustained protection against plant viruses. Nature Plants 3, 16207. https://doi.org/10.1038/nplants.2016.207

Moran, Y., Agron, M., Praher, D., & Technau, U. (2017). The evolutionary origin of plant and animal microRNAs. Nature Ecology & Evolution 1(3), 27. https://doi.org/10.1038/s41559-016-0027

Mosher, R. A., & Baulcombe, D. C. (2008). Bacterial pathogens encode suppressors of RNA-mediated silencing. Genome Biology 9(10), 237. https://doi.org/10.1186/gb-2008-9-10-237

Motulsky, H. J., & Brown, R. E. (2006). Detecting outliers when fitting data with nonlinear regression - a new method based on robust nonlinear regression and the false discovery rate. BMC Bioinformatics 7, 123. https://doi.org/10.1186/1471-2105-7-123

Myles, S., Peiffer, J., Brown, P. J., Ersoz, E. S., Zhang, Z., Costich, D. E., & Buckler, E. S. (2009). Association mapping: critical considerations shift from genotyping to experimental design. The Plant Cell 21(8), 2194-2202. https://doi.org/10.1105/tpc.109.068437

Nagawa, S., Xu, T., & Yang, Z. (2010). RHO GTPase in plants: Conservation and invention of regulators and effectors. Small GTPases 1(2), 78-88. https://doi.org/10.4161/sgtp.1.2.14544

Naramoto, S., Otegui, M. S., Kutsuna, N., de Rycke, R., Dainobu, T., Karampelias, M., Fujimoto, M., Feraru, E., Miki, D., Fukuda, H., Nakano, A., & Friml, J. (2014). Insights into the Localization and Function of the Membrane Trafficking Regulator GNOM ARF-GEF at the Golgi Apparatus in *Arabidopsis*. The Plant Cell 26(7), 3062-3076. https://doi.org/10.1105/tpc.114.125880

National Center for Biotechnology Information (NCBI) (1988) Bethesda (MD): National Library of Medicine (US), National Center for Biotechnology Information.
URL: https://blast.ncbi.nlm.nih.gov/Blast.cgi. (Accessed 01.04.2016)

Navara, S., & Smith, K. P. (2014). Using near-isogenic barley lines to validate deoxynivalenol (DON) QTL previously identified through association analysis. TAG. Theoretical and Applied Genetics Theoretische und Angewandte Genetik, 127(3), 633-645. https://doi.org/10.1007/s00122-013-2247-x

Nielsen, M. E., Feechan, A., Bohlenius, H., Ueda, T., & Thordal-Christensen, H. (2012). *Arabidopsis* ARF-GTP exchange factor, GNOM, mediates transport required for innate immunity and focal accumulation of syntaxin PEN1. Proceedings of the National Academy of Sciences of the United States of America 109(28), 11443-11448. https://doi.org/10.1073/pnas.1117596109

Nishad, R., Ahmed, T., Rahman, V. J., & Kareem, A. (2020). Modulation of plant defense system in response to microbial interactions. Frontiers in Microbiology 11, 1298.

https://doi.org/10.3389/fmicb.2020.01298

Nowara, D., Gay, A., Lacomme, C., Shaw, J., Ridout, C., Douchkov, D., Hensel, G., Kumlehn, J., & Schweizer, P. (2010). HIGS: host-induced gene silencing in the obligate biotrophic fungal pathogen *Blumeria graminis*. The Plant Cell 22(9), 3130-3141. https://doi.org/10.1105/tpc.110.077040

Nunes, C. C., & Dean, R. A. (2012). Host-induced gene silencing: a tool for understanding fungal host interaction and for developing novel disease control strategies. Molecular Plant Pathology 13(5), 519-529. https://doi.org/10.1111/j.1364-3703.2011.00766.x

Oliveira-Garcia, E., & Deising, H. B. (2013). Infection structure-specific expression of beta-1,3-glucan synthase is essential for pathogenicity of *Colletotrichum graminicola* and evasion of beta-glucan-triggered immunity in maize. The Plant Cell 25(6), 2356-2378. https://doi.org/10.1105/tpc.112.103499

Oliveira-Garcia, E., & Deising, H. B. (2016). The glycosylphosphatidylinositol anchor biosynthesis genes *GPI12*, *GAA1*, and *GPI8* are essential for cell-wall integrity and pathogenicity of the maize Anthracnose Fungus *Colletotrichum graminicola*. Molecular plant-microbe interactions : MPMI 29(11), 889-901. https://doi.org/10.1094/MPMI-09-16-0175-R

Opalski, K. S., Schultheiss, H., Kogel, K. H., & Huckelhoven, R. (2005). The receptor-like MLO protein and the RAC/ROP family G-protein RACB modulate actin reorganization in barley attacked by the biotrophic powdery mildew fungus *Blumeria graminis* f.sp *hordei*. The Plant journal : for cell and molecular biology 41(2), 291-303. https://doi.org/10.1111/j.1365-313X.2004.02292.x

Page, M. L. (2017). Gene-silencing spray lets us modify plants without changing DNA. New Scientist 3108.
URL: https://www.newscientist.com/article/2117460-gene-silencing-spray-lets-us-modify-plants-without-changing-dna/ (Accessed 10.02.2017)

Panstruga, R. (2004). A golden shot: how ballistic single cell transformation boosts the molecular analysis of cereal-mildew interactions. Molecular Plant Pathology 5(2), 141-148. https://doi.org/10.1111/j.1364-3703.2004.00208.x

Park, E., Nedo, A., Caplan, J. L., & Dinesh-Kumar, S. P. (2018). Plant-microbe interactions: organelles and the cytoskeleton in action. The New Phytologist 217(3), 1012-1028. https://doi.org/10.1111/nph.14959

Park, M., & Jurgens, G. (2011). Membrane traffic and fusion at post-Golgi compartments. Frontiers in Plant Science 2, 111. https://doi.org/10.3389/fpls.2011.00111

Paudel, B., Zhuang, Y. B., Galla, A., Dahal, S., Qiu, Y. J., Ma, A. J., Raihan, T., & Yen, Y. (2020). *WFhb1-1* plays an important role in resistance against Fusarium head blight in wheat. Scientific Reports 10(1), 7794. https://doi.org/10.1038/s41598-020-64777-9

Pecenkova, T., Hala, M., Kulich, I., Kocourkova, D., Drdova, E., Fendrych, M., Toupalova, H., & Zarsky, V. (2011). The role for the exocyst complex subunits Exo70B2 and Exo70H1 in the plant-pathogen interaction. Journal of Experimental Botany 62(6), 2107-2116. https://doi.org/10.1093/jxb/erq402

Periyannan, S., Milne, R. J., Figueroa, M., Lagudah, E. S., & Dodds, P. N. (2017). An overview of genetic rust resistance: from broad to specific mechanisms. PLoS Pathogens 13(7), e1006380. https://doi.org/10.1371/journal.ppat.1006380

Pliego, C., Nowara, D., Bonciani, G., Gheorghe, D. M., Xu, R., Surana, P., Whigham, E., Nettleton, D., Bogdanove, A. J., Wise, R. P., Schweizer, P., Bindschedler, L. V., & Spanu, P. D. (2013). Host-induced gene silencing in barley powdery mildew reveals a class of ribonuclease-like effectors. Molecular Plant-Microbe Interactions : MPMI 26(6), 633-642. https://doi.org/10.1094/MPMI-01-13-0005-R

Qi, T., Guo, J., Peng, H., Liu, P., Kang, Z. S., & Guo, J. (2019). Host-induced gene silencing: a powerful strategy to control diseases of wheat and barley. International Journal of Molecular Sciences 20(1), 206. https://doi.org/10.3390/ijms20010206

Qi, T., Zhu, X., Tan, C., Liu, P., Guo, J., Kang, Z., & Guo, J. (2018). Host-induced gene silencing of an important pathogenicity factor *PsCPK1* in *Puccinia striiformis* f. sp. *tritici* enhances resistance

of wheat to stripe rust. Plant Biotechnology Journal 16(3), 797-807. https://doi.org/10.1111/pbi.12829

R Core Team. (2018). R: a language and environment for statistical computing. R Foundation for Statistical Computing.
https://www.R-project.org (Accessed 01.10.2017)

Ramirez-Gonzalez, R. H., Borrill, P., Lang, D., Harrington, S. A., Brinton, J., Venturini, L., Davey, M., Jacobs, J., van Ex, F., Pasha, A., Khedikar, Y., Robinson, S. J., Cory, A. T., Florio, T., Concia, L., Juery, C., Schoonbeek, H., Steuernagel, B., Xiang, D., . . . Sequencing, I. W. G. (2018). The transcriptional landscape of polyploid wheat. Science (New York, N.Y.) 361(6403), eaar6089. https://doi.org/10.1126/science.aar6089

Rawat, N., Pumphrey, M. O., Liu, S. X., Zhang, X. F., Tiwari, V. K., Ando, K., Trick, H. N., Bockus, W. W., Akhunov, E., Anderson, J. A., & Gill, B. S. (2016). Wheat *Fhb1* encodes a chimeric lectin with agglutinin domains and a pore-forming toxin-like domain conferring resistance to Fusarium head blight. Nature Genetics, 48(12), 1576-1580. https://doi.org/10.1038/ng.3706

Robinson, D. G., Ding, Y., & Jiang, L. (2016). Unconventional protein secretion in plants: a critical assessment. Protoplasma, 253(1), 31-43. https://doi.org/10.1007/s00709-015-0887-1

Robinson, D. G., Hinz, G., & Holstein, S. E. H. (1998). The molecular characterization of transport vesicles. Plant Molecular Biology 38(1-2), 49-76. https://doi.org/Doi 10.1023/A:1006025802445

Rossum, G. V., & Drake, F. L. (2009). Python 3 reference manual. Scotts Valley, CA: CreateSpace.

Saja, D., Janeczko, A., Barna, B., Skoczowski, A., Dziurka, M., Kornas, A., & Gullner, G. (2020). Powdery mildew-induced hormonal and photosynthetic changes in barley near isogenic lines carrying various resistant genes. International Journal of Molecular Sciences 21(12), 4536. https://doi.org/10.3390/ijms21124536

Scheuring, D., Viotti, C., Kruger, F., Kunzl, F., Sturm, S., Bubeck, J., Hillmer, S., Frigerio, L., Robinson, D. G., Pimpl, P., & Schumacher, K. (2011). Multivesicular bodies mature from the trans-golgi network/early endosome in *Arabidopsis*. The Plant Cell 23(9), 3463-3481. https://doi.org/10.1105/tpc.111.086918

Schmidt, S. M., & Panstruga, R. (2011). Pathogenomics of fungal plant parasites: what have we learnt about pathogenesis? Current Opinion in Plant Biology 14(4), 392-399. https://doi.org/10.1016/j.pbi.2011.03.006

Schweizer P. (2014) Host and nonhost response to attack by fungal pathogens biotechnological approaches to barley improvement. In a Kumlehn J., Stein N. (eds.), Biotechnological approaches to barley improvement. Biotechnology in Aagriculture and Forestry 69, 197-235. https://doi.org/10.1007/978-3-662-44406-1

Schweizer, P., Pokorny, J., Abderhalden, O., & Dudler, R. (1999). A transient assay system for the functional assessment of defense-related genes in wheat. Molecular Plant-Microbe Interactions : MPMI 12(8), 647-654. https://doi.org/Doi 10.1094/Mpmi.1999.12.8.647

Shah, L., Ali, A., Yahya, M., Zhu, Y., Wang, S., Si, H., Rahman, H., & Ma, C. (2018). Integrated control of Fusarium head blight and deoxynivalenol mycotoxin in wheat. Plant Pathology 67(3), 532-548. https://doi.org/10.1111/ppa.12785

Shahid, S., Kim, G., Johnson, N. R., Wafula, E., Wang, F., Coruh, C., Bernal-Galeano, V., Phifer, T., dePamphilis, C. W., Westwood, J. H., & Axtell, M. J. (2018). MicroRNAs from the parasitic plant *Cuscuta campestris* target host messenger RNAs. Nature 553(7686), 82-85. https://doi.org/10.1038/nature25027

Sigrist, C. J. A., de Castro, E., Cerutti, L., Cuche, B. A., Hulo, N., Bridge, A., Bougueleret, L., & Xenarios, I. (2013). New and continuing developments at PROSITE. Nucleic Acids Research 41(Database issue), D344–D347. https://doi.org/10.1093/nar/gks1067

Sinha, S. K. (2010). RNAi induced gene silencing in crop improvement. Physiology and Molecular Biology of Plants : an International Journal of Functional Plant Biology 16(4), 321-332. https://doi.org/10.1007/s12298-010-0036-4

Slominska-Durdasiak, K. M., Kollers, S., Korzun, V., Nowara, D., Schweizer, P., Djamei, A., & Reif, J. C.

(2020). Association mapping of wheat Fusarium head blight resistance-related regions using a candidate-gene approach and their verification in a biparental population. TAG. Theoretical and Applied Genetics. Theoretische und Angewandte Genetik 133(1), 341-351. https://doi.org/10.1007/s00122-019-03463-5

St Clair, D. A. (2010). Quantitative disease resistance and quantitative resistance Loci in breeding. Annual Review of Phytopathology 48, 247-268. https://doi.org/10.1146/annurev-phyto-080508-081904

Staerkel, C., Boenisch, M. J., Kroger, C., Bormann, J., Schafer, W., & Stahl, D. (2013). *CbCTB2*, an O-methyltransferase is essential for biosynthesis of the phytotoxin cercosporin and infection of sugar beet by *Cercospora beticola*. BMC Plant Biology 13, 50. https://doi.org/10.1186/1471-2229-13-50

Stam, P. (1993). Construction of integrated genetic-linkage maps by means of a new computer package - Joinmap. The Plant Journal 3(5), 739-744. https://doi.org/10.1111/j.1365-313X.1993.00739.x

Stam, P. (1995). JoinMap 2.0 deals with all types of plant mapping populations. Plant Genome III Abstracts.

Steiner, B., Buerstmayr, M., Michel, S., Schweiger, W., Lemmens, M., & Buerstmayr, H. (2017). Breeding strategies and advances in line selection for Fusarium head blight resistance in wheat. Tropical Plant Pathology 42(3), 165-174. https://doi.org/10.1007/s40858-017-0127-7

Su, Z. Q., Bernardo, A., Tian, B., Chen, H., Wang, S., Ma, H. X., Cai, S. B., Liu, D. T., Zhang, D. D., Li, T., Trick, H., St Amand, P., Yu, J. M., Zhang, Z. Y., & Bai, G. H. (2019). A deletion mutation in *TaHRC* confers Fhb1 resistance to Fusarium head blight in wheat. Nature Genetics 51(7), 1099-1105. https://doi.org/10.1038/s41588-019-0425-8

Sun, H. Y., Cui, J. H., Tian, B. H., Cao, S. L., Zhang, X. X., & Chen, H. G. (2020). Resistance risk assessment for *Fusarium graminearum* to pydiflumetofen, a new succinate dehydrogenase inhibitor. Pest Management Science 76(4), 1549-1559. https://doi.org/10.1002/ps.5675

Tessmann, E. W., Dong, Y. H., & Van Sanford, D. A. (2019). GWAS for Fusarium head blight traits in a soft red winter wheat mapping panel. Crop Science 59(5), 1823-1837. https://doi.org/10.2135/cropsci2018.08.0492

Tessmann, E. W., & Van Sanford, D. A. (2018). GWAS for Fusarium head blight related traits in winter wheat (*Triticum Aestivum* L.) in an artificially warmed treatment. Agronomy 8(5), 68. https://doi.org/10.3390/agronomy8050068

Tinker, N. A., Fortin, M. G., & Mather, D. E. (1993). Random amplified polymorphic DNA and pedigree relationships in spring barley. TAG. Theoretical and Applied Genetics. Theoretische und Angewandte Genetik 85(8), 976-984. https://doi.org/10.1007/BF00215037

Untergasser, A., Cutcutache, I., Koressaar, T., Ye, J., Faircloth, B. C., Remm, M., & Rozen, S. G. (2012). Primer3-new capabilities and interfaces. Nucleic Acids Research 40(15), e115. https://doi.org/10.1093/nar/gks596

Valadi, H., Ekstrom, K., Bossios, A., Sjostrand, M., Lee, J. J., & Lotvall, J. O. (2007). Exosome-mediated transfer of mRNAs and microRNAs is a novel mechanism of genetic exchange between cells. Nature Cell Biology 9(6), 654-U672. https://doi.org/10.1038/ncb1596

van de Meene, A. M., Doblin, M. S., & Bacic, A. (2017). The plant secretory pathway seen through the lens of the cell wall. Protoplasma 254(1), 75-94. https://doi.org/10.1007/s00709-016-0952-4

Van der Biezen, E. A., & Jones, J. D. (1998). Plant disease-resistance proteins and the gene-for-gene concept. Trends in Biochemical Sciences 23(12), 454-456. https://doi.org/10.1016/s0968-0004(98)01311-5

van Ooijen, J. W., & Jansen, J. (2013). Genetic mapping in experimental populations. Cambridge University Press; 1st edition, 132-137. 978-1-107-01321-6

van Wersch, S., Tian, L., Hoy, R., & Li, X. (2020). Plant NLRs: the whistleblowers of plant immunity. Plant Communications 1(1), 100016. https://doi.org/10.1016/j.xplc.2019.100016

Velasquez, A. C., Castroverde, C. D. M., & He, S. Y. (2018). Plant-pathogen warfare under changing climate conditions. Current Biology : CB 28(10), R619-R634. https://doi.org/10.1016/j.cub.2018.03.054

Venske, E., dos Santos, R. S., Farias, D. D., Rother, V., da Maia, L. C., Pegoraro, C., & de Oliveira, A. C. (2019). Meta-analysis of the QTLome of Fusarium head blight resistance in bread wheat: refining the current puzzle. Frontiers in Plant Science 10. https://doi.org/ARTN 727 10.3389/fpls.2019.00727

Waldron, B. L., Moreno-Sevilla, B., Anderson, J. A., Stack, R. W., & Frohberg, R. C. (1999). RFLP mapping of QTL for fusarium head blight resistance in wheat. Crop Science 39(3), 805-811. https://doi.org/DOI 10.2135/cropsci1999.0011183X003900030032x

Walter, S., Nicholson, P., & Doohan, F. M. (2010). Action and reaction of host and pathogen during Fusarium head blight disease. The New Phytologist 185(1), 54-66. https://doi.org/10.1111/j.1469-8137.2009.03041.x

Wang, F., Shang, Y. F., Fan, B. F., Yu, J. Q., & Chen, Z. X. (2014). Arabidopsis LIP5, a positive regulator of multivesicular body biogenesis, is a critical target of pathogen-responsive MAPK cascade in plant basal defense. PLoS Pathogens 10(7), e1004243. https://doi.org/10.1371/journal.ppat.1004243

Wang, M., & Dean, R. A. (2020). Movement of small RNAs in and between plants and fungi. Molecular Plant Pathology 21(4), 589-601. https://doi.org/10.1111/mpp.12911

Wang, M., Thomas, N., & Jin, H. (2017). Cross-kingdom RNA trafficking and environmental RNAi for powerful innovative pre- and post-harvest plant protection. Current Opinion in Plant Biology 38, 133-141. https://doi.org/10.1016/j.pbi.2017.05.003

Wang, M., Weiberg, A., Lin, F. M., Thomma, B. P., Huang, H. D., & Jin, H. (2016). Bidirectional cross-kingdom RNAi and fungal uptake of external RNAs confer plant protection. Nature Plants 2, 16151. https://doi.org/10.1038/nplants.2016.151

Wang, S. C., Wong, D. B., Forrest, K., Allen, A., Chao, S. M., Huang, B. E., Maccaferri, M., Salvi, S., Milner, S. G., Cattivelli, L., Mastrangelo, A. M., Whan, A., Stephen, S., Barker, G., Wieseke, R., Plieske, J., Lillemo, M., Mather, D., Appels, R., . . . Sequencing, I. W. G. (2014). Characterization of polyploid wheat genomic diversity using a high-density 90 000 single nucleotide polymorphism array. Plant Biotechnology Journal 12(6), 787-796. https://doi.org/10.1111/pbi.12183

Weiberg, A., & Jin, H. (2015). Small RNAs--the secret agents in the plant-pathogen interactions. Current Opinion in Plant Biology 26, 87-94. https://doi.org/10.1016/j.pbi.2015.05.033

Weiberg, A., Wang, M., Lin, F. M., Zhao, H., Zhang, Z., Kaloshian, I., Huang, H. D., & Jin, H. (2013). Fungal small RNAs suppress plant immunity by hijacking host RNA interference pathways. Science 342(6154), 118-123. https://doi.org/10.1126/science.1239705

Werner, B. T., Gaffar, F. Y., Schuemann, J., Biedenkopf, D., & Koch, A. M. (2020). RNA-spray-mediated silencing of *Fusarium graminearum AGO* and *DCL* genes improve barley disease resistance. Frontiers in Plant Science 11, 476. https://doi.org/10.3389/fpls.2020.00476

Wilcoxon, F. (1946). Individual comparisons of grouped data by ranking methods. Journal of Economic Entomology 39, 269. https://doi.org/10.1093/jee/39.2.269

Xu, W. H., Meng, Y., Surana, P., Fuerst, G., Nettleton, D., & Wise, R. P. (2015). The knottin-like Blufensin family regulates genes involved in nuclear import and the secretory pathway in barley-powdery mildew interactions. Frontiers in Plant Science 6 409. https://doi.org/ARTN 409 10.3389/fpls.2015.00409

Xue, S. L., Xu, F., Tang, M. Z., Zhou, Y., Li, G. Q., An, X., Lin, F., Xu, H. B., Jia, H. Y., Zhang, L. X., Kong, Z. X., & Ma, Z. Q. (2011). Precise mapping *Fhb5*, a major QTL conditioning resistance to *Fusarium* infection in bread wheat (*Triticum aestivum* L.). TAG. Theoretical and Applied Genetics. Theoretische und Angewandte Genetik 123(6), 1055-1063. https://doi.org/10.1007/s00122-011-1647-z

Yang, L., & Huang, H. (2014). Roles of small RNAs in plant disease resistance. Journal of Integrative Plant Biology 56(10), 962-970. https://doi.org/10.1111/jipb.12200

Yang, L., Qin, L., Liu, G. S., Peremyslov, V. V., Dolja, V. V., & Wei, Y. D. (2014). Myosins XI modulate host cellular responses and penetration resistance to fungal pathogens. Proceedings of the National Academy of Sciences of the United States of America 111(38), 13996-14001. https://doi.org/10.1073/pnas.1405292111

Yao, E., Blake, V. C., Cooper, L., Wight, C. P., Michel, S., Cagirici, H. B., Lazo, G. R., Birkett, C. L., Waring, D. J., Jannink, J. L., Holmes, I., Waters, A. J., Eickholt, D. P., & Sen, T. Z. (2022). GrainGenes: a data-rich repository for small grains genetics and genomics. Database : The Journal of Biological Databases and Curation 2022, baac034. https://doi.org/10.1093/database/baac034

Yin, C., Jurgenson, J. E., & Hulbert, S. H. (2011). Development of a host-induced RNAi system in the wheat stripe rust fungus *Puccinia striiformis* f. sp. *tritici*. Molecular Plant-Microbe Interactions : MPMI 24(5), 554-561. https://doi.org/10.1094/MPMI-10-10-0229

Yu, G. H., Zhang, X., Yao, J. B., Zhou, M. P., & Ma, H. X. (2017). Resistance against Fusarium head blight in transgenic wheat plants expressing the *ScNPR1* gene. Journal of Phytopathology 165(4), 223-231. https://doi.org/10.1111/jph.12553

Zanke, C., Ling, J., Plieske, J., Kollers, S., Ebmeyer, E., Korzun, V., Argillier, O., Stiewe, G., Hinze, M., Beier, S., Ganal, M. W., & Roder, M. S. (2014). Genetic architecture of main effect QTL for heading date in European winter wheat. Frontiers in Plant Science 5, 217. https://doi.org/10.3389/fpls.2014.00217

Zarsky, V., Kulich, I., Fendrych, M., & Pecenkova, T. (2013). Exocyst complexes multiple functions in plant cells secretory pathways. Current Opinion in Plant Biology 16(6), 726-733. https://doi.org/10.1016/j.pbi.2013.10.013

Zhang, B., Karnik, R., Wang, Y., Wallmeroth, N., Blatt, M. R., & Grefen, C. (2015). The *Arabidopsis* r-SNARE VAMP721 interacts with KAT1 and KC1 K+ channels to moderate K+ current at the plasma membrane. The Plant Cell 27(6), 1697-1717. https://doi.org/10.1105/tpc.15.00305

Zhang, T., Zhao, Y. L., Zhao, J. H., Wang, S., Jin, Y., Chen, Z. Q., Fang, Y. Y., Hua, C. L., Ding, S. W., & Guo, H. S. (2016). Cotton plants export microRNAs to inhibit virulence gene expression in a fungal pathogen. Nature Plants 2(10), 16153. https://doi.org/10.1038/nplants.2016.153

Zhang, Z., Henderson, C., Perfect, E., Carver, T. L., Thomas, B. J., Skamnioti, P., & Gurr, S. J. (2005). Of genes and genomes, needles and haystacks: *Blumeria graminis* and functionality. Molecular Plant Pathology 6(5), 561-575. https://doi.org/10.1111/j.1364-3703.2005.00303.x

Zhang, Z. W., Ersoz, E., Lai, C. Q., Todhunter, R. J., Tiwari, H. K., Gore, M. A., Bradbury, P. J., Yu, J. M., Arnett, D. K., Ordovas, J. M., & Buckler, E. S. (2010). Mixed linear model approach adapted for genome-wide association studies. Nature Genetics 42(4), 355-U118. https://doi.org/10.1038/ng.546

Zhao, S. Z., Li, A. Q., Li, C. S., Xia, H., Zhao, C. Z., Zhang, Y., Hou, L., & Wang, X. J. (2017). Development and application of KASP marker for high throughput detection of *AhFAD2* mutation in peanut. Electronic Journal of Biotechnology 25, 9-12. https://doi.org/10.1016/j.ejbt.2016.10.010

Zheng, Z., Gao, T., Hou, Y., & Zhou, M. (2013). Involvement of the anucleate primary sterigmata protein *FgApsB* in vegetative differentiation, asexual development, nuclear migration, and virulence in *Fusarium graminearum*. FEMS Microbiology Letters 349(2), 88-98. https://doi.org/10.1111/1574-6968.12297

Zhu, C., Liu, T., Chang, Y. N., & Duan, C. G. (2019). Small RNA functions as a trafficking effector in plant immunity. International Journal of Molecular Sciences 20(11), 2816. https://doi.org/10.3390/ijms20112816

Zhu, C. S., Gore, M., Buckler, E. S., & Yu, J. M. (2008). Status and prospects of association mapping in plants. The Plant Genome 1(1), 5-20. https://doi.org/10.3835/plantgenome2008.02.0089

Zhu, Z. W., Chen, L., Zhang, W., Yang, L. J., Zhu, W. W., Li, J. H., Liu, Y. K., Tong, H. W., Fu, L. P., Liu, J. D., Rasheed, A., Xia, X. C., He, Z. H., Hao, Y. F., & Gao, C. B. (2020). Genome-wide association analysis of Fusarium head blight resistance in Chinese elite wheat lines. Frontiers in Plant Science 11, 206. https://doi.org/10.3389/fpls.2020.00206

Zierold, U., Scholz, U., & Schweizer, P. (2005). Transcriptome analysis of *mlo*-mediated resistance in the epidermis of barley. Molecular Plant Pathology 6(2), 139-151. https://doi.org/10.1111/j.1364-3703.2005.00271.x

Zulak, K. G., Cox, B. A., Tucker, M. A., Oliver, R. P., & Lopez-Ruiz, F. J. (2018). Improved detection and monitoring of fungicide resistance in *Blumeria graminis* f. sp. *hordei* with high-throughput genotype quantification by gigital PCR. Frontiers in Microbiology 9, 706.

https://doi.org/10.3389/fmicb.2018.00706

Appendix: Supplemental tables and figures

Supplementary Data M1: Important chemicals used in experiments described in here.

Chemicals	Company
Acetic acid	Carl Roth
Agarose	Biozym
Ampicillin Sodium Salt	Carl Roth
Bentonite	Sigma-Aldrich
Benzimidazole	Fluka
5-Bromo-4-chloro-3-indolyl-β-D-glucuronic	Biosynth
Calcium chloride dihydrate	Carl Roth
Calcium nitrate tetrahydrate	Carl Roth
Celite 545	Merck
Diethyl pyrocarbonate (DEPC)	Carl Roth
Dipotassium hydrogen phosphate trihydrate	Carl Roth
Disodium dihydrogen pyrophosphate –	Sigma-Aldrich
Ethanol (96 %)	Carl Roth
Ethanol (>= 99.5%)	Carl Roth
Ethidium bromide [10g/l]	Carl Roth
Ethylenediaminetetraacetic acid disodium salt	Carl Roth
Glucose	Carl Roth
Glycerol	Carl Roth
Glycine	Carl Roth
Hydrochloric acid, 37% fuming	Carl Roth
Isoamyl alcohol (99.9 %)	Carl Roth
Isopropanol	Carl Roth
Kanamycin	Carl Roth
Magnesium chloride hexahydrate	Merck
Magnesium sulfate heptahydrate	Carl Roth
Methanol	Carl Roth
Microagar	Duchefa
3-(N-morpholino) propanesulfonic acid (MOPS)	Carl Roth
Phytoagar	Duchefa

Chemicals	Company
Potassium acetate	Carl Roth
Potassium chloride	Carl Roth
Potassium dihydrogen phosphate	Carl Roth
Potassium ferricyanide (III)	Carl Roth
Potassium hexacyanoferrate(II) trihydrate	Carl Roth
Potassium nitrate	Carl Roth
Potato Extract Glucose Agar	Carl Roth
Rubidium chloride	Sigma-Aldrich
Saccharose	Applichem
Sodium acetate trihydrate	Carl Roth
Sodium chloride	Carl Roth
Sodium dihydrogen phosphate monohydrate	Carl Roth
Sodium hydroxide	Carl Roth
Disodium hydrogen phosphate dihydrate	Carl Roth
Spectinomycin dihydrochloride pentahydrate	Sigma-Aldrich
Trichloroacetic acid	Sigma-Aldrich
Tris(hydroxymethyl)aminomethane	Carl Roth
Tryptone	Otto Nordwald
Triton X-100	Carl Roth
Tween-20	Sigma
Yeast extract	Duchefa

Supplementary Data M2: The media composition for bacterial and fungal cultures used in the experiments with additional information.

Medium	Composition	Additional information
LB (Lysogeny Broth) medium (liquid)	1% (w/v) Tryptone 0.5% (w/v) Yeast extract 0.5% (w/v) NaCl	pH 7.0 Sterilization at 121 °C for 20 min
LB medium (solid)	1% (w/v) Tryptone 0.5% (w/v) Yeast extract 0.5% (w/v) NaCl 1.5 % (w/v) Microagar	pH 7.0 Sterilization at 121 °C for 20 min
LB medium for chemical competent cells preparation	LB (liquid) + 2.5 mM $MgSO_4$ 2.5 mM MgCl	pH 7.0 $MgSO_4$ and MgCl sterilized by filtering (0.2 µm filter)
SOC (Super Optimal Broth) medium	2% (w/v) Tryptone 0.5% (w/v) Yeast extract 10 mM NaCl 2.5 mM KCl 10 mM $MgCl_2$ 10 mM $MgSO_4$ 20 mM Glucose	Sterilization at 121 °C for 20 min before adding glucose. Final sterilization by filtering throught a 0.2 m filter.
SNA (Saltwater Nutrient Agar) medium	7.35 mM KH_2PO_4 10 mM KNO_3 2 mM $MgSO_4$ 6.7 mM KCL 1.1 mM Glucose 0.3 mM Saccharose 1.2 % (w/v) Microagar	Sterilization at 121 °C for 20 min
PDA (Potato Dextrose Agar) medium	0.5 % (w/v) Mikroagar 3.9 % (w/v) Potato-Extract-Glucose-Agar	Sterilization at 121 °C for 20 min

The pH adjustment, if not written otherwise, was performed with 5M NaOH / 3M HCl.

The LB media, if necessary, were supplemented with the indicated antibiotics that were kept at -20°C.
Medium Concentration
Ampicillin 100 mg/l (dissolved in 50% (v/v) EtOH + 50% (v/v) H_2O)
Kanamycin 50 mg/l (dissolved in H_2O)
Spectinomycin 100 mg/l (dissolved in H_2O)

All media are stored at room temperature (RT).

Supplementary Data M3: The solutions used in the experiments described in Material and Methods.

Solution	Solution Composition	Additional information
Benzimidazole	40 mg/ml benzimidazole in 96 % ethanol	Stored at -20°C
Calcium nitrate	1 M $Ca(NO_3)_2$	pH 10.0 Sterilization at 121 °C for 20 min Stored at 4°C
DEPC water 0.1%	0.1% DEPC	RT for 60 min, then sterilization at 121 °C for 15 min
EDTA	0.5 M EDTA	pH 8.0 Sterilization at 121 °C for 15 min
FES buffer	0.1 M Glycine 0.06 M K_2HPO_4 1% $Na_2H_2P_2O_7$ 3% Bentonite 1.25% Celite	pH 8.9 Sterilization at 121 °C for 20 min
GUS-staining solution (1.4 M)	20 % (v/v) Methanol 0.1 % (w/v) X-Gluc 20 % (v/v) Phosphate buffer 10 mM EDTA 0.001 % Triton-X 1.4 mM $K_4Fe(CN)_6$ 1.4 mM $K_3Fe(CN)_6$	pH 6.8-7.2
GUS-staining solution (3 M)	20 % (v/v) Methanol 0.1 % (w/v) X-Gluc 20 % (v/v) phosphate buffer 10 mM EDTA 0.001 % Triton-X 3 mM $K_4Fe(CN)_6$ 3 mM $K_3Fe(CN)_6$	pH 6.8-7.2
Sodium dihydrogen phosphate	0.5 M NaH_2PO_4	Sterilization at 121 °C for 20 min
Sodium hydrogen phosphate	0.5 M Na_2HPO_4	Sterilization at 121 °C for 20 min
Phosphate buffer for GUS-solution	50% sodium dihydrogen phosphate buffer 50% sodium hydrogen phosphate buffer	pH 6.5 (pH adjustment with sodium dihydrogen phosphate)

Solution	Solution Composition	Additional information
TAE (50x)	2 M Tris-HCl (pH 8.4) 1 M Acetic acid 50 mM EDTA	pH 8.0 Sterilization at 121 °C for 20 min
Transformation buffer I (for the preparation of chemical competent cells)	0.03 M Potassium acetate 0.1 M RbCl 0.05 M $MgCl_2$ 0.01 M $CaCl_2$	pH 5.8 Sterilization by filtering throught a 0.2 µm filter. Stored at -20°C
Transformation buffer II (for the preparation of chemical competent cells)	0.01 M MOPS 0.01 M RbCl 0.075 M $CaCl_2$ 15 % (w/v) Glycerol	pH 7.0 Sterilization by filtering throught a 0.2 µm filter. Stored at -20°C
QBT buffer – for isolation of B. graminis DNA	750 mM NaCl 50 mM MOPS 15% (v/v) Isopropanol 0.15% (v/v) Triton X-100	Adjastment to pH 7.0 before adding isopropanol and Triton X-100
QC Washbuffer – for isolation of B. graminis DNA	1 M NaCl 50 mM MOPS 15% (v/v) Isopropanol	
QF Elutions-buffer – for isolation of B. graminis DNA	1.25 M NaCl 50 mM MOPS 15% (v/v) Isopropanol	Adjastment to pH 8.5 before adding isopropanol
TCA	7.5% (w/v) $C_2HCl_3O_2$ 50% (v/v) Methanol	
Sodium acetate	3 M CH_3COONa	pH 5.2 (pH adjasment with glacial acetic acid) Sterilization at 121 °C for 20 min
Phytoagar solution for big shooting plates	1 % (m/v) Phytoagar 20 mg/l Benzimidazole	
Phytoagar solution for small shooting plates	0.5 % (m/v) Phytoagar 10 mg/l Benzimidazole	

The pH adjustment if not written otherwise was performed with 5M NaOH / 3M HCl. Solutions were stored at RT if not written otherwise.

Supplementary Data M4: Specifications of the barley and wheat variaties used in the PhD thesis.

Name	Species	Country of origin	Genebank[1]	Growth habit	Status of accession[3]	Maintainer
Golden Promise	Barley	United Kingdom	HOR 4654	Spring	TC	deleted
Manchuria	Barley	China	HIR9634	Spring	AC/IC	-
Pallas	Barley	Sweden	BCC 1402	Spring	AC/IC	deleted
Ingrid	Barley	Sweden	BCC 1390	Spring	AC/IC	NordGen Växter-Sweden
HOR728	Barley	Greece	HOR 728	Spring	L	-
Hanna	Barley	Germany	HOR 808	Spring	AC/IC	deleted
Black Hulless	Barley	USA	HOR 4940	Spring	AC/IC	-
Morex	Barley	USA	BCC 906	Spring	AC/IC	-
Arina	Wheat	Swizerland	TRI 15243	Winter	AC/IC	Delley Samen und Pflanzen AG - Swizerland
Apache	Wheat	France	TRI 7466	Winter	AC/IC	Limagrain Verneuil Holding - France
Julius	Wheat	-	TRI 15890	Winter	AC/IC	KWS Lochow GMBH - Germany
Florett	Wheat	France	TRI 30124	Winter	AC/IC	deleted
Biscay	Wheat	Germany	-	Winter	AC/IC	deleted
Chinese Spring	Wheat	China	TRI 12922	Spring	L	-
Rubens	Wheat	-	-	Winter	AC/IC	deleted
History	Wheat	-	-	Winter	AC/IC	deleted

[1] IPK genebank identifier

[2] status of accession: AC/IC: advanced/improved cultivar; L: landrace; TC: traditional cultivar

The informations presented in the table are obtained from websites: https://urgi.versailles.inra.fr/siregal/siregal/accessionAction.do?collectionId=126, https://ec.europa.eu/food/plant/plant_propagation_material/plant_variety_catalogues_databases/search/public/index.cfm?event=SearchForm&ctl_type=A (maintainer), and https://gbis.ipk-gatersleben.de/gbis2i/faces/index.jsf

Supplementary Data M5: Vectors

- **pUbiGUS** vector is described by Schweizer et al. (1999). It contains 1850 nt fragment of the maize polyubiquitin1 promoter, coding region of the *uidA* gene (GUS) and CaMV 35S terminator.

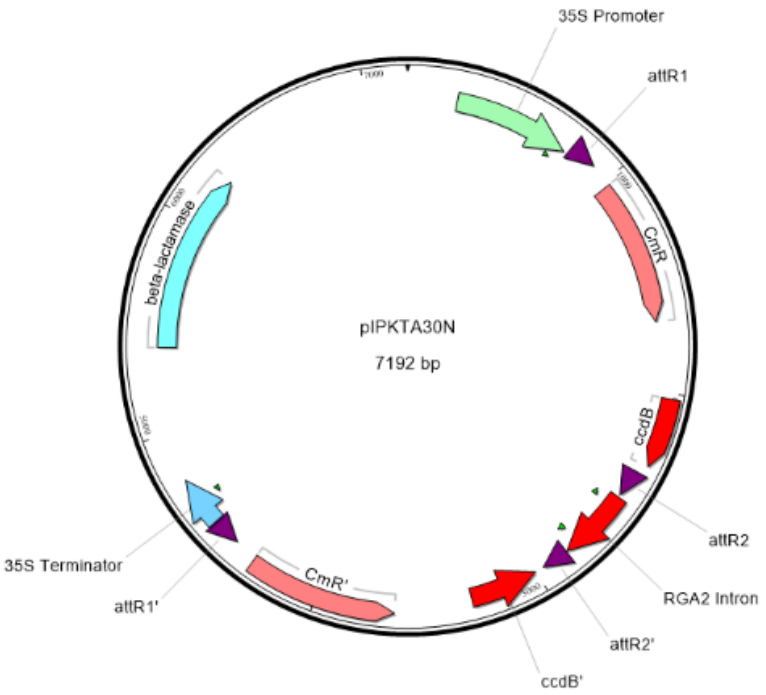

- **pIPKTA30N** vector was generated and described by Douchkov et al. (2005). It was developed as Gateway destination vector and is based on pUC18 backbone. It contains CaMV 35S promoter and terminator, ccdB gene, chloramphenicol resistance gene, and four *att*R adaptor sequences. The plasmid confers resistance to ampicillin (Douchkov et al., 2005).

- **pIPKTA36** vector was described by Douchkov et al. (2005). It is RNAi vector, silencing the expression of the barley *Mlo* gene, and causing *mlo*-mediated resistance to powdery mildew.

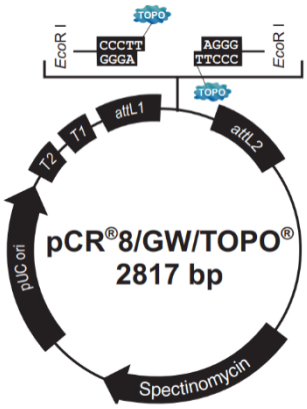

- **pCR™8/GW/TOPO®** vector (from Invitrogen, Carlsbad, USA (Catalog number: K250020)) contains TOPO Cloning site, that allows cloning of *Taq*-amplified PCR product, as well as *att*L1 and *att*L2 sites, allowing recombinational cloning of a sequence in the entry vector with a Gateway destination vector (Landy, 1989). The vector confers resistance to spectinomicin. pUC origin of replication to obtain high-copy replication in *E. coli*. It also contains priming sites (GW1, GW2, M13 forward priming site and M13 reverse priming site) allowing sequencing of the insert (Invitrogen, Carlsbad, USA).

- Presented vectors (**BSMV-VIGS α, BSMV-VIGS β and BSMV-VIGS γ**) are described by Meng et al. (2009). The subgenomes of BSMV are under the CaMV 35S promoter. The created transcripts are cleaved at the 3'terminus by the HDV ribozyme. The plasmids confer resistance to ampicillin and the nopaline-synthase (NOS) terminator.

Supplementary Data M6: cDNA synthesis protocol.

Step	Protocol
DNAse treatment	**1 µg RNA** **1 µl 10X reaction buffer with $MgCl_2$** **1 µl DNAse I** **DEPC-treated H_2O to 10 µl** **Incubation 30 min at 37°C** **1 µl EDTA** **Incubation 10 min at 65°C**
First-strand cDNA synthesis	**1 µl Oligo(dT)** **Incubation 5 min 65°C, then cooling on ice** **4 µl 5X Reaction Buffer** **0.5 µl RNase Inhibitor (Thermo Scientific)** **2 µl dNTP Mix 10mM (Thermo Scientific)** **1 µl (200U) RevertAid Reverse Transcriptase** **0.5 µl DEPC-treated H_2O** **Incubation 60 min at 42°C**

Supplementary Data M7: Transformation efficiency equation.

$CFU/\mu g = CFU/pgDNA * 1 * 10^6 pg/\mu g * V_a/V_p$

CFU = Colony forming units
pg DNA = amount of DNA used for transformation
$1 \cdot 10^6$ pg = conversion from pg to µg
V_a = transformation volume
Vp = volume of plated cells on plates containing LB mediu

Supplementary Data R1: Values to Figure R 2.

Manchuria									
	TA36	GTF1	CYP51	GPI	BEC1011	GLS	GTF1(1)	GTF2	HO06F11
Number of values	7	4	1	-	5	2	5	6	5
Median	0.01718	0.9416	0.930049	-	1.211	0.8458	1.234	1.113	0.9674
Mean	0.0146	0.9384	0.930049	-	1.219	0.8458	1.185	1.142	1.003
Std. Deviation	0.006953	0.1409	-	-	0.07578	0.1036	0.3961	0.1728	0.2301
Std. Error of Mean	0.002628	0.07045	-	-	0.03389	0.07326	0.1772	0.07055	0.1029
Hanna									
	TA36	GTF1	CYP51	GPI	BEC1011	GLS	GTF1(1)	GTF2	HO06F11
Number of values	7	4	3	2	8	5	-	-	-
Median	0.2957	0.9665	1.276	1.849	0.7461	0.7868	-	-	-
Mean	0.256	0.9373	1.271	1.849	0.8367	0.8094	-	-	-
Std. Deviation	0.1218	0.3108	0.4755	1.095	0.3835	0.2376	-	-	-
Std. Error of Mean	0.04605	0.1554	0.2745	0.7743	0.1356	0.1063	-	-	-
Golden Promise									
	TA36	GTF1	CYP51	GPI	BEC1011	GLS	GTF1(1)	GTF2	HO06F11
Number of values	4	3	3	2	4	-	-	-	-
Median	0.07607	0.5935	0.6944	1.088	0.789	-	-	-	-
Mean	0.1197	0.8418	0.6235	1.088	0.8392	-	-	-	-
Std. Deviation	0.1196	0.4314	0.3535	0.1208	0.456	-	-	-	-
Std. Error of Mean	0.05982	0.2491	0.2041	0.08544	0.228	-	-	-	-

Supplementary Data R2: Values to Figure R 3.

Genotype	Manchuria	Hanna	Pallas	HOR728	Ingrid	Golden Promise
Number of values	14	9	2	5	6	10
Median	0,1605	0,1566	0,1446	0,08308	0,122	0,08949
Mean	0,173	0,1507	0,1446	0,09772	0,1067	0,1033
Std. Deviation	0,08408	0,06628	0,005837	0,03211	0,03347	0,04933
Std. Error of Mean	0,02247	0,02209	0,004128	0,01436	0,01366	0,0156

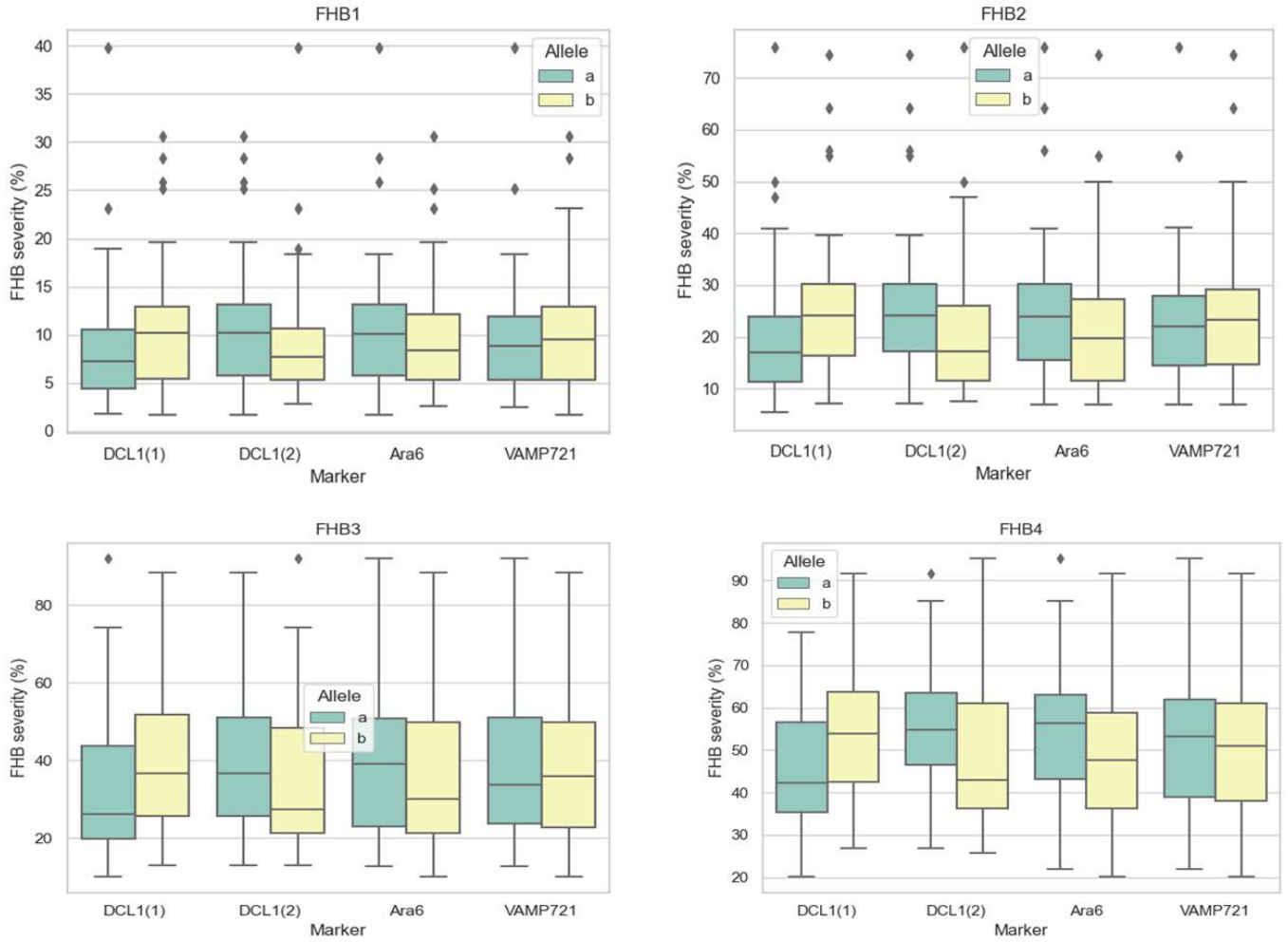

Supplementary Data R3: Association of the FHB infection at the different stages of FHB disease development in a biparental population 'Apache x Biscay' and allelic variant of the four markers.

Allelic variants are marked as a and b. Marker DCL1(1) and marker DCL1(1) are located in the *Dicer1* gene. Marker Ara6 is located in Rab5-like GTPase *Ara6* and marker VAMP721 in the *VAMP721* gene. *Refers to P ≤ 0.05; **Refers to P ≤ 0.01

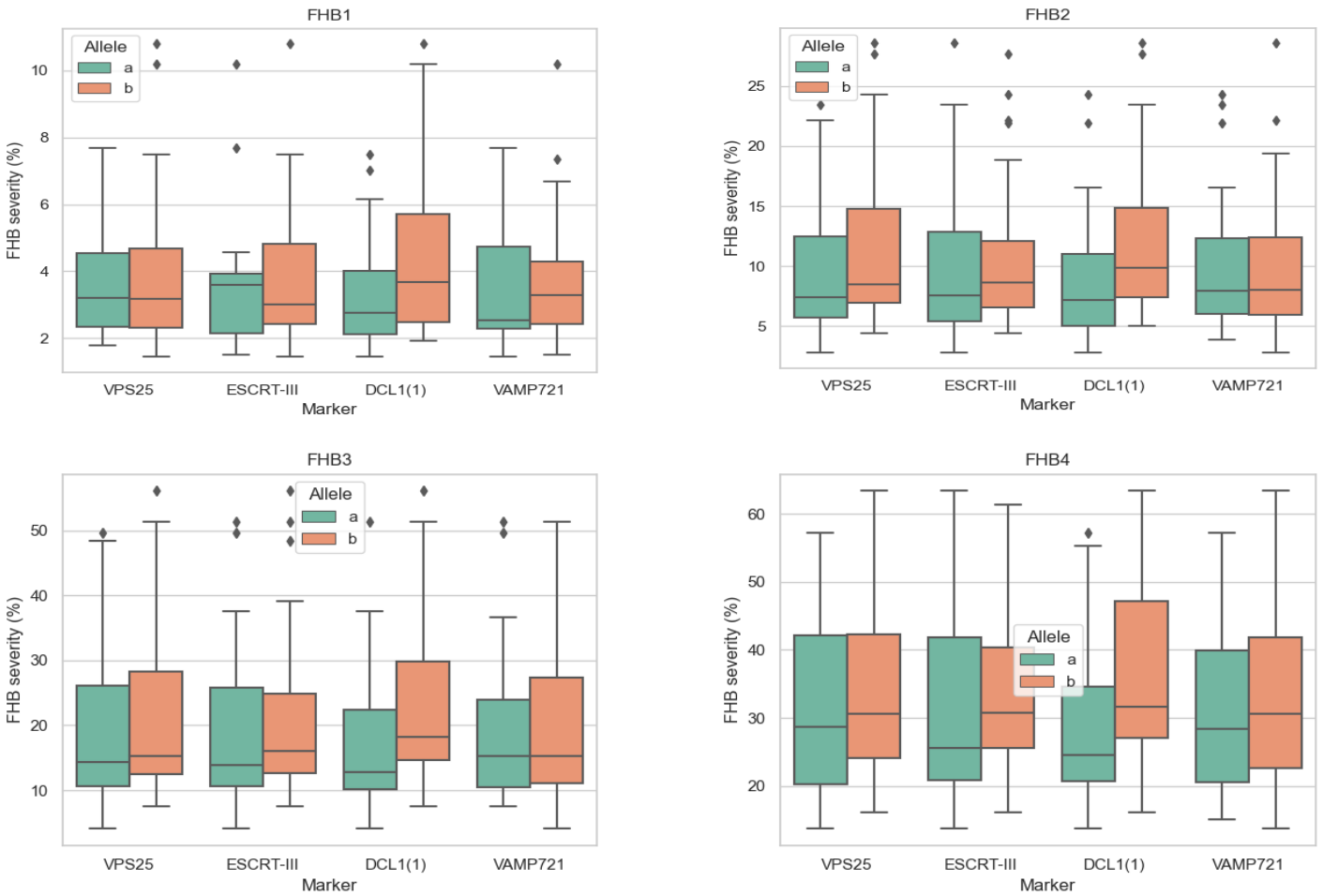

Supplementary Data R4: Association of the FHB infection at the different stages of FHB disease development in a biparental population 'History x Rubens' and allelic variant of the four markers.

Allelic variants are marked as a and b. Marker DCL1(1) and marker DCL1(1) are located in the *Dicer1* gene. Marker Ara6 is located in Rab5-like GTPase *Ara6* and marker VAMP721 in the *VAMP721* gene. *Refers to P ≤ 0.05; **Refers to P ≤ 0.01

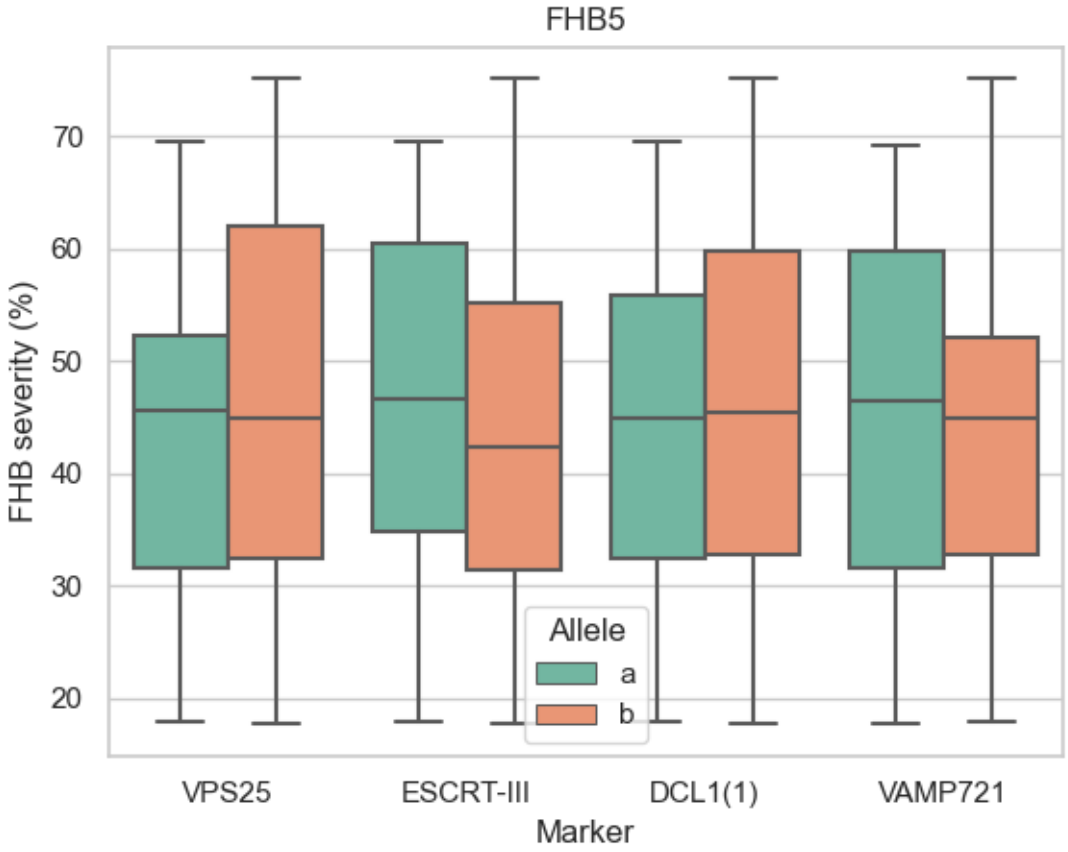

Supplementary Data R5: Association of the FHB infection at the latest stage of FHB disease development in a biparental population 'History x Rubens' and allelic variant of the four markers.
Allelic variants are marked as a and b. Marker DCL1(1) and marker DCL1(1) are located in the *Dicer1* gene. Marker Ara6 is located in Rab5-like GTPase *Ara6* and marker VAMP721 in the *VAMP721* gene. *Refers to P ≤ 0.05; **Refers to P ≤ 0.01

Supplementary Data R6: sRNA sequences and their targets in Fusarium graminearum.
The table presents eight *Fusarium* genes, sRNAs targeting these genes, sRNA lengths, their induction in infected FHB' Morex' spike in comparison to the heathy barley spike. Length of sRNA similarity to *Fusarium* transcript and function of the target fungal genes.

tag_ID	sRNA sequence	lengh of sRNA	Fold Induction	Targer gene in *Fusarium*	Max hit length in *Fusarium*	BlastX
sRNAtag2035	CGGCAACGGATATCTCGGCTCTCA	24	>100	FGSG_09048T0	18	bifunctional dethiobiotin synthetase
sRNAtag114	ACTCTCGGCAACGGATATCTCGGCTCTCGC	30	4.6		18	
sRNAtag225	ACTCTCGGCAACGGATATCTCGGCTCTCG	29	8.1		18	
sRNAtag324	CTCTCGGCAACGGATATCTCGGCTCTCG	28	4.3		18	
sRNAtag1274	TCGGCAACGGATATCTCGGCTCTCGCA	27	3.7		18	
sRNAtag558	TCTCGGCAACGGATATCTCGGCTCTCG	27	13.5		18	
sRNAtag363	TCTCGGCAACGGATATCTCGGCTCTCGC	28	8.6		18	
sRNAtag1214	TCGGCAACGGATATCTCGGCTCTCG	25	15.2		18	
sRNAtag665	TCGGCAACGGATATCTCGGCTCTCGC	26	10.8		18	
sRNAtag176	CGGCAACGGATATCTCGGCTCTCGC	25	13.1		18	
sRNAtag118	CGGCAACGGATATCTCGGCTCTCG	24	12		18	
sRNAtag1206	TCTCGGCAACGGATATCTCGGCT	23	4.2		18	
sRNAtag737	CGGCAACGGATATCTCGGCT	20	3.5		18	
sRNAtag883	ACGGCCTGCCAACCCTGGAAACGGTT	26	4.4	FGSG_02471T0	17	related to transcription factor medusa
sRNAtag157	AGGAAGCTGACGAGCGGGAGGCCCT	25	3.5	FGSG_10970T0	21	anucleate primary sterigmata protein b
sRNAtag612	TAACCTTGTGGTCGTGGGTTCG	22	36	FGSG_01104T0	20	phenylalanyl-tRNA synthetase alpha chain
sRNAtag368	AACCTTGTGGTCGTGGGTTCG	21	26.4		20	
sRNAtag493	TCCGGAGACGCCGGCGGGGGCCTCGGG	27	19.3	FGSG_06175T0	20	phospholipase d
sRNAtag850	TCCGGAGACGCCGGCGGGGGCCTCGG	26	7.5		20	
sRNAtag599	GCCTACCATGGTGGTGACGGGTGACG	26	3.1	FGSG_08039T0	20	sugar transporter
sRNAtag1323	GCCGTCGGTGCAGATCTTGGTGGTAGTAGCA	31	3.1	FGSG_09183T0	18	o-methyltransferase
sRNAtag596	ATTTCCCGAGCCGGGATGTGGCGGT	25	3.5	FGSG_06195T0	17	succinate dehydrogenase
sRNAtag1105	CCGAGCCGGGATGTGGCGGT	20	6.6		17	
sRNAtag1191	CGAGCCGGGATGTGGCGGT	19	5.3		17	

tag_ID	sRNA sequence	lengh of sRNA	Fold Induction	Targer gene in *Fusarium*	Max hit length BlastX in *Fusarium*
sRNAtag678	TCCCGAGCCGGGATGTGGCGGT	22	5		17
sRNAtag564	CCCGAGCCGGGATGTGGCGGT	21	4.5		17
sRNAtag554	TTCCCGAGCCGGGATGTGGCGGT	23	4.4		17
sRNAtag766	GAGCCGGGATGTGGCGGT	18	16.7		17
sRNAtag402	AGCCGGGATGTGGCGGT	17	27.9		16
sRNAtag792	TCCCGAGCCGGGATGTGGCGG	21	10.1		17
sRNAtag961	CGAGCCGGGATGTGGCGG	18	4.9		17
sRNAtag800	TTCCCGAGCCGGGATGTGGCGG	22	3.4		17
sRNAtag1277	TTTCCCGAGCCGGGATGTGGCGG	23	3.1		17
sRNAtag613	GAGCCGGGATGTGGCGG	17	27		17

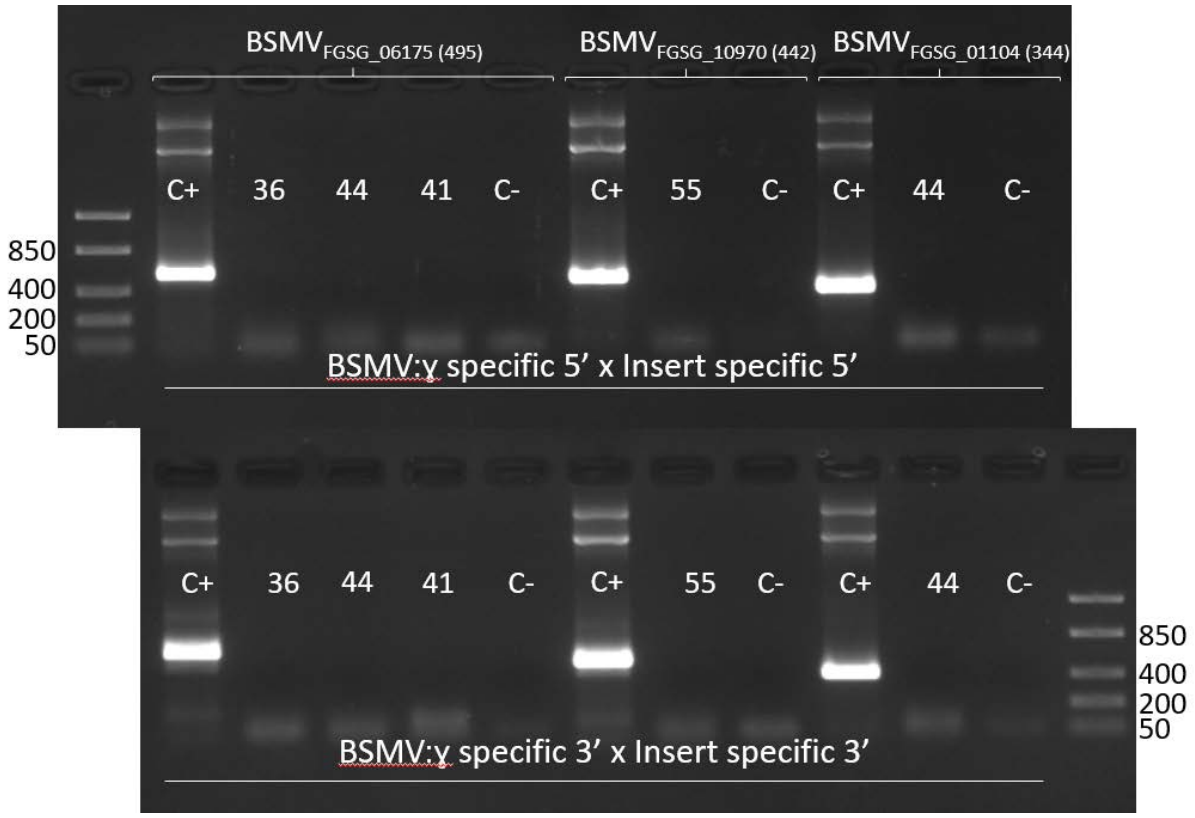

Supplementary Data R7: Stability of the long inserts (344, 442 and 495 nt) at the time when 'Apogee' spikelet is inoculated with FHB (~20th day of the experiment).

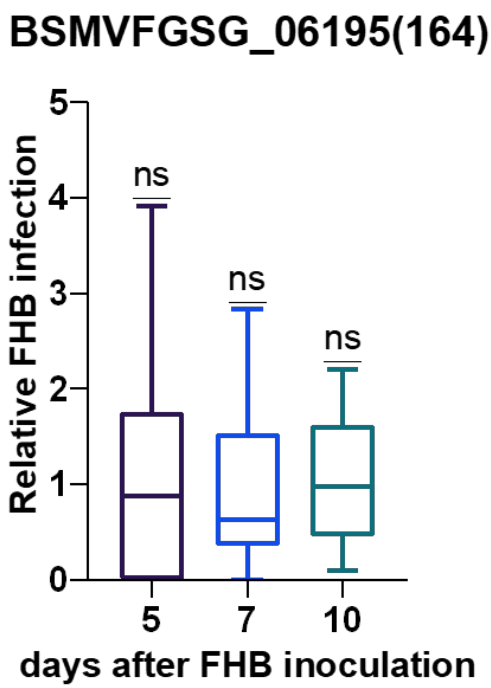

Supplementary Data R8: Relative FHB infection of 'Apogee' wheat plants inoculated with recombinant BSMV, carrying FGSG_06195(164) insert.

FHB severity was compared to the control plants carrying BSMV:00 and set as 1. Assessment of FHB severity was made 5, 7 and 10 days after *Fusarium* inoculation of the wheat spike.

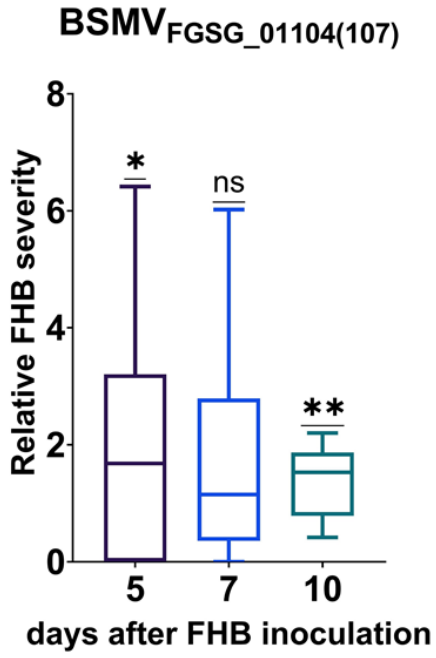

Supplementary Data R9: Relative FHB infection of 'Apogee' wheat plants inoculated with recombinant BSMV, carrying FGSG_01104(107) insert.

FHB severity was compared to the control plants carrying BSMV:00 and set as 1. Assessment of FHB severity was made 5, 7 and 10 days after *Fusarium* inoculation of the wheat spike.

Supplementary Data R10: Gene expression analysis and stability of the BSMV.

insert	sample	Relative gene expression	Stability of the insert	Relative FHB infection (10 days)
FGSG_06175(104)	1	0.364466	0.8	N
FGSG_06175(104)	2	1.167385	0.1	1.324382
FGSG_06175(104)	3	1.866937	1	0.441461
FGSG_06175(104)	4	0.981945	0.7	1.117447
FGSG_06175(104)	5	0.486907	0.4	1.229783
FGSG_06175(104)	6	2.032303	1	0.441461
FGSG_06175(104)	7	0.389887	1	0.945987
FGSG_06175(104)	8	1.302001	1	0.389524
FGSG_06175(104)	9	0.540184	1	1.135184
FGSG_06175(104)	10	0.733599	1	1.040586
FGSG_06175(104)	11	0.889614	1	0.794629
FGSG_06175(104)	12	0.312901	1	1.087885
FGSG_06175(104)	13	0.480328	1	0.927067
FGSG_06175(104)	14	1.758511	0.8	0.827739
FGSG_06175(104)	15	0.832901	1	0.971213
FGSG_06175(180)	1	0.549411	0.9	0.065286
FGSG_06175(180)	3	1.778984	0.9	0.447679
FGSG_06175(180)	4	1.193344	0.3	1.2535
FGSG_06175(180)	5	1.352452	0.8	1.175156
FGSG_06175(180)	6	1.181885	0	0.96997
FGSG_06175(180)	7	0.95481	0.5	1.19381
FGSG_06175(180)	8	2.084665	0.9	0.820744
FGSG_06175(180)	11	1.168114	0.6	0.820744
FGSG_06175(180)	12	0.141232	0	0.261146
FGSG_06175(180)	13	0.901177	0.7	1.392778
FGSG_06175(180)	14	1.740035	0.6	0.208917
FGSG_06175(180)	15	0.798732	0.5	1.19381
FGSG_06175(180)	16	1.395828	0.2	1.114222
FGSG_06175(180)	17	0.946102	0	0.835667
FGSG_10970(233)	2	1.54896	0.3	0.550689
FGSG_10970(233)	4	1.304392	0	1.376724
FGSG_10970(233)	5	1.1834	0.2	0.917816
FGSG_10970(233)	6	0.968837	0	0.295012
FGSG_10970(233)	7	0.362165	0.1	0.295012
FGSG_10970(233)	8	1.278549	0.2	0.642471
FGSG_10970(233)	9	1.141896	0	N
FGSG_10970(233)	10	1.098941	0	0.295012
FGSG_10970(233)	11	1.011519	0	2.569884

Acknowlegment

First and foremost, I would like to thank my supervisor Dr. Patrick Schweizer, who made it possible for me to work on my PhD, thanks to whom I was lucky enough to be part of the 'Cerealpath' project. I will always remember him as a wonderful boss, open to my ideas, patient and supportive, a great scientist who loved what he did and inspired others.

I would also like to sincerely thank Dr. Dimitar Douchkov, who, although not officially my supervisor, was the person who first proofread my dissertation and helped me improve it. I thank him for his many valuable comments, for his support, for being open to my many questions and his patience.

I would like to thank Prof. Reif, for becoming my supervisor. I thank him for helping me in a situation that was difficult for everyone, for his understanding, for encouraging me to complete my doctoral thesis, and for helping me write my publication.

I would also like to thank Professor Desing, for agreeing to be my supervisor, for his patience, correcting my PhD thesis and for his guidance.

I thank Dr. Chen, who was my mentor, for her help, especially at the beginning of my PhD. Thanks to her guidance, getting started in IPK seemed much easier. Dr. Chen taught me many important methods and shared her knowledge, for which I am grateful.

I would like to thank very much Dr. Helmut Bäumlein, who became temporary head of the PSG group. Dr. Bäumlein was very understanding, gave me many valuable comments and helped me a lot during this very difficult time.

I would like to thank Dr. Victor Korzun, who was always helpful and encouraged me to write a publication. My two-month stay at KWS, I always remember very fondly, and thanks in part to the internship, I was able to publish my research. I would like to thank all the people in the KWS Breeding Technologies Cereals group, especially Sonja Kollers, who took care of me after I arrived at KWS and guided me there.

I would also like to thank Stefanie Lueck, who helped me with the design of the primers using the bioinformatics tools she created herself, as well as familiarized me with many laboratory techniques. I would also like to thank Daniel Nowara, with whom I discussed many of the issues/problems that arose during my PhD and who gave me many valuable suggestions. I would also like to appreciate the rest of the group forming PSG, for their support, pleasant atmosphere and helpful discussions.

Many thanks to Dr. Leps, for her help with many official matters. Thanks to her, staying in Germany has become much easier for our family.

Finally, thank to the CerealPath community, including the scientific representatives, the industry representatives, and especially other early-stage researchers, thanks to whom the time spent training, was great.

I would like to thank my wonderful husband Piotrek, for always being there for me, his support, patience and love. To my mother, for a tremendous amount of help, being a great mother and grandmother and for supporting me always and everywhere. For the time, for being always ready to help, for being a great grandmother to my daughters, I wanted to thank Piotr's mom - Danusia. Aunt Jola for helping me, for being there for me, for being a loving grandmother to my girls. To my beloved grandmother, for always being with me. To the rest of my wonderful family and friends, for their support. Finally, to my dear girls, Michasia and Stefcia, for being my joy and love.

Curriculum vitae

Name	Karolina Maria Słomińska-Durdasiak
Nationality	Polish
Gender	female
EDUCATION	
2019	International Spring School „Computational Biology Starter", Gatersleben
2016-2017	Trainings in disease cereal control as a part of Cerealpath programme
02.2015 – 07.2015	University of Natural Resources and Life Sciences in Vienna (Austria) – Erasmus+ Programme
10.2010 - 09.2015	Warsaw University of life sciences, Faculty of Horticulture, Biotechnology and Landscape Architecture – Biotechnology
03.2014 – 09.2015	Master of Science –specialization: biotechnology in plant production; master thesis: "Preliminary studies on the role of HvCKX5 gene in barley development"
10.2010 – 02.2014	Bachelor of Science – bachelor thesis: "Influence of silencing of selected genes on tomato susceptibility to the potato cyst nematode infestation"
EXPERIENCE	
Since 03.2016	Early Stage Researcher at Leibniz-Institute of Plant Genetics and Crop Plant Research in Gatersleben (Germany) "Host-induced gene silencing (HIGS) as a biotechnological and natural tool for controlling barley diseases"
15.02.2015 -30.06.2015	Research project in Department of Applied Genetics and Cell Biology in University of Natural Resources and Life Sciences in Vienna (Austria) "Establishing a non-radioactive translation efficiency method in plant Arabidopsis thaliana", as a trainee under ERASMUS + programme
02.2014 – 02.2015	Research for Master's thesis in Plant Breeding and Acclimatization Institute – National Research Institute in Department of Functional Genomics (Poland)

List of publications

1. Kangara N., Marchal C., Ndougonna C. & and Słomińska-Durdasiak K. M. (2017) Genetically modified organisms as an option for crop management for disease and pest resistance. In a Paschke M. (ed.), Zurich-Basel Plant Science Center: PSC Summer Schools 2014 and 2016, Agriculture in transformation – Concepts for agriculture production systems that are socially fair, environmentally safe and economically viable. 103-107.
2. Llabata, P., Richter, J., Faus, I., Słomińska-Durdasiak, K., Zeh, L. H., Gadea, J., & Hauser, M. T. (2019). Involvement of the eIF2α Kinase GCN2 in UV-B Responses. Frontiers in Plant Science 10, 1492. https://doi.org/10.3389/fpls.2019.01492
3. Słomińska-Durdasiak, K. M., Kollers, S., Korzun, V., Nowara, D., Schweizer, P., Djamei, A., & Reif, J. C. (2020). Association mapping of wheat Fusarium head blight resistance-related regions using a candidate-gene approach and their verification in a biparental population. TAG. Theoretical and Applied Genetics. Theoretische und Angewandte Genetik 133(1), 341–351. https://doi.org/10.1007/s00122-019-03463-5

Oral presentations and posters

Presentations

1. 14 th European Fusarium Seminar, Tulln, Austria (2018) “Host-induced gene silencing as natural resistance strategy of wheat against Fusarium head blight”

Posters

1. V Biotechnology Symposium, Spytkowice, Poland (2014) “Influence of changes in the expression of selected genes on tomato susceptibility to the potato cyst nematode infestation”
2. IPK Institute´s Days; Leibniz Institute of Plant Genetics and Crop Plant Research (IPK), Gatersleben, Germany (2016) “Host-induced gene silencing (HIGS) as a biotechnological and natural tool for controlling cereal diseases”
3. 20 th EUCARPIA General Congress, Zurich, Switzerland (2016) “Role of HvCKX5 and HvCKX4b genes in growth and reproductive development of barley” (2 nd author)
4. Plant Science Student Conference 2017; Leibniz-Institute of Plant Biochemistry; Halle (Saale), Germany (2017) “Host-induced gene silencing as resistance strategy against pathogens”
5. International Plant Immunity Symposium 2018; Göttingen (2018) “Host-induced gene silencing (HIGS) as a biotechnological and natural tool for controlling cereal diseases”

Declaration under oath

I declare under penalty of perjury that this thesis is my own work entirely and has been written without any help from other people. I used only the sources mentioned and included all the citations correctly both in word or content.

_____ _____

Date Signature of the applicant